

A study on TAP38:
its regulation, site of action
and antagonistic function towards STN7



Dissertation
zur Erlangung des Doktorgrades der Fakultät für Biologie
der Ludwig-Maximilians-Universität München

Vorgelegt von
Qiuping Liu
aus München

A study on TAP38:
its regulation, site of action
and antagonistic function towards STN7



Dissertation
zur Erlangung des Doktorgrades der Fakultät für Biologie
der Ludwig-Maximilians-Universität München

Vorgelegt von
Qiuping Liu
aus München

Erstgutachter: Prof. Dr. Dario Leister
Zweitgutachter: Prof. Dr. Peter Geigenberger
Tag der Einreichung: 8. 6. 2013
Tag der mündlichen Prüfung: 8.8.2013

Summary

Variations in light quality and quantity induce imbalances in the excitation of the two photosystems, PSI and PSII, due to their distinct absorption spectra, leading to an impairment of electron transport across the thylakoid membrane. To counteract such fluctuations, land plants and algae evolved a short-term acclimation mechanism called state transitions which involves the reversible phosphorylation of the light harvesting complex of PSII (LHCII) and is regulated by the redox state of the plastoquinone pool (PQ pool). The protein kinase STN7 and protein phosphatase TAP38 form an antagonistic pair in catalyzing the reversible (de)phosphorylation of LHCII. An in depth characterization of TAP38 revealed that TAP38 is an intrinsic thylakoid membrane protein with its N-terminus facing the stroma. TAP38 was enriched in the stroma lamellae, as shown by fractionation and immunogold labeling approaches. Furthermore, it could be shown that TAP38 protein levels remain on a constantly high level being permanently active irrespective of the redox status. This was supported by TAP38 being able to significantly overaccumulate in the presence of an overreduced PQ pool (i.e. in the *psad1-1* and *psae1-3* background). Based on BN-PAGE and sucrose gradient centrifugation assays, no stable association of TAP38 with any of the photosynthetic complexes could be determined, whereas a localization of TAP38 in the close proximity of PSI was revealed by Co-IP using lines expressing GFP- and HA-tagged TAP38. Regarding the long term acclimatory response, *tap38-1* and *oeTAP38* lines behaved essentially like WT and microarray analyses revealed no significant differential regulation at the transcriptional level. Finally, additional substrates of TAP38 were detected, both in the thylakoid membrane and the stroma, suggesting a function of TAP38 beyond state transitions.

Zusammenfassung

Aufgrund der unterschiedlichen Lichtabsorptionsmaxima der zwei Photosysteme, PSI und PSII, können Veränderungen in der Lichtqualität und Quantität eine ungleiche Anregung der Photosysteme hervorrufen und somit die Effizienz des Elektronentransports über die Thylakoidmembran beeinträchtigen. Um solche Schwankungen auszugleichen, haben Algen und Landpflanzen einen reaktionsschnellen Anpassungsmechanismus entwickelt, den sogenannten „*State Transitions-Mechanismus*“, der auf einer reversiblen Phosphorylierung des Lichtsammelkomplexes des PSII (LHCII) beruht und über den Redoxzustand des Plastochinon-Pools (PQ-pool) reguliert wird. Für die reversible (De) Phosphorylierung von LHCII sind die Phosphatase TAP38 bzw. die Kinase STN7 verantwortlich. Eine weiterführende Charakterisierung von TAP38 haben gezeigt, dass es sich bei TAP38 um ein integrales Thylakoidmembranprotein handelt, dessen N-Terminus der Stromaseite zugewandt ist. Mittels Thylakoidfraktionierung und Immunogoldmarkierung konnte zudem nachgewiesen werden, dass TAP38 hauptsächlich in den Stromathylakoiden lokalisiert ist. Des Weiteren konnte gezeigt werden, dass sowohl die TAP38 Proteinmenge als auch die enzymatische Aktivität von TAP38 ungeachtet des Redox-Status konstant bleibt. Diese Ergebnisse wurden durch die Beobachtung unterstützt, dass eine starke Überexpression von TAP38 in der Gegenwart eines stark reduzierten PQ Pools gestützt (z.B. im genetischen Hintergrund von *psad1-1* und *psae1-3*) möglich ist. Basierend auf BN-PAGE-Analysen und Saccharose-Gradientenzentrifugation konnte keine stabile Assoziation von TAP38 mit Photosynthese-Komplexen nachgewiesen werden. Co-IP-Experimente lieferten jedoch deutliche Hinweise für eine Interaktion von TAP38 mit PSI-Antennenproteinen. Bezüglich der Langzeitanpassung (LTR) verhielten sich sowohl *tap38-1* als auch *oeTAP38* wie der Wildtyp. Auch Microarray-Analysen dieser Linien zeigten keine signifikante Veränderung auf Transkriptebene. Abschließend konnten weitere putative Substrate von TAP38 in Thylakoidmembran- und Stromaextrakten detektiert werden, was auf eine zusätzliche Funktion von TAP38 neben dem State-transitions Mechanismus schließen lässt.

Index

Summary	i
Zusammenfassung	ii
Index	iii
List of Figures	vii
List of Tables	viii
Abbreviations	ix
Units	x
1 Introduction	1
1.1 Photosynthesis	1
1.2 The linear electron flow (LEF) and cyclic electron flow (CEF)	3
1.3 Adaptation to light changes	5
1.3.1 Nonphotochemical quenching (NPQ)	5
1.3.2 D1 turnover and PSII repair	6
1.3.3 State transitions	7
1.3.4 Long term response (LTR)	16
1.4 Reversible phosphorylation in chloroplasts	17
1.4.1 STN8	18
1.4.2 Further chloroplast kinases.....	19
1.4.3 PBCP and other phosphatases.....	19
1.5 Aims of this work	20
2 Materials and Methods	22
2.1 Plant material.....	22
2.1.1 Generation of transgenic <i>A. thaliana</i> lines expressing GFP-tagged TAP38	22
2.1.2 Generation of transgenic <i>A. thaliana</i> lines expressing HA-tagged TAP38.....	22
2.2 Growth and light conditions	23
2.3 Total protein extraction	24
2.4 Isolation of thylakoid membranes	24
2.5 Chloroplast isolation and separation of soluble membrane fraction	24

2.6 Purification of recombinant His-tagged TAP38 proteins.....	25
2.7 Chlorophyll fluorescence analysis.....	25
2.7.1 Measurement of standard photosynthetic parameters	25
2.7.2 State Transition measurements via PAM fluorometry	25
2.8 Photosynthetic Acclimation Analysis	26
2.8.1 Chlorophyll fluorescence measurement during LTR.....	26
2.8.2 Chlorophyll a/b ratio measurement during LTR	26
2.9 SDS-PAGE and immunoblot analysis.....	26
2.10 BN- and 2D-PAGE.....	26
2.11 Sucrose gradient fractionation of thylakoid complexes	27
2.12 2D protein separation by isoelectric focusing (IEF) and SDS-PAGE gel Electrophoresis	27
2.13 Coomassie or Ponceau S staining of proteins on PVDF membrane	28
2.14 Crosslinking	28
2.15 Co-Immunoprecipitation (Co-IP).....	28
2.16 Mass spectrometry analysis and database searches.....	29
2.17 Immunogold labeling	29
2.18 cDNA synthesis and real-time PCR	30
2.19 mRNA expression profiling	30
2.20 Salt extraction and trypsin treatment of thylakoid membranes.....	30
2.21 Fractionation of state 1 and 2 thylakoids.....	31
2.22 Phosphorylation Inhibitory assay	31
3 Results	32
3.1 Topology studies on TAP38 protein	32
3.1.1 TAP38 is accessible to trypsin digestion at the stroma side of thylakoids	32
3.1.2 TAP38 is anchored in the thylakoid membrane mainly by electrostatic interactions ...	33
3.2 Differential localization of TAP38 within the thylakoid membrane.....	35
3.2.1 TAP38 localizes predominantly to stroma lamellae fractions.....	35
3.2.2 Immunogold labeling suggests a stroma lamellae localization of TAP38	35
3.3 TAP38 is not regulated by the redox state of the Plastoquinone pool	36
3.3.1 Constant expression of TAP38 under different light conditions.....	36
3.3.2 TAP38 still active in state 2	37

3.3.3 TAP38 accumulates and functions normally in mutant lines with over-reduced PQ pool	38
3.4 TAP38 co-localizes with its putative substrate LHCII and depends on its expression.....	43
3.4.1 TAP38 co-localizes with its putative substrate LHCII.....	43
3.4.2 TAP38 expression is decreased in mutants defective in LHCII accumulation	44
3.5 TAP38 is not directly associated with PSI or other major photosynthetic complexes	46
3.5.1 TAP38 is not associated with major photosynthetic complexes in BN and sucrose gradient ultracentrifugation	46
3.5.2 The expression of TAP38 is affected in a mutant lacking PSI but not in mutants lacking any other of the major photosynthetic complexes	47
3.6 Pull down assay using functional N-terminal HA-Fusion line and C-terminal GFP-Fusion Line of TAP38.....	49
3.6.1 Expression of TAP38-HA and TAP38-GFP proteins in the <i>tap38-3</i> mutant background	49
3.6.2 Pull down of putative interactors of TAP38 using HA- or GFP-tagged lines.....	51
3.7 At low light TAP38 is present in lower amounts compared to STN7.....	52
3.8 Is TAP38 the true counter player of STN7?.....	53
3.8.1 Response of <i>tap38-3</i> and <i>oeTAP38</i> to the long term acclimation as monitored by chlorophyll a/b ratios and F_v/F_m values	54
3.8.2 Microarray analyses on <i>tap38</i> and <i>oeTAP38</i> show no significant changes on transcriptome level	56
3.9 Generation of thylakoid hyper- and hypo-phosphorylation double mutants.....	57
3.10 Second dimension protein separation by isoelectric focusing and SDS-PAGE gel electrophoresis.....	59
4 Discussion	62
4.1 TAP38 is not regulated by the PQ pool redox in contrast to the counteracting kinase STN7	62
4.2 TAP38 is present in lower amounts than STN7	64
4.3 TAP38 accumulation is regulated at the transcript level and correlates with the presence of LHCII and PSI.....	65
4.4 TAP38 localized close to PSI.....	67
4.5 The function of TAP38 and STN7 in the long term response (LTR)	69
4.6 Potential new substrates of TAP38	71
Appendix 1	74

Appendix 2	75
Appendix 3	76
5 References	77
Acknowledgements	92
Curriculum vitae	93
Declaration/Eidesstattliche Erklärung	95

List of Figures

Figure 1 Schematic cartoon of a land plant chloroplast.	1
Figure 2 Lateral heterogeneity of thylakoid membrane complexes.	3
Figure 3 Scheme of linear electron flow (LEF).....	4
Figure 4 State transition models.	9
Figure 5 Scheme of PSI and PSII remodeling during state 1-to-2 transition.	12
Figure 6 Topology studies on TAP38.	33
Figure 7 Differential localization of TAP38 within the thylakoid membrane.	34
Figure 8 TAP38 is neither regulated at the protein nor activity level by the redox state of the PQ pool.....	37
Figure 9 Ectopic expression of TAP38 in mutants with highly-reduced PQ pool (<i>psae1-3</i> and <i>psad1-1</i>)......	39
Figure 10 TAP38 could accumulate and functions normally in the double mutants with further over-reduced PQ pool.....	42
Figure 11 TAP38 co-localizes with its putative direct substrate LHCII and depends on its expression.....	43
Figure 12 TAP38 is not directly associated with PSI or other major photosynthetic complexes.	45
Figure 13 TAP38 is crosslinked to high molecular weight complexes.	47
Figure 14 The expression of TAP38 is affected in mutants lacking PSI but not in mutants lacking any of the other photosynthetic complexes	48
Figure 15 Generation of a functional N-terminal HA and C-terminal GFP Fusion lines of TAP38.	50
Figure 16 Immunodetection of TAP38 in the elutions of co-immunoprecipitation with HA-and GFP-affinity matrixes.....	51
Figure 17 In low light acclimated plants TAP38 is accumulated in lower amounts compared to STN7.	53
Figure 18 Measurement of LTR-acclimation of <i>TAP38</i> mutant and overexpressor plants.....	55
Figure 19 Venn diagram depicting the overlap of genes whose expression was found in Microarray analysis to be differentially regulated.	57
Figure 20 LHCII phosphorylation in hyper- and hypo-phosphorylation mutants.....	58
Figure 21 Second dimension-IEF gel analyses of thylakoid and stromal proteins.	60
Figure 22 Simplified State transitions model indicating the working dynamic of TAP38.	68
Figure S1 Identification of homozygous <i>tap38-3</i> lines.	74
Figure S2 Chl a/b ratios of <i>TAP38</i> mutant and overexpressor plants during LTR acclimation....	75
Figure S3 Overexpression of STN7 in the double mutant <i>tap38-1</i> oe <i>STN7</i>	76

List of Tables

Table 1 Chlorophyll Fluorescence Parameters of 4-week-old double mutants of oeTAP38 and PSI defective mutants (psad1-1, psae1-3).	40
Table 2 Results of the Mass Spectrometry analysis on the Co-IP elutions.	52
Table 3 Quantification of TAP38 and STN7 in low light adapted thylakoid membranes.	53

Abbreviations

1-qL	measure for the fraction of open PSII reaction centers	NDH	NADPH dehydrogenase complex
2D	2-dimensional	NP40	Nonidet P-40
<i>A. thaliana</i>	<i>Arabidopsis thaliana</i>	NPQ	non-photochemical energy quenching
ATP	adenosine-5'-triphosphate	oe	overexpressor
ATPase	ATP synthase	oeSTN7	overexpressor of STN7
β -DM	n-dodecyl β -D-maltoside	oeTAP38	overexpressor of TAP38
BN	Blue Native	P680	PSII reaction center
CaCl ₂	calcium chloride	P700	PSI reaction center
CcdA	CcdA, cytochrome c defective A	pLHCII	phosphorylated lightharvesting complex of photosystem II
cDNA	complementary DNA	P-Thr	phosphothreonine
CDS	coding sequence	PSI/II	Photosystem I/II
CEF	cyclic electron flow	PAGE	polyacrylamide gel electrophoresis
Chl a/b	chlorophyll a/b	PAM	pulse amplitude modulation
<i>C. reinhardtii</i>	<i>Chlamydomonas reinhardtii</i>	PAR	photosynthetically active radiation
CSK	chloroplast sensor kinase	PCR	polymerase chain reaction
Cyt	cytochrome	PVDF	polyvinylidene fluoride
Cyt <i>b₆f</i>	cytochrome <i>b₆f</i> complex	pLHCII	phosphorylated LHCII
D	dark	PP2C	protein phosphatase 2 C
DBMIB	2,5-dibromo-6-isopropyl-3-methyl-1,4-benzoquinone	PBCP	Photosystem II Core Phosphatase
DCMU	3-(3,4-dichloro-phenyl)-1,1-dimethylurea	PQ/ PQH ₂	plastoquinone (oxidized)/plastoquinol (reduced)
DNA	deoxyribonucleic acid	PTK	plastid transcription kinase
DTT	dithiothreitol	PVDF	polyvinylidene fluoride
EDTA	ethylene diamine tetraacetic acid	Φ_{II}	effective quantum yield of photosystem II
Fm/ m'	maximum fluorescence in the dark/ light	Q _A	the primary quinone electron acceptor of PSII
F ₀	fluorescence after dark adaptation	Q _B	secondary quinone electron acceptor of PSII
FR	far-red light	Q _o	the quinol oxidation site of the Cyt <i>b₆f</i> complex
FV	variable fluorescence	qL	photochemical quenching
GFP	green fluorescent protein	qT	fluorescence quenching because of state transition
HA	human influenza hemagglutinin	RNA	ribonucleic acid
HEPES	4-(2-hydroxyethyl)-1-piperazineethanesulfonic acid	RT-PCR	real-time PCR
HL	high light	SD	standard deviation
IEF	isoelectric focusing	SDS	sodium dodecyl sulphate
IPTG	isopropyl β -D-1-thiogalactopyranoside	Ser	serine
KCl	potassium chloride	SEM	Scanning electron microscopy
KOH	potassium hydroxide	SIG1	chloroplast sigma factor 1
LED	light-emitting diode	STN7	thylakoid-associated Ser-Thr protein kinase
LEF	linear electron flow		State Transition 7 (<i>A. thaliana</i>)

LHCI/II	light harvesting complex I/II	STN8	thylakoid-associated Ser-Thr protein kinase
LL	low light		State Transition 8 (<i>A. thaliana</i>)
LTR	long-term response	STR	short-term response
mRNA	messenger RNA	STT7	thylakoid-associated Ser-Thr protein kinase (<i>C. Reinhardtii</i>)
MS	mass spectrometry		
NaCl	sodium chloride	TAP38/ PPH1	Thylakoid-Associated Phosphatase of 38 kDa/ Protein Phosphatase 1 (<i>A. thaliana</i>)
NADP ⁺	oxidized nicotinamide adenine dinucleotide phosphate	Thr	threonine
NADPH	reduced nicotinamide adenine dinucleotide phosphate	TM	transmembrane domain
NaOH	sodium hydroxide	Tris	tris (hydroxymethyl) aminomethane
		WT	wild type

Units

°C	degree Celcius	μ	micro
cm	centimetre	M	molar
δ	delta	m	meter
Da	Dalton	min	minutes
g	gram	mL	milliliter
g	gravity	mM	millimolar
h	hour	mol	molar
k	kilo	nm	nanometer
kDa	Kilodalton	s	second
L	liter	v	volume

1 Introduction

1.1 Photosynthesis

Photosynthesis refers to a process by which prokaryotes, algae and plants use light energy to synthesize organic compounds. In plants, this process occurs in a specialized organelle called chloroplast, which is surrounded by a double membrane system, the outer and inner envelope membrane. The chloroplast contains a complex internal membrane system named thylakoid membrane, which consists of stacked membrane domains (grana), unstacked membrane areas (stroma lamellae) and the connection parts (margin) (Figure 1). The internal space encircled by the thylakoid membrane is the lumen and the corresponding area outside the thylakoids is called stroma (Figure 1) (Buchanan et al., 2002).

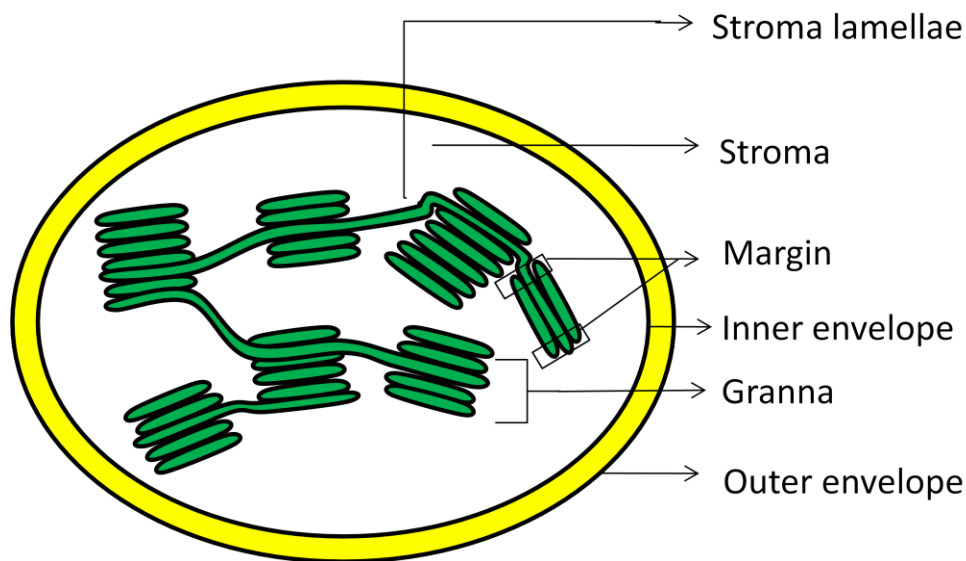


Figure 1 Schematic cartoon of a land plant chloroplast.

Chloroplasts have two envelopes (inner envelope and outer envelope). The internal membrane (thylakoids) is constituted of stacked thylakoids (grana), unstacked thylakoids (stroma lamellae) and the connection parts (margin). The space outside of thylakoids is stroma (white area) and the space surrounded by the thylakoids is the lumen (green area). Modified from Buchanan et al., 2002

The chloroplasts of algae and land plants are supposed to derive from cyanobacteria by endosymbiotic association with a eukaryotic cell (Buchanan et al., 2002). The endosymbiotic theory is supported by abundant evidence provided by electron microscopy and molecular biology (Margulis, 1992). During evolution, most genes of the cyanobacterial endosymbiont were

transferred to the nucleus of the eukaryotic host, whereas only a small part remained in the organelle. Due to this integration, 18% of the nuclear genome of the reference plant *Arabidopsis thaliana* (*A. thaliana*) shows signs of cyanobacterial origin (Martin et al., 2002).

The oxygen-evolving photosynthesis in algae and plants is a reduction-oxidation process including two steps. The first step which occurs in the thylakoid membranes involves oxidation of H₂O to O₂ and production of ATP and NADPH using energy absorbed by photosynthetic pigments. In a second step, the carbon reduction cycle (also called Calvin-Benson cycle) converts CO₂ into carbohydrate by consumption of ATP and NADPH generated during the first part of the reaction. In the whole process, H₂O serves as the ultimate electron source and CO₂ is used as the final electron acceptor (Buchanan et al., 2002).

A plant photosystem consists of the following principal components: light harvesting pigments complexes (antenna), electron carriers and reaction center. The pigments are mainly chlorophyll a (Chl a) and chlorophyll b (Chl b) with light absorption spectra of wavelengths between 400-700 nm peaking at 430 nm (blue) and 680 nm (red). Carotenoids, a second group of pigments participating in light absorption, absorb light between 400 and 500 nm. Chlorophyll a is present both in the antenna and reaction center complexes, whereas chlorophyll b and carotenoids are only found in antenna complexes. Chlorophylls are associated with proteins and form the light-harvesting complexes (LHCs) of the photosystems. The reaction centre represents the place where the initial charge separation takes place. Plants contain two photosystems designated Photosystem I (PSI) and Photosystem II (PSII), which have different absorbance maxima regarding their special pigments: PSI at 700 nm; PSII at 680 nm (Buchanan et al., 2002).

Besides the two photosystems, there are other photosynthetic complexes in the thylakoid membrane, such as the Cytochrome *b₆f* complex and the ATP synthase. The complexes display a heterogenic distribution pattern within the thylakoid membrane: PSII is primarily localized in the grana; PSI and ATP synthase are mainly found in stroma lamellae; the Cytochrome *b₆f* complex (Cyt *b₆f*) is distributed quite evenly throughout the membrane. Although PSII and PSI cooperate in electron transport primarily in a linear way, the ratio of PSII to PSI is variable depending on species and environmental conditions (Figure 2).

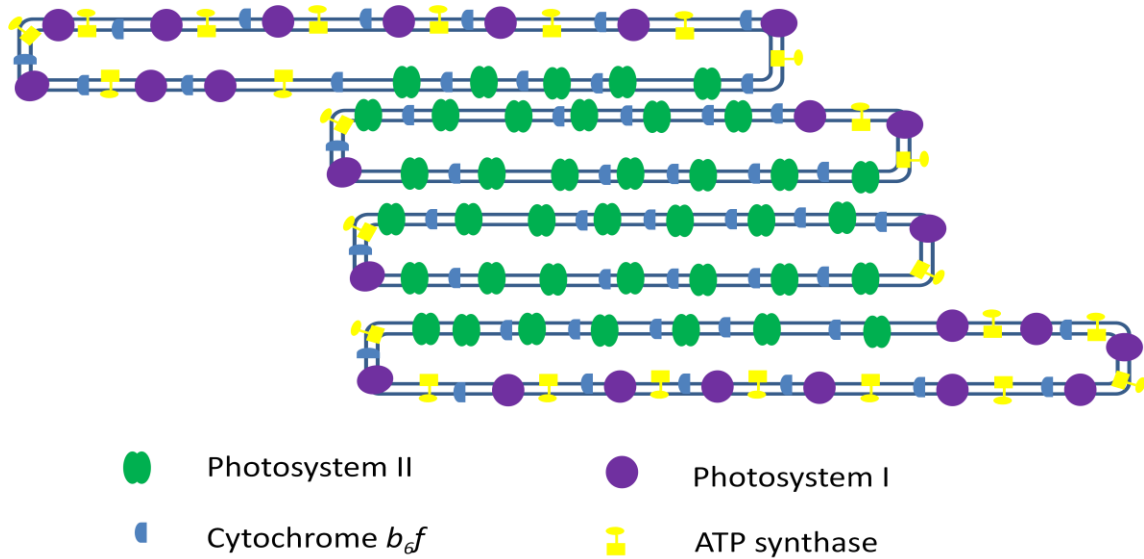


Figure 2 Lateral heterogeneity of thylakoid membrane complexes.

PSI and ATP synthase are almost exclusively distributed in unstacked thylakoid membrane (stroma lamellae), whereas PSII is localized primarily in the grana region, whereas Cytochrome *b₆f* complex is more evenly distributed. Modified from Buchanan et al., 2002

1.2 The linear electron flow (LEF) and cyclic electron flow (CEF)

The four major photocomplexes together with serial electron carriers comprise the pathway for linear electron flow (LEF) which starts at PSII. Upon excitation of the PSII reaction center (P680) by light, electrons are released from P680 to pheophytin which transfers electrons to a tightly bound plastoquinone (PQ) Q_A , and further transferred to another loosely bound plastoquinone molecule Q_B to produce fully reduced Q_B^{2-} . The oxidized P680 will be re-reduced by electrons generated by the splitting of H_2O . During this procedure, oxygen and protons are released into the lumen. Q_B^{2-} turns into plastoquinol (PQH_2), Q_BH_2 , by taking up two protons from the stroma side of the thylakoid membrane. This mobile electron carrier then transfers the electrons to Cyt *b₆f* and releases the protons into the lumen. Subsequently, the electrons are transferred to luminal plastocyanin (PC), which is a small soluble electron carrier, as the electron acceptor of PC, contains chlorophylls of its own and is capable to be excited by light similarly to PSII and transfer electron to ferredoxin (Fd) leaving an electron gap that can be filled by electron transferred from PC. Finally, Fd transfer electrons through the ferredoxin-NADP⁺ reductase (FNR) to NADP⁺, generating NADPH. Consequently, a proton gradient is generated which promotes the synthesis of ATP via the ATP synthase using ADP and P_i (Figure 3).

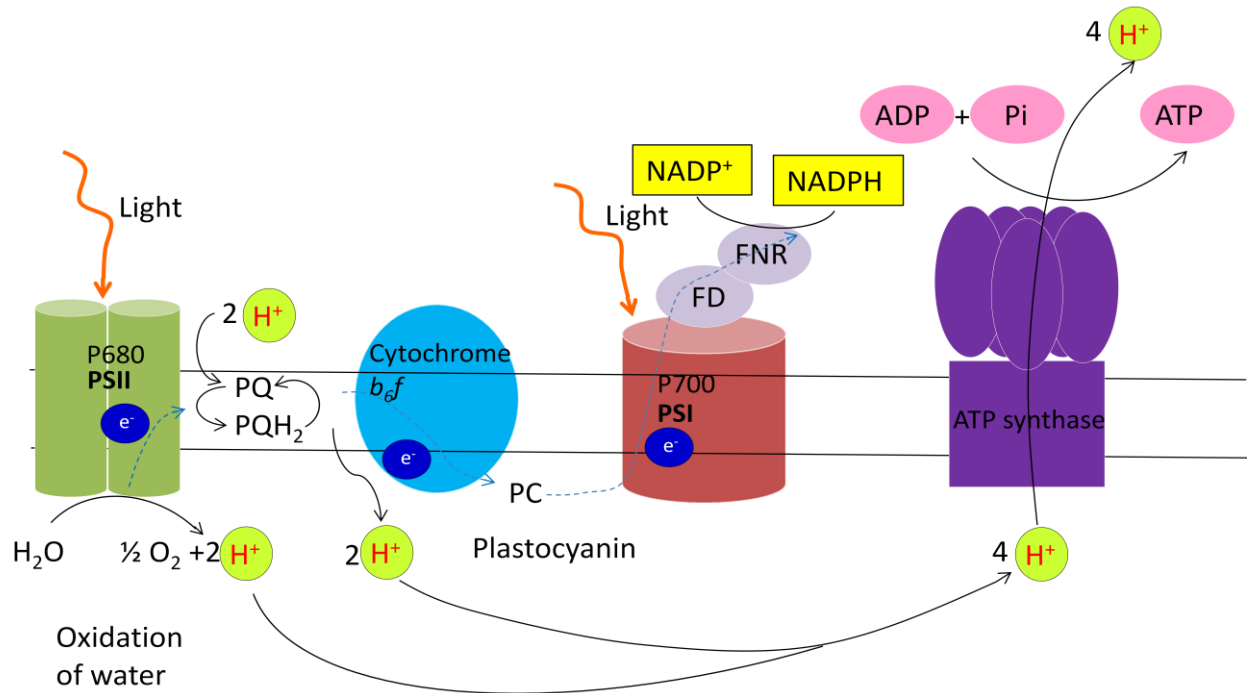


Figure 3 Scheme of linear electron flow (LEF).

Photosystem I (PSI, P700); photosystem II (PSII, P680); oxidized/reduced plastoquinone (PQ/PQH₂); plastocyanin (PC); ferredoxin (Fd); ferredoxin-NADPH-oxidoreductase (FNR); Modified from Buchanan et al., 2002

Alternatively, plants can perform cyclic electron flow (CEF), which is driven by PSI alone and produces exclusively ATP. CEF involves all the components in LEF and electron transfer from PSII (P700) to Fd. However, CEF reinjects electrons to PQ which can be mediated via two pathways: the NADH dehydrogenase-like complex (NDH)-dependent pathway (NDH-CEF) (Peng et al., 2011) and a second pathway which is sensitive to antimycin and depends on the Cyt b_6/f complex using a Q-cycle-derived mechanism (AA-sensitive CEF) (Joliot and Joliot, 2006). In the first pathway, Fd transfers electrons to PQ through NDH whereas the second route is carried out through a ferredoxin-plastoquinone reductase (FQR). Additionally, two components PGRL1 and PGR5 were described to be involved in the AA-sensitive CEF and both of them are found in PSI preparations and interacting with each other (DalCorso et al., 2008; Munekage et al., 2002). Recent findings indicate that PGRL1 is actually the elusive FQR enzyme based on *in vitro* enzyme activity (donation and acceptance properties for electrons), interaction with Cyt b_6/f and other biochemical evidences (Hertle et al., 2013). Since the Calvin-Benson cycle requires an optimal ratio of ATP to NADPH ideally 3:2 and LEF solely cannot accomplish this, CEF is

regarded as an option to compensate the too low levels of ATP generated by LEF (Eberhard et al., 2008) especially under high light or other stress conditions (Johnson, 2011).

1.3 Adaptation to light changes

Light environment can vary in intensity and quantity in time ranges of seconds, minutes up to hours, days and seasons and these variations affect the efficiency of photosynthesis. Many mechanisms are evolved by plants to counteract such changing conditions: nonphotochemical quenching (NPQ) dissipate excess light energy as heat under high light (Horton and Hague, 1988); D1 turnover serve as PSII self repair cycle (Vasilikiotis and Melis, 1994); state transitions readjust the size of two photosystems when they are differentially excited by changes of light qualities normally under weak light (Allen and Forsberg, 2001); long term response (LTR) readjust the stoichiometry of the photosystems under long time change of light quality (Bailey et al., 2004; Bailey et al., 2001; Fey et al., 2005b; Pfannschmidt et al., 2003).

1.3.1 Nonphotochemical quenching (NPQ)

Excess absorption of light energy leads to increased production of harmful reactive oxygen species as side products of photosynthesis which cause pigments bleaching or death in extreme cases. To minimize the damage, plants evolved a series mechanism to balance the absorption and utilization of light energy (Muller et al., 2001). When light energy exceeds the capacity of plant for carbon fixation, non-photochemical quenching (NPQ) processes will occur and dissipate excess energy as heat resulting in decreased chlorophyll fluorescence (fluorescence quenching) (Horton and Hague, 1988). This process is named corresponding to photochemical quenching (qP) which refers to fluorescence quenching due to the photochemical charge separation in the PSII reaction center (Horton and Ruban, 2005). NPQ can be subdivided into three different components according to different response to inhibitors and different relaxation kinetics (Horton and Hague, 1988). The primary quenching component is the de-excitation quenching or high-state quenching (qE) which is regulated by pH gradient across the thylakoid membrane and it is reversible. Moreover, the qE component acts very fast to changes of light condition (seconds to minutes) and can quench up to 80% of the singlet Chl which has the possibility to form triplet Chl and produce damaging singlet oxygen and other highly reactive species (Bassi and Caffarri, 2000; DemmigAdams et al., 1996). The Xanthophyll cycle which converts violaxanthin to zeaxanthin and the PSII antenna protein PsbS are both necessary for this quenching mechanism.

The second component, qT , is due to state transition, a second mechanism allows for the relocation of LHCII between the two photosystems PSII and PSI (Allen and Forsberg, 2001; Haldrup et al., 2001). Compared to qE , qT is slower and unlikely to significantly contribute to photoprotection during exposure to high light. However, this process represents an important acclimation response under weak light conditions (Mullineaux and Rausch, 2005) (see chapter 1.3.3). The third NPQ component refers to photoinhibition and therefore is called qI . It is the slowest quenching process and occurs when qE quenching process becomes either irreversible or slowly reversible, e.g. under strong high light or prolonged stress conditions where the protective capacity of qE has been exceeded. Overall, qI is not well characterized so far (Demmig-Adams et al., 1996; Horton and Hague, 1988; Muller et al., 2001).

1.3.2 D1 turnover and PSII repair

To compensate photoinhibition, which represents the damage of PSII during excess light exposure, plant also developed a sophisticated D1 repair cycle (Kruse, 2001). PSII is a specialized water-to-plastoquinone oxidoreductase, which can extract electrons and protons from water and transfer the electron to plastoquinone. The oxidation of water is a very strong reaction and causes irreversible photodamage to PSII especially the reaction center protein D1. In order to deal with this, photosynthesis has evolved a highly specialized repair mechanism to replace the damaged D1 (D1 turnover) and reassemble PSII (Vasilikiotis and Melis, 1994). Under high irradiance stress, the enhanced turnover of D1 is accompanied by lowered amount of PSI and increased accumulation of PSII with photoinactivated reaction center where damaged D1 is degraded and replaced (Aro et al., 2005; Fristedt et al., 2009; Vasilikiotis and Melis, 1994). Initially, D1 phosphorylation was suggested as a marker for PSII migration from grana to stroma lamellae where D1 was dephosphorylated and damaged PSII was reassembled with newly synthesized D1 (Aro et al., 1993). However, the *stn8* mutant which was devoid of PSII core and D1 phosphorylation, employed normal D1 turnover (Bonardi et al., 2005). However, using feasible high light, Tikkanen et al. (2008) could show that degradation of D1 was retarded in *stn8* mutant and it was caused by impaired PSII disassembly of PSII. More recent results further confirmed that in *stn8* mutant, D1 degradation was delayed but the reasons resided in changes of thylakoids ultrastructure and hindered relocation of the FtsH protease from grana to stroma lamellae (Fristedt et al., 2009).

1.3.3 State transitions

1.3.3.1 Different light absorption of PSI and PSII

Each photosystem (PSI and PSII) consists of an array of light-harvesting antennae and a photochemical reaction center. The antennas of PSI and PSII have a different protein and pigment composition and therefore the two photosystems display distinct light absorption properties. PSI and PSII act in series and while PSI can absorb wavelengths longer than 680 nm, PSII is poorly excited by far red light (Taiz and Zeiger, 2010). Due to the connection in linear electron transport, the two photosystems have to work at the same rate to reach efficient energy conversion. However, cyclic electron flow, which is driven by PSI alone, requires a proportional rate of primary photochemistry between these two photosystems (Allen, 1984a, b; Arnon et al., 1954; Finazzi et al., 2002). Moreover, the incident light quality and quantity keeps changing and certain habitats show altered spectral composition, like water allows the passing of short wavelength and shadowing by other plants enriches the light spectrum by far red light, thus causing preferentially excitation of one photosystem over the other. To achieve optimal photosynthetic efficiency, it is necessary for the plant to adjust the light-absorption ability of the two photosystems. Therefore, plants and algae evolved two mechanisms to cope with such alteration in light composition and rebalance energy distribution between PSI and PSII, state transitions and the adjustment of photosystem stoichiometry composition (long term response).

1.3.3.2 Simplified model of state transitions

State transitions, which were found 40 years ago, involves reversible association of LHCII with PSII and PSI and can occur in a time scale of minutes (Bonavent and Myers, 1969; Murata, 1969). This process is suggested to be regulated by the redox state of the plastoquinone pool (PQ pool) (Allen et al., 1981; Vener et al., 1995; Vener et al., 1997) When the PQ pool becomes reduced under light conditions that favor PSII excitation, the PQH₂ binds to the Q_o site of the Cyt *b₆f* complex leading to the activation of the LHCII kinase which subsequently phosphorylates LHCII (pLHCII) and facilitates its movement to PSI (Allen, 1983, 1992; Michel et al., 1991; Telfer et al., 1983). Thus, the capacity of PSI to absorb light energy is increased and this state is called state 2. Light conditions that favor state 2 include low light (LL) and light of wavelengths that preferentially excite PSII (e.g. red light). On the contrary, when plants or algae are exposed to light conditions that preferentially excite PSII, the PQ pool becomes oxidized, leading to the

deactivation of the kinase. In this case, the LHCII phosphatase dephosphorylates pLHCII and drives its dissociation from PSI and re-binding to PSII (Bennett, 1983). This state is called state 1 and induced by several light conditions, e.g. darkness (D), high light (HL) and light with wavelengths that preferentially excite PSI (e.g. far red light, FR) (Figure 4). However, new results based on thylakoids fractionation show that two photosystems may share the same LHCII antenna through a subtle mechanism in grana margins to complete redistribution of excitation energy. This is challenging the traditional view, which suggests energy redistribution depends on LHCII migration upon phosphorylation or dephosphorylation during state transitions (Tikkanen et al., 2008b).

In other words, light intensity also exerts effects on the redox state of the PQ pool leading to alteration in LHCII phosphorylation and state transition. Dark conditions result in oxidized PQ pool and state 1 whereas low light induce more phosphorylation of LHCII being considerate as state-2 condition (Bonardi et al., 2005). However, recent findings reveal that reversible phosphorylation caused by changes of light intensities does not result in different excitation of two photosystems, i.e. the two photosystems remains equally excited irrespective of the extent of LHCII phosphorylation (Tikkanen et al., 2010). In the case of high light, the PQ pool is rather reduced but the LHCII is actually dephosphorylated and not attached to PSI, displaying a state1-like situation. Most likely, the signal from stromal ferredoxin-thioredoxin system deactivates the LHCII kinase (Grieco et al., 2012).

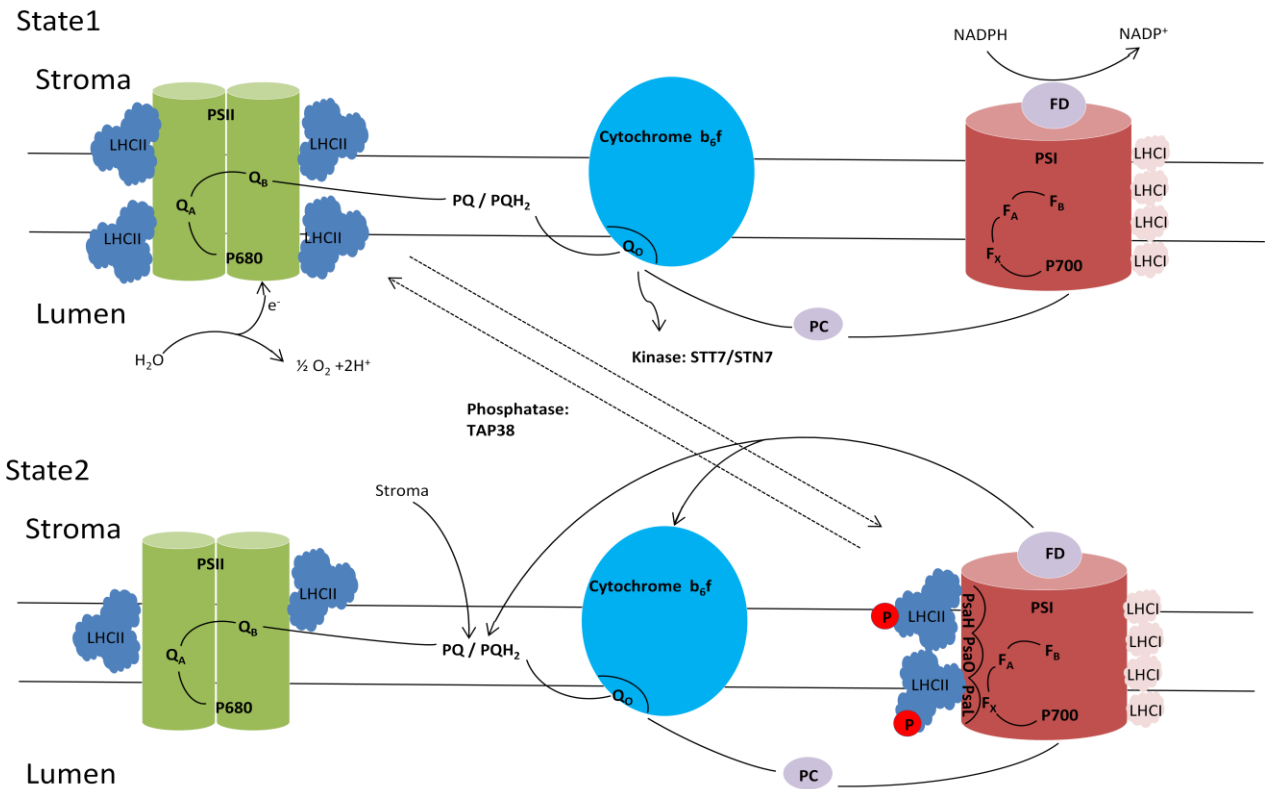


Figure 4 State transition models.

In case the light favors the excitation of PSII, the PQ pool becomes reduced. This leads to the binding of PQH₂ to the Q_o site of the Cytochrome *b₆f* complex. Thereby the STT7/STN7 kinase is activated which then phosphorylates the LHCII. The phosphorylated versions of the antenna subsequently disassociate from PSII and attach to PSI on the side of PsaH, PsaO and PsaF opposing the LHCI belt. This state is called state 2. If PSI is preferentially excited, the PQ pool will be oxidized leading to the opposite result: the kinase cannot be activated and the pLHCII will be dephosphorylated by the LHCII phosphatase TAP38 in higher plant, and then move back to PSII. This state is called state 1. Red circles with a “P” letter indicate phosphorylation effects. Modified from Lemeille and Rochaix (2010)

1.3.3.3 Remodeling of the two photosystems during state transitions

In plants, the PSII core complex is a dimer (C₂) and each core complex is composed of the D1, D2, CP47 and CP43 proteins. The peripheral PSII antenna (light harvesting complex of PSII, LHCII) is comprised of six pigment binding proteins, Lhcb1-6. Out of these, Lhcb1-3 are the major (most abundant) proteins, that form homo- and hetero-trimers (Jansson, 1999). The minor LHCII proteins Lhcb4 (CP29), Lhcb5 (CP26), and Lhcb6 (CP24) are present as monomers. In *Chlamydomonas reinhardtii* (*C. reinhardtii*), there are four types of major LHCI (type I-IV) and

two types of minor LHCII, CP29 and CP 26. C₂ is associated strongly with two copies of CP29, CP26 and LHCII at each side of the dimer to form the C₂S₂ supercomplex in spinach (Boekema et al., 1995) and *C. reinhardtii* (Nield et al., 2000). In higher plants, further two copies each of CP24 and LHCII trimer attach to each border of C₂S₂ with medium strength (M-trimer), forming the C₂S₂M₂ supercomplex. Additional LHCII are able to loosely associate with this large supercomplex, C₂S₂M₂, hence they are called L-trimers (Dekker and Boekema, 2005). In state 2, the residues of Thr-27 of the major LHCII (Lhcb1 and Lhcb2) and Thr-7 of the minor LHCII, CP29, are commonly phosphorylated (Hansson and Vener, 2003; Michel et al., 1991). Phosphorylated LHCII are predominantly found in stroma lamellae where PSI is located; on the contrary, nonphosphorylated LHCII preferentially located to grana (Andersson et al., 1982; Bassi et al., 1988). Takahashi et al. (2006) identified CP29, CP26 and major LHCII in isolated PSI-LHCI-LHCII supercomplexes in *C. reinhardtii*. These indicate that migration of LHCII during state transitions is caused by reversible phosphorylation (Black et al., 1986; Larsson et al., 1983). The M trimer is suggested to migrate between PSII and PSI in state transitions as shown by reduced amounts of C₂S₂M₂ in plants adapted to state 2 (Kouril et al., 2005). Furthermore, when the attachment of the M trimer to PSII is decreased state transitions are concomitantly increased (Kovacs et al., 2006).

Recently, remodeling of such PSII supercomplexes was indicated to be part of state transitions in *C. reinhardtii* (Iwai et al., 2008). The PSII supercomplex remodeling involves reversible phosphorylation of PSII core proteins precedes and facilitates state transitions. Furthermore, in the mutants lacking the Psb27 protein, a stabilizer of PSII, state transitions are accelerated (Dietzel et al., 2011). In plants, these supercomplexes are also found in various composition orders in the grana membranes (Dekker and Boekema, 2005). *A. thaliana* mutants deficient in Lhcb proteins (Lhcb3 or Lhcb4) or the small PSII subunit protein PsbW exhibit accelerated kinetics of state transitions, which might be caused by changes of the LHCII structure and/or PSII supercomplex formation (Caffarri et al., 2009). The depletion of TSP9, a small intrinsically unstructured and thylakoid-soluble protein, changes the stability and organization of PSII and further reduces the ability of state transitions in *A. thaliana*. Therefore TSP9 phosphorylation is suggested to facilitate the dissociation of LHCII from PSII (Fristedt et al., 2009).

The redistribution of LHCII between the two photosystems is suggested to be caused by an altered molecular affinity of phosphorylated or nonphosphorylated forms of LHCII trimers for

PSI or PSII or by generating of more grana margins through microstructure rearrangement of the thylakoid membrane (Allen and Forsberg, 2001; Barber, 1982; Bennett, 1983).

PSI is present as a monomer located in the stroma lamellae, and its core consists of at least 14 proteins named PsaA-B, PsaN, and PsaO (Scheller et al., 2001). Light harvesting complexes of PSI (LHCI) are associated with PsaJ/G/F proteins, leaving PsaH/L/O subunits on the opposite side uncovered (Ben-Shem et al., 2003). And these accessible subunits are supposed to be the docking site for mobile LHCII in state 2. In mutants lacking the PsaH or PsaL protein, state transitions are reduced to 20% or 30% of WT level, respectively, even though STT7/STN7 kinase activity and LHCII composition are not affected. LHCII becomes phosphorylated but similar fluorescence signatures during both state 1 and state 2 suggests that LHCII is still attached to PSII in state 2 in those mutants (Lunde et al., 2000). Moreover, a mutant lacking PsaO also shows 50% reduction in state transitions when PsaH/L are not affected (Jensen et al., 2004). However, loss of PsaH or PsaL results in 80% - 90% reduction in PsaO suggesting that the involvement of PsaH or PsaL in state transitions could be indirect (Jensen et al., 2004). In absence of the docking site, a large number of phosphorylated LHCII (pLHCII) remained attached to PSII in state 2. In supportive of this, electron microscopic studies revealed that the potential docking site of LHCII on PSI are associated with LHCII trimer and possibly some minor LHCII in *C. reinhardtii* (Kouřil et al., 2005). Also, more major LHCII proteins were cross linked to PSI subunits PsaH/L under state 2 compared to state 1 in *A. thaliana* (Zhang and Scheller, 2004).

A model was proposed by Minagawa et al., (2011) for the molecular remodeling of photosystems during state transitions in *C. reinhardtii*: C₂S₂ supercomplexes can form megacomplexes by the linkage of LHCII. When the major LHCII becomes phosphorylated, the megacomplex disassembles into supercomplexes, which subsequently separate from the major LHCII and minor LHCII upon phosphorylation of the minor LHCII and core proteins. Several phosphorylated major and minor LHCII then accumulate to aggregated structures which were shown to be more efficient in dissipating energy than the monomeric form (Iwai et al., 2008). Considering the long migration distance between PSII (localized in grana) and PSI (localized in the stroma lamellae), this aggregated form is advantageous to quench excess energy. And the aggregates were observed to be present substantially in the grana and stroma lamellae regions. Some of these aggregates were shown to migrate to PSI to increase its efficiency, thereby completing the state 1-to-2 transition (Minagawa, 2011) (Figure 5).

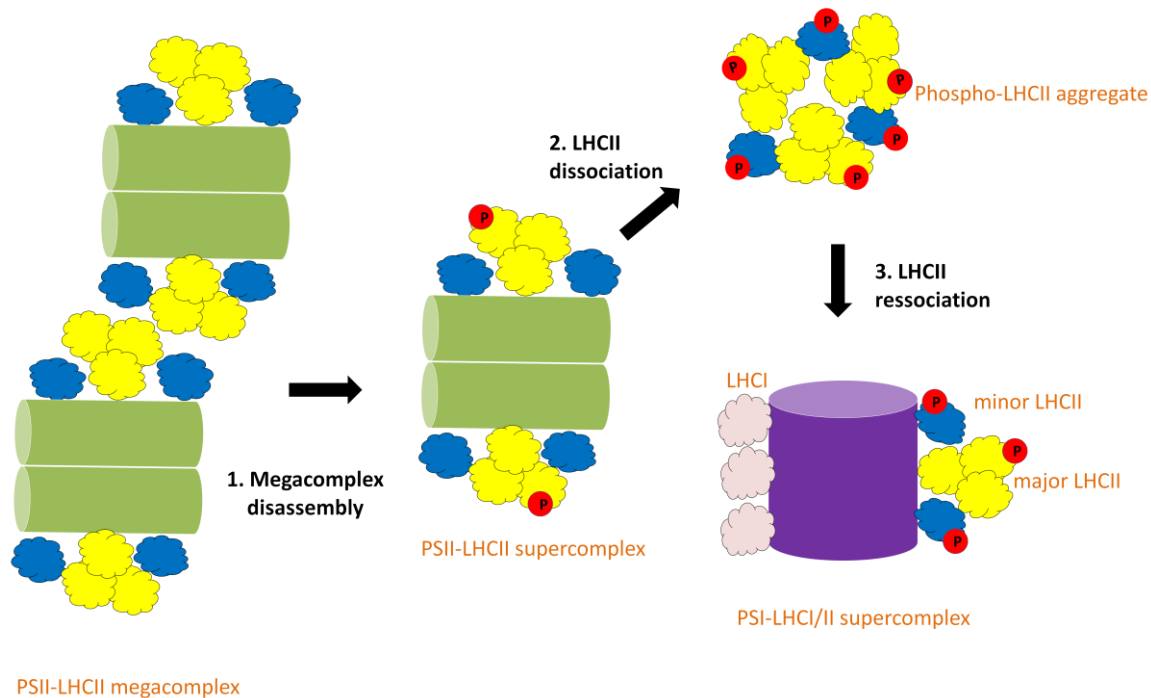


Figure 5 Scheme of PSI and PSII remodeling during state 1-to-2 transition.

Upon phosphorylation of the major LHCII, the megacomplex of PSII disassembles into supercomplexes. (2) Phosphorylation of minor LHCII (CP26 and CP29) and PSII core proteins promote the dissociation of LHCII trimers and minor LHCII from the PSII core complex. The pLHCII complexes tend to aggregate together. (3) Binding of some LHCII (both major and minor) to PSI complete the transition from state 1 to state 2. PSII is indicated by double-column of light-green color; PSI is indicated by a single column of purple color; LHCII trimer are depicted as yellow clouds; minor LHCII are depicted as blue clouds; LHCI is depicted as light-purple cloud; red circles with a "P" letter indicate phosphorylation effects. Redrawn from Minagawa et al., (2011)

1.3.3.4 LHCII kinase STT7/STN7

The identification of kinases involved in state transitions was not successful until ten years ago. The first identified kinase involved in state transitions was the thylakoid associated kinase 1 (TAK1), which interacts with the Cyt *b₆f* complex and LHCII according to co-immunoprecipitation (CoIP) experiments. It is well known that the Cyt *b₆f* complex plays a crucial role in the state transition by activating the kinase (Wollman and Lemaire, 1988). The *TAK1* antisense lines with lower amounts of TAK1 protein relative to WT are impaired in state transitions and have concomitantly lower amounts of pLHCII in state 2 relative to wild type (WT) (Snyders and Kohorn, 2001). Indeed, TAK1s were shown to be phosphorylated and two

additional TAK proteins, TAK2 and TAK3 were identified and expected to phosphorylate TAK1, suggesting a kinase cascade that controls LHCII phosphorylation and regulates state transition (Snyders and Kohorn, 1999). However, the chloroplast locations of TAK2 and TAK3 could not be reproduced (Schliebner et al., 2008).

Later, a serine-threonine protein kinase, STT7, which mediates state transitions in *C. reinhardtii* was identified by screening for mutants defective in state transitions using fluorescence video imaging. The *stt7* mutant showed an unchanged fluorescence signature and constant phosphorylation level of LHCII during state transitions (Depege et al., 2003). STT7 was shown to interact with the Cyt *b₆f* complex (especially the Rieske protein), LHCII and PSI by CoIP and sucrose gradient ultracentrifugation both in state 1 and state 2. In addition the interaction with CP29 was exclusively detected under state 2 condition (Lemeille et al., 2009). Using tagged lines of *STT7* the topology was studied which demonstrated that the transmembrane domain separates the N-terminus in the lumen from its C-terminus in the stroma (Depege et al., 2003). Furthermore, there are two Cysteine residues Cys⁶⁸ and Cys⁷³ in the N-terminal region which are conserved between STT7 and STN7 (the land plant variant of STT7), and are essential for STT7/STN7 activity (Depege et al., 2003; Lemeille et al., 2009; Wunder et al., 2013). The amount of STT7/STN7 becomes decreased under prolonged state1 and HL conditions but the degradation could be prevented by Cysteine proteases inhibitors. Interestingly, STT7 itself seems to be phosphorylated as shown by intestinal phosphatase (CIP) treatment, after which the migration pattern of this protein is changed (Depege et al., 2003). This observation was confirmed by Mass Spectrometry (MS) analysis which demonstrated that the Ser⁵³³ site is exclusively phosphorylated during state 1 to state 2 transition in dependence of STT7 itself (Lemeille et al., 2010). However, Ser⁵³³ is not conserved in STN7 and its phosphorylation is not crucial for state transition and degradation/accumulations for STT7 (Lemeille et al., 2010). STT7-dependent phosphorylation of CP29 was also proved to be essential for state transitions (Tokutsu et al. 2009; Lemeille et al. 2010).

The ortholog of STT7, STN7 was confirmed to have the same function as STT7 in *A. thaliana* (Bellafiore et al., 2005). The state transitions were abolished in *stn7* mutants as shown by fluorescence measurement. Moreover, the STN7 function in LHCII phosphorylation was confirmed indirectly *in vitro*. Also, STN7 is localized in the thylakoid membrane and is able to undergo autophosphorylation (Bellafiore et al., 2005). Besides the homology with STT7 in its kinase domain and the Cysteine-motif at the N-terminus, STN7 contains four unique

phosphorylation sites (Ser⁵²⁶, Thr⁵³⁷, Thr⁵³⁹ and Thr⁵⁴¹) at the C-terminus and two additional Cysteine residues in the catalytic domain on the stromal side (Puthiyaveetil, 2011; Reiland et al., 2009). Like in the case of STT7, the phosphorylation sites of STN7 are demonstrated not to be crucial for state transitions but may play a role in its turnover (Willig et al., 2011). In WT and the *STN-4A* mutant, in which these four phosphorylation sites are substituted by Alanine to prevent phosphorylation, the amount of STN7 decreases when *A. thaliana* plants are shifted from state 2 to state 1. Whereas, *STN-4D* mutants, in which these phosphorylation sites are changed to Aspartic acid to mimic permanent phosphorylation, show very stable STN7 levels irrespective of the light condition. STN8, CSK and TAP38 were tested to be irrelevant for the phosphorylation or dephosphorylation of STN7 (Willig et al., 2011). STN7-dependent phosphorylation of CP29 was identified to be essential for PSII disassembly under high-light condition (Fristedt and Vener, 2011; Lemeille et al., 2010; Tokutsu et al., 2009). Furthermore, TSP9 is also phosphorylated by STN7 as shown by *in vitro* phosphorylation experiment and phosphorylation of TSP9 was indicated to facilitate the dissociation of LHCII from PSII (Fristedt et al., 2009).

Under low light, STT7/STN7 is activated by PQH₂ via the Cyt *b₆f* complex. Basically, binding of PQH₂ to the Q_o site of Cyt *b₆f* changes the position of Rieske protein from distal position to a proximal position. This position conversion leads to a conformational change of the Cyt *b₆f* complex which further mediates the activation of the kinase (Finazzi et al., 2001; Zito et al., 1999). On the contrary, under high light the PQ pool is reduced, but the kinase is deactivated via the thioredoxin system. The stromal thioredoxin signal is supposed to be transduced by proteins like CcdA and Hcf164 to the conserved two Cysteines on the luminal side thereby deactivating STN7 (Depege et al., 2003). However, a new model was proposed for STN7 regulation on the basis of the discovery that two additional conserved Cysteines in the catalytic domain on the stromal side might act as an additional redox sensor (Puthiyaveetil, 2011). Under low light conditions, PQH₂ activates STN7 via reducing the disulfide bond formed between the two Cysteines on the luminal side. To this end, PQH₂ has to bind to the Q_o site of Cyt *b₆f* and reduce the disulfide bond directly or indirectly through Rieske protein. Under high light, the reduction of the stromal exposed two conserved Cysteines by thioredoxin could be responsible for the deactivation of the kinase (Puthiyaveetil, 2011). Since STT7 does not contain the same stromal Cysteine motif, it might be either not inhibited by thioredoxin under highlight or inhibited through Cysteine residues located somewhere else in the protein, e.g. the two closely placed Cysteines in the middle of the kinase domain (Puthiyaveetil, 2011).

1.3.3.5 LHCII phosphatase TAP38/ PPH1

Under light conditions that preferentially excite PSI (e.g. far red light), the PQ pool becomes oxidized leading to the inactivation of STN7. The pLHCII associated with PSI becomes then dephosphorylated by a LHCII phosphatase resulting in the dissociation of the mobile LHCII pool from PSI. Early findings suggested a PP2C type phosphatase that can not be inhibited by microcystin and okadaic acid but depends on the presence of divalent cations to be responsible for LHCII dephosphorylation (Cohen, 1989; Hammer et al., 1995; Sun et al., 1989). Only recently, this protein phosphatase was identified by two independent groups, and named TAP38/PPH1 (Pribil et al., 2010; Shapiguzov et al., 2010). The *tap38* mutant and *oeTAP38* (overexpression line of *TAP38*) are both impaired in state transitions as monitored by PAM fluorometry and the recording of 77K fluorescence emission spectra. Furthermore, the level of pLHCII under all light conditions seems to be inversely proportional to the amount of the TAP38 protein and the intensity of the PSI-LHCI-LHCII band in BN-PAGE (Pribil et al., 2010). Although recombinant TAP38 protein is able to dephosphorylate pLHCII (Pribil et al., 2010), additional support for direct dephosphorylation of pLHCII by TAP38 was not available. TAP38 is predicted to contain a chloroplast transit peptide (cTP) at its N-terminus, a transmembrane domain near its C-terminal end and a PP₂C (phosphatase 2C) signature near the N-terminus. Fractionation experiment demonstrated that TAP38/PPH1 is localized in thylakoid membrane, especially the stroma lamellae region (Pribil et al., 2010; Shapiguzov et al., 2010). The constant expression levels of TAP38 under far-red light and low light is an indication for TAP38 not to be regulated at the protein levels, in contrast to STN7 (Bellafiore et al., 2005; Lemeille et al., 2009; Pribil et al., 2010; Shapiguzov et al., 2010; Wunder et al., 2013). Previous results derived from *in vitro* experiment further suggest that the LHCII phosphatase activity is redox independent (Silverstein et al., 1993).

1.3.3.6 Various environmental factors that involved in state transition

Besides light, various environmental factors can affect state transitions (e.g. high and low temperature and oxygen concentration). Moderate heat in the dark for a short term is suggested to induce transition from state 1 to state 2 accompanied by phosphorylation of LHCII and increase of PSI emission in 77 K measurements (Nellaepalli et al., 2011). These alterations of fluorescence emission and LHCII phosphorylation could not be observed in the *stn7* mutant. Similarly, no state transitions were observed in cold-adapted plants (10 °C) under low light as

monitored by 77 K measurement. Phosphorylation of LHCII is detectable both under dark and low light but to a less extent under normal growth temperature, suggesting a reduced electron transport rate in cold (Nellaepalli et al., 2011). Nellaepalli et al. (2011) also suggests that dark anaerobiosis condition induces nonphotochemical reduction of the PQ pool by generating more reducing equivalents (NADPH) which leads to transition from state 1 to state 2 mediated by NDH activity. This conclusion is based on the observation that LHCII phosphorylation and absorption cross-section of PSI are increased in WT but abolished in the *crr2-2* mutant (NDH mutant) (Nellaepalli et al., 2012).

LHCII plays an important role in stability of the thylakoid membrane, and its migration during state transitions is suggested to cause structural changes of the thylakoid membrane (Dekker and Boekema, 2005). This notion is supported by the finding that isolated thylakoids undergo large-scale structural change when they are subjected to salt solution (mimic the state 1 to state 2 transition) (Arvidsson and Sundby, 1999; Ryrie, 1983). In line with this, thylakoid membrane was found to undergo demodulation during state transitions. Specifically, upon transition from state 1 to state 2, the lateral and/or vertical connections around the highly curved margins area of thylakoid membrane were broken and subsequently the demodulation spreads over the whole thylakoid membrane system. The rearrangement resulted in increased chloroplast diameter and unstacked grana leading to a disordered and undulating morphology of the membrane network (Chuartzman et al., 2008).

Apparently electron flow switches from LEF to CEF in *C. reinhardtii* in state 2 given that 80% of LHCII are mobile (Delosme et al., 1996). This hypothesis is supported by the finding that the PSII inhibitor DCMU which blocks the plastoquinone binding site of photosystem II, only disturbs the reduction of the Cyt *b₆f* complex in state 1 but not in state 2 (Finazzi et al., 1999). This is consistent with the observation of that CEF acts independently from PSII activity. Since CEF can increase the ATP/NADPH ratio, depletion of ATP is suggested to induce state 2 (Bulte et al., 1990). However, this is not the case for *A. thaliana*, because only 20 - 25% LHCII migrate during state transition (Allen, 1996).

1.3.4 Long term response (LTR)

Longer lasting changes in light quality are counterbalanced by the long term response (LTR), a process which balances the energy absorption by changing the stoichiometry and/or the antenna size of the photosystems (Bailey et al., 2004; Bailey et al., 2001; Fey et al., 2005a;

Pfannschmidt, 2003). This process involves degradation and assembly of the photosystems and regulatory modifications in photosystem gene expression (Meurer et al., 1998; Walters, 2005). It was shown that de novo synthesis of chlorophyll a and its binding proteins, as well as of core proteins of photosystems encoded in chloroplast were controlled at the transcriptional level by the redox state of PQ pool ((Murakami et al., 1997; Pfannschmidt et al., 1999). This was supported by subsequent studies (Kovacs et al., 2000). Since many photosynthetic genes are encoded in the nucleus, the signal from the PQ pool has to be transmitted within and outside of the chloroplast under a special regulation mechanism (Dietzel et al., 2008; Nott et al., 2006). However, recent discoveries suggest that *A. thaliana* adjusts its photosystem stoichiometry mainly by modifying the amount of PSI complexes (Fey et al., 2005; Pesaresi et al., 2009). The ratio of chlorophyll a to chlorophyll b (Chl a/b) and steady fluorescence to maximum fluorescence (F_s/F_m) are indicators for such changes in photosystem stoichiometry (Bailey et al., 2001; Dietzel et al., 2008).

The Chloroplast sensor kinase (CSK) was suggested to adjust photosystem stoichiometry by sensing the oxidized form of PQ and to undergo autophosphorylation induced by an oxidized PQ pool (Puthiyaveetil et al., 2008). Loss of CSK was demonstrated to affect transcription of photosynthetic plastid-encoded genes and adjustment of the PSII/PSI ratio. In more detail, the transcription of plastid encoded PSI subunits cannot be decreased during state 1 condition. Plastid transcription kinase (PTK) and Chloroplast sigma factors were found to be interaction partners of CSK, involved in chloroplast gene regulation. Therefore, a phosphorylation cascade was postulated to regulate photosystem stoichiometry adjustment (Puthiyaveetil et al., 2012).

Another kinase reported to be involved in LTR is STN7 which is described as the LHCII kinase involved in state transition (Bonardi et al., 2005). While WT showed changes in Chl a/b ratio and the F_s/F_m value when acclimated to either state 1 or state 2, the *stn7* mutant displayed no alterations in these parameters indicating that the *stn7* mutant is impaired in the LTR. However, other mutants defective in state transitions undergo normal LTR, suggesting that these two regulatory pathways are distinct and might diverged downstream of STN7 (Bonardi et al., 2005; Pesaresi et al., 2009). In consistency with that, state transitions are activated by a reduced PQ pool but LTR is induced by an oxidized PQ pool (Puthiyaveetil et al., 2012).

1.4 Reversible phosphorylation in chloroplasts

Reversible phosphorylation can affect the stability, activity or subcellular localization of target proteins, and around one-third of all eukaryotic proteins are supposed to undergo reversible

phosphorylation (Olsen et al., 2006). Besides redox regulation, reversible protein phosphorylation is definitely another key regulation factor for cellular functions and signal transduction in response to environmental changes (Cohen, 2000; Schliebner et al., 2008). A recent proteomic study identified 174 phosphoproteins in *A. thaliana*, and they are predicted to be localized in the chloroplast with high confidence (Reiland et al., 2009). Protein kinases (PKs) and protein phosphatases (PPs) are needed for reversible phosphorylation of proteins. It is estimated that about 3.8% of the nuclear encoded genes code for protein kinases (1050 genes). Since about 2100 genes are supposed to be imported into chloroplast of *A. thaliana*, and 3.8% of them are protein kinases, there should be about 80 kinases present in the chloroplast (Bayer et al., 2012; Richly and Leister, 2004). A complete survey of the *A. thaliana* genome revealed about 220 PPs to exist (Schliebner et al., 2008). Out of these, only 27 PPs were clearly predicted to be localized in the chloroplast and only 9 of them were actually confirmed to do so (Schliebner et al., 2008). Apparently, the numbers of PPs in the chloroplast is much lower than the PKs.

1.4.1 STN8

STN8 is a homolog of STN7, as they share high sequence and structural similarities (Depege et al., 2003). Unlike STN7, STN8 is not required for LHCII phosphorylation and state transitions, but plays an essential role in the phosphorylation of PSII core proteins (Bellafiore et al., 2005; Bonardi et al., 2005). In the *stn8* T-DNA insertion mutant, the phosphorylation levels of PSII subunits (D1, D2, CP43, PsbH) is dramatically reduced compared to WT and *stn7* mutant (Bonardi et al., 2005; Tikkanen et al., 2008a). Notably, in the *stn7 stn8* double mutant, overall thylakoid phosphorylation, including that of PSII and LHCII, is totally abolished, indicating that these two kinases share a certain overlap in their substrates. Although phosphorylation was suggested to influence D1 degradation, thus affecting the repair of PSII under high light, there is actually no difference between *stn8* and WT regarding D1 synthesis and its degradation (Bonardi et al., 2005; Koivuniemi et al., 1995). Depletion of STN8 and consequently reduction in PSII phosphorylation leads to delayed D1 degradation and significant rearrangement of the thylakoid membrane network in the *stn8* mutant (Tikkanen et al., 2008a).

Moreover, the calcium-sensing receptor (CaS) was also identified as a substrate of STN8 (Vainonen et al., 2008). CaS is a 40kD protein localized in the chloroplast and particularly enriched in stroma lamellae. Its phosphorylation level is markedly increased under high light in *A. thaliana*. In *C. reinhardtii*, CaS is essential for the expression of LHCSR3 which plays an

important role in qE quenching under high light; therefore, the *cas* mutant is more sensitive to high light and impaired in PSII recovery (Petroustos et al., 2011). Interestingly, the phosphorylation of CaS depends on calcium availability and is mediated by STN8 whereas its dephosphorylation is supposed to be carried out by TAP38, the major counteractor of STN7 (Pribil et al., 2010; Vainonen et al., 2005).

Recently, MS analyses identified PGRL1, the newly confirmed FQR of cyclic electron flow, as a substrate of STN8, and the *stn8* mutant displayed a faster transition from CEF to LEF during a shift from dark-to-light (Reiland et al., 2011). Reiland et al. (2011) also suggest that the large subunit of RuBisCo (RbcL), CP29 and two unknown proteins are phosphorylated by STN8. This finding was in line with previous results which showed that RbcL and CP29 were phosphorylated (Lemeille et al., 2010; Lohrig et al., 2009). However, CP29 was also indicated to be phosphorylated by STN7 under high light (Fristedt and Vener, 2011). This again supports that STN7 and STN8 have overlapping substrates.

1.4.2 Further chloroplast kinases

Chloroplast casein kinase 2 (cpCK2) originally identified in mustard is localized to the stroma. It has a homolog in *A. thaliana* (At2g23070) which is able to phosphorylate parts of the plastid transcription machinery and RNA binding proteins. The plastid sigma factor AtSIG6 was identified to be its substrate (Ogrzewalla et al., 2002; Salinas et al., 2006). The binding properties of AtSIG6 changed upon phosphorylation leading to differences in gene expression in chloroplasts and to an impaired plant growth (Schweer et al., 2010). Furthermore, CSK was identified as an interaction partner of cpCK2 which provides a link between plastid transcription control and redox sensing (Puthiyaveetil et al., 2010). It seems that cpCK2 is the main kinase for stromal components, as stroma phosphorylation depends equally on ATP and GTP, a co-substrate of CK2, and a large set of phosphoproteins contain a phosphorylation motif specific for cpCK2 (Bayer et al., 2012; Reiland et al., 2009).

1.4.3 PBCP and other phosphatases

Besides TAP38/PPH1 which counteracts predominantly STN7 in reversible protein phosphorylation (Pribil et al., 2010; Shapiguzov et al., 2010), another chloroplast protein phosphatase, PBCP, was identified recently in *A. thaliana* to be responsible for the dephosphorylation of PSII core proteins. In the *pbcP* mutants, the dephosphorylation of PSII core

proteins was deficient under far red light conditions, whereas this phenotype can be reversed by overexpressing PBCP (Samol et al., 2012). Via MS and Western blot analyses, it could be confirmed that the substrates of PBCP significantly overlapped with STN8. Interestingly, overexpression of PBCP resulted in less pLHCII in state 2 and influenced the kinetics of state transitions, suggesting a certain substrate overlap between PBCP and TAP38 (Samol et al., 2012), similar to STN7 and STN8 (Bonardi et al., 2005). Consistent with this, TAP38 also dephosphorylates D1/D2 to certain degree (Pribil et al., 2010).

1.5 Aims of this work

TAP38 and STN7 form an antagonistic pair regarding the reversible phosphorylation of the light harvesting complex of PSII (LHCII) and therefore state transitions (Bellafiore et al., 2005; Pribil et al., 2010; Shapiguzov et al., 2010). The activity and amount of STN7 are both regulated by the redox of state plastoquinone (PQ) pool, while previous findings from *in vitro* dephosphorylation experiments showed that the LHCII phosphatase is insensitive to redox regulation (Bellafiore et al., 2005; Lemeille et al., 2009; Willig et al., 2011; Wunder et al., 2013). However, since its identification no further investigations were done in this direction. Furthermore, it is unclear whether the LHCII phosphatase TAP38 is associated with other proteins or protein complexes and whether TAP38 directly or indirectly dephosphorylates LHCII. Also an involvement of TAP38 in the long term response (LTR) was discussed, as *stn7* mutants are devoid of LTR (Bonardi et al., 2005). As thylakoids kinases and phosphatases show a complicated overlap in substrates and the number of phosphoproteins exceeds that of phosphatase and kinases markedly (Bayer et al., 2012; Reiland et al., 2009; Richly and Leister, 2004; Schliebner et al., 2008), the possibility that TAP38 target other substrates than beyond LHCII is feasible.

To address the TAP38 topology, trypsin digestion and salt extraction experiments were performed. Also, spatial and temporal localization of TAP38 was assayed by approaches of thylakoid fractionation and immunogold labeling. Its sensitivity to redox regulation was studied by different light treatments and via phosphorylation inhibition assays, as well as by TAP38 overexpression in genetic mutant backgrounds with over-reduced PQ pool. Furthermore, lines expressing HA- and GFP- tagged TAP38 were generated and applied in co-immunoprecipitation experiments to identify putative interacting components of TAP38. In order to identify additional putative substrates of TAP38 other than LHCII, double mutants *stn7 oeTAP38* and *tap38-1*

oe*STN7* showing thylakoid hyper- and hypo-phosphorylation were generated and used in 2D-IEF SDS PAGE. As TAP38 is supposed to be the counteracting enzyme of *STN7*, effects of TAP38 on the long term response were analyzed.

2 Materials and Methods

2.1 Plant material

The *A. thaliana* wild type Columbia-0 (Col-0) used in this study as the wild type (WT) was obtained from NASC (Nottingham *Arabidopsis* Stock Centre, accession number N1092). Previously described transgenic lines employed in this study were: *hcf136* (Meurer et al., 1998), *psad1-1* (Ihnatowicz et al., 2004), *psad1d2* (Ihnatowicz et al., 2004), *petc-1* (Maiwald et al., 2003), *psae1-3* (Ihnatowicz et al., 2007), as *LHCB2.1* (Andersson et al., 2003); *chaos* (Klimyuk et al., 1999); *tap38-1* (Pribil et al., 2010), TAP38 overexpressor (oeTAP38) (Pribil et al., 2010) and *stn7* (Bonardi et al., 2005), STN7 overexpressor (oeSTN7) (Wunder et al., 2013). Seeds of TAP38 knock-out line *tap38-3* (GABI_232H12) were obtained from GABI-Kat. This line carries a T-DNA insertion in the Columbia (Col-0) background. Homozygous lines were selected via PCR, Western blotting and PAM measurements (Figure S1). The primers specific for detection of T-DNA insertion were LBgk1 (5'CCCATTTGGACGTGAATGTAGACAC) and TAP38-3s (5'GCATTGCAAGCTGGATCGTTG), and primers for detection of *TAP38* gene were TAP38-3s and TAP38-3as (5'TCATCAACACCCTTCTTTAAC).

2.1.1 Generation of transgenic *A. thaliana* lines expressing GFP-tagged TAP38

To generate a TAP-GFP-line, the native TAP38 sequence was cloned into the plant expression vector pB7YWG2 under Cauliflower Mosaic Virus (CMV) 35s promoter by Gateway Cloning strategy using primers PinFw (5'GGGGACAAGTTTGTACAAAAAAGCAGGCTTCACTGAGTCATGGCGCTTC) and PinRev (5'GGGGACAAGTTTGTACAAAAAAGCTGGGT AAGATAGATGTGAAGACATCCATATGCC). The vector containing green fluorescence protein (GFP) sequence was at the C-terminus of TAP38. GFP construct was introduced into *tap38-3* using floral-dipping technique (Clough and Bent, 1998). Transgenic plants were selected by the Basta herbicide and several independent homozygous T-DNA insertion lines of the T3 generation were obtained. Then the expression of TAP38 fused to GFP was analyzed by Western blotting with a TAP38 antibody and antibody specific for the GFP. The restoration of state transition process was used as an indicator for the expression of functional TAP38 (see PAM measurement).

2.1.2 Generation of transgenic *A. thaliana* lines expressing HA-tagged TAP38

A mutant line expressing TAP38 with a HA-tag fused to its N-terminus was generated in following steps. First a cTP sequence of TAP38 and one copy of the HA sequence (PYDVDPDYA) flanked by the restriction site of BamHI were cloned into pDONOR using the primers: HA1Fw (CACCAGTGCATGGCGCTTCTG) and HA2Rev (GTGGATCCAGCGTAATCTGGAACATCGTATGGGTAAACGGTGACGACCATACGTG). In parallel, the BamHI restriction site was fused to the full CDs of TAP38 without its cTP and introduced into the same vector using the primers HA3Fw (5'GTGGATCCTACCCATACGATGTTCCAGATTACGCTTGCTCCGCGATTGCGATCGAC) and HA4Rev (5'TTAAGATAGATGTGAAGACATCCATATG). After BamHI restriction at these constructs, the two fragments were ligated and inserted into the pB7FWG2 vector which was previously relieved GFP sequence from it. Finally, a construct was obtained containing a cTP, two HA sequence repeats and the mature TAP38 coding sequence fused together. Transformation of TAP38-HA construct into *tap38-3*, BASTA selection and segregation and insertion analysis were performed as described above (see chapter 2.1).

2.2 Growth and light conditions

Plants were grown on soil under controlled conditions in a growth chamber on a 12/12 h day-night regime with 100 $\mu\text{mol photons m}^{-2} \text{s}^{-1}$ at light phase. PSI- and PSII-light were generated as described before with minor modifications (Fey et al., 2005b; Pfannschmidt et al., 2009; Pfannschmidt et al., 1999; Wagner et al., 2008). In detail, PSI light (20 $\mu\text{mol photons m}^{-2} \text{s}^{-1}$) was generated by white fluorescent lamps of Osram (39 W) filtered through two layers of red foil (Lee Filters, transmittance 50% at 650 nm, 027 Medium Red) and PSII light (30 $\mu\text{mol photons m}^{-2} \text{s}^{-1}$) was generated by the same lamp filtered through one layer of orange foil (Lee Filters, transmittance 50% at 560 nm, 405 Orange). Further light conditions were obtained as follows: low light (LL) was provided by cool-white fluorescence strip lamps at an intensity of 50 $\mu\text{mol photons m}^{-2} \text{s}^{-1}$; high light (HL) of 800 $\mu\text{mol photons m}^{-2} \text{s}^{-1}$ was generated by an Osram Powerstar HQIBT-D/400 W lamp; far red light (FR) was emitted by LEDs at an intensity of 3.0 $\mu\text{mol photons m}^{-2} \text{s}^{-1}$. WT, *tap38-1*, *hcf136*, *petc-1*, *psad1d2*, *chaos*, asLHCB2, *psad1-1*, *psae1-3* plants grown on 1 \times MS medium including vitamins (Duchefa[®]) at 50 $\mu\text{mol photons m}^{-2} \text{s}^{-1}$ (Wunder et al., 2013). For all experiments, 4-week-old soil grown plants were used if not indicated otherwise.

2.3 Total protein extraction

Total protein extracts were prepared as described (Haldrup et al., 1999). About 0.1 g of frozen leaf material from 6-week-old *A. thaliana* plant grown on MS plates was homogenized in 200 µl solubilization buffer (100 mM Tris pH 8.0, 50 mM EDTA pH 8.0, 0.25 M NaCl, 1 mM DTT, 0.7% SDS). The homogenate was then heated up to 65 °C for 10 min. Insoluble material was removed by centrifugation at 10000 g for 10 min and the protein concentration in the supernatant was determined by the amido black assay according to (Schaffne and Weissman, 1973).

2.4 Isolation of thylakoid membranes

Thylakoids were isolated based on the protocol of Bassi et al. (1995) with modifications. In brief, leaf material of *A. thaliana* plants was homogenized in ice cold isolation buffer (0.5% milk powder, 0.4 M sorbitol, 0.1 M Tricine-KOH pH 7.8, 20 mM NaF and freshly prepared protease inhibitor [0.2 mM PMSF, 1 mM Benzamidine, 5mM Aminocaproic acid]) and filtered through 2 layers of Mirocloth (Calbiochem). After centrifugation at 1500 g for 10 min at 4 °C the membrane pellet was resuspended in ice cold resuspension buffer (20 mM HEPES-KOH pH 7.5, 10 mM EDTA, 20 mM NaF) supplemented with protease inhibitors. After 10 min of incubation on ice, a centrifugation step was carried out at 10000 g for 10 min at 4 °C. At last, TMK buffer (10 mM Tris-HCl pH 6.8, 10 mM MgCl₂, 20 mM KCl, 20 mM NaF) was used to resuspend the thylakoid pellet and the chlorophyll concentration was determined in aqueous 80% acetone (Lichtenthaler, 1987; Porra, 2002).

2.5 Chloroplast isolation and separation of soluble membrane fraction

Chloroplasts were isolated from plant leaves as described by Aronsson and Jarvis (2002) with modifications. In general, 20 g leaf material was homogenized in 200 ml HB buffer (0.45 M Sorbitol, 20 mM Tricine-KOH pH 8.4, 10 mM EDTA, 10 mM NaHCO₃), filtered through 2 layers Microcloth and centrifuged at 600 g for 6 min. The pellet was resuspended in 0.8 ml RB buffer (0.3 M Sorbitol, 20 mM Tricine-KOH pH 8.4, 2.5 mM EDTA, 5 mM MgCl). In parallel, a Percoll gradient which is comprised of 7.5 ml light layer (40% Percoll, 1xRB) on the top and 3.5 ml of heavy layer (80% Percoll, 1x RB) at the bottom was made. The resuspended pellet was then placed on the top of the Percoll gradient and centrifuged at 6500 g for 20 min with low acceleration and no break. The green band between the two layers was the intact chloroplast. To

obtain membrane and soluble fractions (e.g. thylakoid and stroma fractions), chloroplasts were resuspended in 10 volumes of RB buffer and then mechanically sheared by pushing the samples 20-40 times through a thin needle on ice. After centrifugation for 30 min at 42000 g, 4 °C, the collected supernatant and pellet represented soluble and membrane fractions, respectively. The concentration of the soluble protein was determined using the Bradford Protein Assay (Biorad, Munich, Germany).

2.6 Purification of recombinant His-tagged TAP38 proteins

The coding sequences of STN7 and TAP38 without cTPs were cloned into pProExHTa (STN7) or pET151 vector (TAP38) (Invitrogen) providing an N-terminal-6x His-tag (Invitrogen) for each protein (Pribil et al., 2010; Wunder et al., 2013). Then the recombinant proteins were expressed in 500 ml cultures of the *Escherichia coli* (*E. coli*) strain BL21-CodonPlus® (DE3)-RIPL (Stratagene), as inclusion bodies. The purification of inclusion bodies was performed as described (Wunder et al., 2013) and subsequently recombinant protein was purified under denaturing conditions according to Ni-NTA batch purification procedure (Qiagen).

2.7 Chlorophyll fluorescence analysis

2.7.1 Measurement of standard photosynthetic parameters

After plants were adapted to the dark for 30 min, minimal fluorescence (F_0) was determined. Then white light ($5000 \mu\text{mol photons m}^{-2} \text{s}^{-1}$) were given in pulses (0.8 s) to measure the maximum fluorescence (F_m). In the meanwhile, maximum quantum yield of PSII was calculated according to the ratio ($F_v/F_m = (F_m - F_0)/F_m$). A 10-min actinic light ($40 \mu\text{mol photons m}^{-2} \text{s}^{-1}$) was applied before the steady-state fluorescence (F_s) was measured. F_m' was determined after exposure to further saturation pulses ($0.8 \text{ s}, 5000 \mu\text{mol photons m}^{-2} \text{s}^{-1}$) (Maxwell and Johnson, 2000). At the end, minimal fluorescence of light adapted plants (F_0') as determined after switching off the actinic red light. The light dependence of the photosynthetic parameters, the effective quantum yield of PSII (Φ_{II}), qP or qL, representing the fraction of PSII receptors that remains open or oxidized were calculated according to the following equations: $\Phi_{II} = (F_m' - F_s)/F_m'$, $1 - qP = 1 - (F_m' - F_s)/(F_m' - F_0)$, and $1 - qL = 1 - (F_m' - F_s)F_0/((F_m' - F_0)F_s)$ (Maxwell and Johnson, 2000). Average values are based on measurements of 6 plants.

2.7.2 State Transition measurements via PAM fluorometry

State transitions were measured by pulse-amplitude modulation fluorometry (PAM) as described (Pribil et al., 2010; Ruban and Johnson, 2009). The quenching of chlorophyll fluorescence due to state transitions (qT) was calculated according the equation $qT = (F_m1 - F_m2)/F_m2$ (Jensen et al., 2000).

2.8 Photosynthetic Acclimation Analysis

The development of the long term response (LTR) was monitored on the basis of measurements of steady state fluorescence (F_s) and chlorophyll a/b ratios as described before (Fey et al., 2005b; Pesaresi et al., 2009). PSI and PSII lights were set as described, and then plants were initially grown for 10 d under white light, followed an acclimation period. In detail, plants were grown under PSI or PSII light for 6 d (PSI or PSII plants) or they were first acclimated to PSI light for 2 d followed by 4 d under the PSII light source or *vice versa* (PSI-II or PSII-I plants).

2.8.1 Chlorophyll fluorescence measurement during LTR

Chlorophyll fluorescence parameters (F_s/F_m , Φ_{II} and $1-qP$) were measured according to chapter 2.7.1.

2.8.2 Chlorophyll a/b ratio measurement during LTR

Plant material was harvested under the respective growth light and grinded in liquid nitrogen. The pigments were extracted with 80% buffered acetone. Chlorophyll concentrations and chlorophyll a/b ratios were determined and calculated according to Porra et al. (1989).

2.9 SDS-PAGE and immunoblot analysis

Standard SDS-PAGE (8-15% acrylamide) was performed according to Laemmli (1970) if not indicated otherwise. Immunoblot analyses with phosphothreonine-specific antibodies (p-Thr, Cell Signaling), polyclonal antibodies raised against the mature TAP38 protein (Pribil et al., 2010), STN7 (Wunder et al., 2013), ACTIN (Dianova), PsaA/B, PsaD, PetC, LHCB2, LHCA1, PSII subunit D2, ATP synthase β -subunit or ATP synthase γ -subunit (all from Agrisera) were performed as described before (Ihnatowicz et al., 2008).

2.10 BN- and 2D-PAGE

Thylakoids were prepared from 4-week-old plants as described (chapter 2.4) and then crosslinked by DTSSP (chapter 2.14) or not. For BN-PAGE, thylakoids samples equivalent to

100 µg of chlorophyll were solubilized in solubilization buffer (750 mM 6-aminocaproic acid, 5 mM EDTA [pH 7], 50 mM NaCl) for 10 min with 1% (w/v) n-dodecyl-β-D-maltoside (β-DM) or for 1h with 1.5% digitonin or 2% Nonidet P-40 (NP40) on the ice. Followed by centrifugation at 16000 g for 20 min (β-DM) or 1h (digitonin or NP40), the soluble material was fractionated using nondenaturing BN-PAGE at 4 °C as described (Heinemeyer et al., 2004). After electrophoretic separation, the first dimension gel was either subjected to immunoblot analysis or 2D-PAGE after incubation in Laemmli buffer including 100 mM DTT. For 2D-PAGE, a single denatured lane of the BN gel was placed on top of a reducing 12% acrylamid SDS gel and subsequently fractionated by electrophoresis (Schagger and Vonjagow, 1991). The 2D gel was either stained with Coomassie brilliant blue (CBB) or subjected to immunoblot analysis with antibodies against LHCB2, LHCA1, PSII subunit D2, PetC, ATP synthase β-subunit, PsaB, and PsaD as described in chapter 2.9.

2.11 Sucrose gradient fractionation of thylakoid complexes

Sucrose gradients were prepared by freezing of 11 ml of 0.4 M sucrose, 20 mM Tricine-NaOH pH 7.5, 0.06% NP40 and subsequent thawing at 4 °C. Prior to thylakoid isolation (chapter 2.4) WT plants were exposed to PSI or PSII light. Thylakoids were washed twice with 5 mM EDTA (pH 7.8) and diluted to a final chlorophyll concentration of 1 mg ml⁻¹. NP40 was added at a final concentration of 1% and solubilization was carried out at 4 °C for 1 h. The non-solubilized fraction was pelleted at 16000 g for 1 h at 4 °C and the supernatant as loaded on the afore prepared sucrose gradients. After centrifugation at 195000 g for 21 h at 4 °C, the gradient was divided into 16 or 19 fractions (numbered from the top). All fractions were separated via a 12% SDS-PAGE and either stained with Coomassie brilliant blue or analyzed by Western blotting with antibodies against LHCB2, LHCA1, PSII subunit D2, PetC, ATPase β or γ, PsaB, and PsaD.

2.12 2D protein separation by isoelectric focusing (IEF) and SDS-PAGE gel Electrophoresis

Protein separation via IEF was performed as described before (Qi et al., 2012; Stael et al., 2012). Thylakoids corresponding to 50 µg chlorophyll or 500 µg stromal proteins were precipitated in 80% acetone and resuspended in rehydration buffer (7 M urea, 2 M thiourea, 2% (w/v) CHAPS, 0.5% (v/v) Pharmalyte (GE Healthcare), 0.002% (w/v) bromophenol blue, 18.2 mM DTT). Then protein buffer was applied to Immobiline™ Drystrips (gradient pH 3–10 NL,

GE Healthcare). The strips were placed in a Multiphor II focusing unit (GE Healthcare) and run according to the manufacturer's protocol. Afterwards, the strip was first equilibrated in SDS equilibration buffer (6 M urea, 75 mM Tris-HCl [pH 8.8], 29.3% [v/v] glycerol, 2% [w/v] SDS, 0.002% [w/v] bromophenol blue) containing DTT (100mg per 10 ml buffer) for 20 min and subsequently in the SDS equilibration buffer supplemented with iodoacetamide (250 mg per 10 ml buffer) for another 20 min period. After equilibration, proteins were separated by 12% at SDS-PAGE.

2.13 Coomassie or Ponceau S staining of proteins on PVDF membrane

For Coomassie brilliant staining (CBB), proteins on PVDF membrane were incubated in staining solution (0.1% Coomassie brilliant blue R-250 dissolved in 50% methanol) for 2 min with gentle agitation, followed by rinsing with 50% methanol to remove any background staining. Staining of protein bands can be completely removed by washing with 100% methanol.

For Ponceau S staining (P.S.), proteins were stained with 0.1% (w/v) Ponceau S in 1% (v/v) acetic acid for 2 min prior to block the membrane. Washes with 100% methanol fully removed the protein staining and the membranes could afterwards be blocked as usual.

2.14 Crosslinking

Thylakoids were isolated as described in chapter 2.5 and resuspended in 20 mM HEPES/KOH (pH 7.5). Following chlorophyll measurement, thylakoids were diluted to a concentration of 0.5 mg ml⁻¹ chlorophyll. Then, 100 µl thylakoids preparations were washed 5 times with 500 µl HEPES/KOH (20 mM, pH 7.5) to remove any potential EDTA and subsequently supplied with 1 mM DTSSP (3, 3'-dithiobis [sulfosuccinimidylpropionate]) (Pierce, Thermo Science). After incubation in the dark for 1h at 0 °C, the reaction was quenched by addition of 30 mM Tris (pH 7.6). Samples were centrifuged at 5000 g for 2 min, and the pellet was resuspended in corresponding buffer for BN (see chapter 2.10).

2.15 Co-Immunoprecipitation (Co-IP)

GFP/HA-tagged proteins were pulled down using the GFP-Trap®-A (Chromotek) or Anti-HA Affinity Matrix (Roche). To this end, thylakoids corresponding to 500 µg of Chl (crosslinked by DTSSP or not) were resuspended in dilution buffer (20 mM Tris pH 7.5, 150 mM NaCl, 0.5 mM EDTA) to a Chl concentration of 1 mg ml⁻¹, and solubilized in the presence of 1% (w/v) NP40 for 1h on the rotor at 4 °C. Solubilized thylakoids were separated from the unsolubilized

material by centrifugation 1h at 13000 g, 4°C, and were applied to 25 µl of equilibrated GFP-Trap beads or HA-Affinity Matrix beads. Following 2 h of incubation at 4 °C on a rotor and subsequent six washes with 500 µl dilution buffer (incl. 1% [w/v] NP40), proteins were eluted from the beads by incubation with 100 µl 4×SDS loading buffer (200 mM Tris-HCl pH 6.8, 8% SDS, 40% glycerol, 4% β-mercaptoethanol, 50 mM EDTA) at 95 °C for 10 min. Beads were pelleted by centrifugation at 5000 g 2 min. Subsequently, the solution was applied to 8% SDS–PAGE and electrophoresis was performed until all proteins had migrated into the separating gel (indicated by pre-stained marker proteins). The gel slice (containing the eluted proteins) was excised, washed twice in ddH₂O for 10 min, and further analyzed by mass spectrometry (MS) (Armbruster et al., 2010).

2.16 Mass spectrometry analysis and database searches

LC-MS analyses were performed by Mass-Spectrometry Group (LMU) on an LTQ-Orbitrap XL system. To this end, trypsin-digested peptides were loaded on a fritless 100 µm capillary, packed in-house with ProntoSIL C18 ace-EPS (ProntoSIL C18 ace-EPS, Bischoff Analysentechnik und -geräte GmbH, Leonberg, Germany) by using a quaternary HPLC pump (Flux, Basel, Switzerland) including a CTC autosampler. A gradient of 5-80% (v/v) acetonitrile in 0.1% (v/v) formic acid was then passed through the column over a period of 80 min. The eluted peptides were introduced directly into the LTQ orbitrap XL MS at a flow rate of 250 nl min⁻¹ and a spray voltage of 1.3 kV. The LTQ-Orbitrap was operated via Instrument Method files of Xcalibur to acquire a full high-resolution MS scan between 400 and 2000 m/z. The SEQUEST algorithm was used to interpret MS spectra. Results were interpreted on the basis of a conservative set of criteria: only results with dCn (delta normalized correlation) scores greater than 0.2 were accepted, all fragments had to be at least partially tryptic and the cross-correlation scores (Xcorr) of single-charged, double-charged or triple-charged ions had to be greater than 2, 2.8, or 3.5, respectively. Spectra were manually evaluated to match the following criteria: distinct peaks with signals clearly above noise levels, differences in fragment ion masses in the mass range of amino acids, and fulfilment of consecutive b and y ion series.

2.17 Immunogold labeling

Intact chloroplasts were isolated from *tap38-3* and WT as described (chapter 2.15) and then subjected to one freeze and thaw cycle to strip off the chloroplast envelopes. 40 µl of TAP38

peptide specific antibody was incubated with 50 µg of chloroplast in 200 µl labeling-buffer (50 mM HEPES pH 8.0, 330 mM Sorbitol, 150 mM NaCl, 0.5 mM BSA) on a rotor for 2 h at 4 °C. Afterwards the sample was washed twice with 400 µl labeling-buffer followed by centrifugation at 200 g for 2.5 min. Next, 20 µl of secondary antibody (Anti-Rabbit IgG-Gold antibody, SIGMA) was added, and the reaction was incubated on a wheel for 1h at 4 °C. Again the sample washed with 400 µl labeling-buffer for 5 times. The immune-labeled envelope-free chloroplasts were resuspended in 20 µl labeling-buffer and subjected for SEM analysis (AG Wanner, LMU).

2.18 cDNA synthesis and real-time PCR

Total leaf RNA extraction was performed according to the instructions of Maxwell 16 Tissue LEU, Total RNA Purification Kit (Promega). cDNA was synthesized using 500 ng of total RNA according to the manufacturer's instructions (iScrip cDNA Synthesis Kit, Bio-Rad) and then diluted 1:70. Real-time PCR reaction (20 µl) consisted of 2 µl cDNA dilution, 10 µl iQSYBR Green Supermix (Bio-Rad), 1 µl of each primer and 6 µl of water. The iQ5 Multi-Color Real-Time qPCR Detection System (Bio-Rad) was used to monitor the reaction. The PCR program comprised an initial denaturation step (95 °C for 3 min) and 40 thermal cycles (10 s denaturation at 95 °C, 30 s annealing at 55 °C and 10 s elongation at 72 °C). The primers used to amplify *TAP38* were TPA1-2 sense (5'ACATGGGAATGTGCAGCTTG) and TPA1-2-3 antisense (5'GTGAAGACATCCATATGCCA). UBIQUITIN and CYTOCHROME B5 were amplified as internal controls as described, using the primers Ubiquitin_forward (5'GGAAAAA GGTCTGACCGACA), Ubiquitin-reverse (5'CTGTTCACGGAACCCAATTC), Cytochrome_B5_forward (5'CGACACTGCAAGGGACATGA) and Cytochrome_B5_reverse (5'ACGTATG TCCTAGTTGCTGGAACA) (Wunder et al., 2013). All reactions were performed in triplicate with at least two biological replicates.

2.19 mRNA expression profiling

Total RNA was isolated from 4-week-old plants (WT, *tap38-1*, *oeTAP38*) using the RNeasy Microarray Tissue Mini Kit (QIAGEN), a final amount of 1mg total RNA of each genotype was sent to NASC for microarray analysis.

2.20 Salt extraction and trypsin treatment of thylakoid membranes

Salt and trypsin treatments were prepared according to the protocol of Karnauchov et al. (1997) with minor modifications. In brief, fresh isolated thylakoids were resuspended to a final

concentration of 0.5 mg chlorophyll ml⁻¹ in 2 M NaBr, 2 M NaSCN, 0.1 M Na₂CO₃ or 0.1 M NaOH dissolved in HM buffer (10 mM HEPES-KOH, pH 8.0, 5 mM MgCl₂). After incubation on ice for 30 min, the samples were centrifuged at 7000 g for 10 min at 4 °C. Supernatants were transferred to new reaction tubes and pellets were gently pipetted by adding HM buffer. After washing with HM buffer, pellets were collected by spinning at 16000 g for 30 min. Supernatants and pellets were directly solubilized in SDS sample buffer, separated by SDS-PAGE and subsequently subjected to Western blot analysis.

For trypsin treatment, intact thylakoids with a concentration of 0.5 mg ml⁻¹ chlorophyll were resuspended with HS buffer (10 mM HEPES-KOH, pH 8.0, 0.1 M sucrose) and incubated with 1 µg ml⁻¹ trypsin at 20 °C for 0, 1, 5, 15 or 30 min. Reactions were topped by adding 1 mg ml⁻¹ soybean trypsin inhibitor. Then the entire assays were subjected to SDS-PAGE followed by Western blot analysis using PsbO as control.

2.21 Fractionation of state 1 and 2 thylakoids

WT plants grown in a climate chamber under controlled conditions (100 mmol m⁻² s⁻¹, 12/12 h dark/light cycles) were shifted to PSI (state 1) or PSII (state 2) light as mentioned in chapter 2.2. Thylakoid fractionation was performed as previously described (Shapiguzov et al., 2010). Briefly, thylakoids at a concentration of 0.6 mg of chlorophyll per ml were incubated with 1% digitonin for 5 min and then stepwise centrifuged at 1000 g for 10 min, 10000 g for 30 min, 40000 g for 60 min and 140000 g for 90 min. The respective supernatant was collected and used for the next centrifugation. Pellets collected centrifugation at 10000 g, 40000 g and 140000 g were defined as grana, margins and stroma lamellae, respectively. Thylakoids equivalent to 2.5 µg Chl were loaded onto SDS-PAGE and analyzed by Western blotting.

2.22 Phosphorylation Inhibitory assay

Thylakoids were isolated from 18 h dark-adapted plants in the darkness (without the addition of NaF addition). Then aliquots of thylakoids equivalent to 6 µg chlorophyll were prepared in 20 µl phosphorylation buffer (20 mM Tris-HCl pH7.5, 5 mM MgCl₂, 1 mM MnCl₂, 25 µM ATP) containing different NaF concentrations. Following illumination under 60 µmol photons m⁻² s⁻¹ for 15 min, reactions were stopped by adding the same volume of 4×SDS loading buffer (200 mM Tris-HCl pH 6.8, 8% SDS, 40% glycerol, 4% β-mercaptoethanol, 50 mM EDTA) and analyzed by Western blot.

3 Results

3.1 Topology studies on TAP38 protein

3.1.1 TAP38 is accessible to trypsin digestion at the stroma side of thylakoids

TAP38 is localized in the thylakoid membrane and contains a putative N-terminal chloroplast transit peptide (cTP) according to the computational prediction. Furthermore, TAP38 possesses a phosphatase 2C signature and a transmembrane domain at its very C-terminus (Pribil et al. 2010) (Figure 6a). To clarify, whether the N-terminal part of TAP38 is actually facing towards the lumen or stroma, thylakoids were isolated and treated with $1\mu\text{g ml}^{-1}$ trypsin at 20 °C.

Samples were taken after different time points and the presence of TAP38 was determined by Western blot analysis using an antibody specifically raised against several amino acids at the very N-terminus. Since the TAP38 protein contains multiple trypsin cleavage sites at the N-terminus, that also comprise the sequence of the antibody epitope, a digestion of the N-terminus would result in the loss of TAP38 detectability. PsbO, an extrinsic subunit of photosystem II, (PSII) located on the luminal side of the thylakoid membrane was also analyzed as a control.

TAP38 was gradually degraded over time and disappeared completely after 30 min of trypsin treatment (Figure 6b). On the contrary, PsbO remained unaffected by trypsin in the same experiment indicating that the isolated thylakoids were intact during the course of the experiment (Figure 6b). This result suggests that trypsin digestion only occurred at the stromal side and that the major part of TAP38 (at least its N-terminus) is exposed to this side of the thylakoid membrane. It can be concluded that TAP38 is embedded in the thylakoid membrane with a single transmembrane helix and with the N-terminus facing the chloroplast stroma.

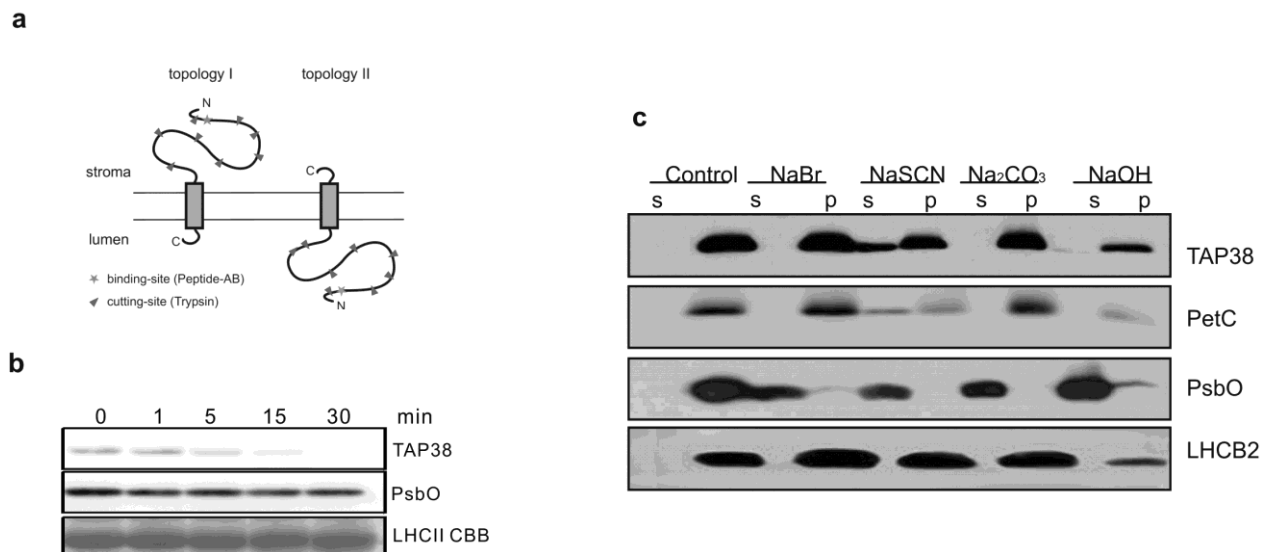


Figure 6 Topology studies on TAP38.

(a) Prediction of TAP38 topology. Asterisks indicate the TAP38 antibody binding sites and triangles represent trypsin cutting sites. (b) Time-course of a WT thylakoid digestion with $1\mu\text{g ml}^{-1}$ trypsin at $20\text{ }^{\circ}\text{C}$. Thylakoids were resuspended in HS buffer (10 mM HEPES-KOH, pH 8.0, 0.1 M sucrose) to a final concentration of 0.5 mg ml^{-1} chlorophyll and samples were taken at 0, 1, 5, 15 and 30 minutes after trypsin treatment. The reactions were stopped by addition of $50\text{ }\mu\text{g ml}^{-1}$ protease inhibitor from soybean followed by a separation on 12% SDS-PAGE. TAP38, as well as PsbO, were immunodetected by specific antibodies after Western blotting. The same membrane was stained with Coomassie brilliant blue (CBB) and the LHCII region was shown as a loading control.

3.1.2 TAP38 is anchored in the thylakoid membrane mainly by electrostatic interactions

In order to experimentally elucidate how TAP38 is anchored in the membrane, i.e. by inserting into the membrane or extrinsically attaching to it, thylakoids were treated with solutions of chaotropic salts or alkaline pH as described by (Karnauchov et al., 1997) and the resulting fractions were assayed by Western blotting. Membrane integral protein PetC, transmembrane protein LHCII and lumen associated protein PsbO were detected as controls. It turned out that TAP38 was still present in the membrane in the presence of 0.1M NaCO_3 and 2 M NaBr , but could be released partially by NaSCN and NaOH (Figure 6c). In all cases, the behavior of TAP38 resembled that of the PetC protein which has one transmembrane domain and integrated into the

thylakoid membrane mainly by electrostatic nature. Taken together, TAP38 is an integral transmembrane protein with its N-terminus facing the stroma.

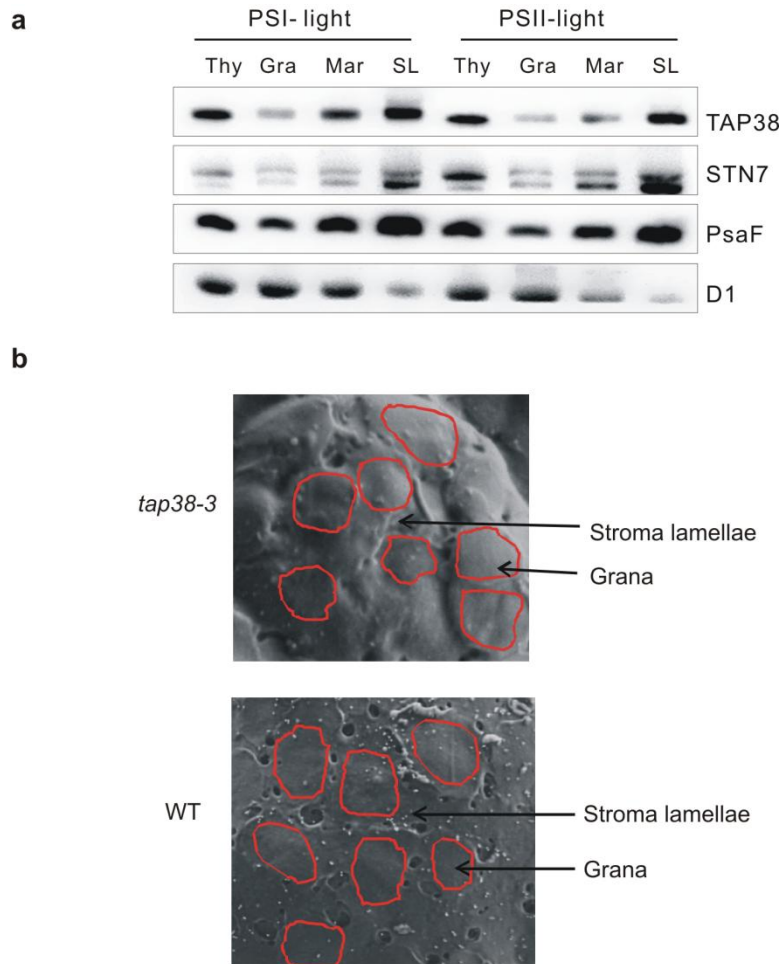


Figure 7 Differential localization of TAP38 within the thylakoid membrane.

(a) TAP38 localization by differential fractionation analysis. After WT plants were adapted to either PSI or PSII light for 2 h, thylakoids were isolated and resuspended at $0.6 \text{ mg chlorophyll ml}^{-1}$. After incubation with 1% digitonin for 5 min, thylakoids were centrifuged at 1000 g for 10min, 10000 g for 30 min, 40000 g for 60 min and 140000 g for 90 min to collect grana, margins and stroma lamellae, respectively. Thylakoids and all collected fractions equivalent to $2.5 \mu\text{g}$ of chlorophyll were loaded onto a SDS-PAGE and analyzed by Western blot using TAP38, STN7, PsaF and D1 specific antibodies. (b) SEM images of Immunogold-labeled TAP38 on envelope-free chloroplasts. Intact chloroplasts were isolated from WT and *tap38-3* under LL as described (chapter 2.5). Following the incubation with TAP38 first and gold-labeled secondary antibodies, the envelope-free chloroplasts were analyzed by scanning electron microscopy (AG Wanner, LMU) (2.17). Red circles indicate the grana stack areas; immunogold-labeled TAP38 is represented by white dots.

3.2 Differential localization of TAP38 within the thylakoid membrane

3.2.1 TAP38 localizes predominantly to stroma lamellae fractions

To specifically localize TAP38 within the thylakoid membrane, thylakoids from PSI and PSII light-adapted WT plants were isolated, solubilized with digitonin and further divided into grana, margin and stroma lamellae fractions via differential centrifugation. These fractions were analyzed by immunoblotting using antibodies against TAP38. The quality and purity of the collected fractions was assessed with antibodies against the subunits of photosynthetic complexes, PsaF and PsbA (D1). Western blots showed results demonstrated that the marker proteins were significantly enriched in the expected fractions. In detail, PSI complexes were found mainly in the stroma lamellae, whereas the grana contained predominantly PSII (Allen and Forsberg, 2001). The TAP38 protein was significantly enriched in the stroma lamellae fraction and its distribution pattern closely resembled that of PSI marker PsaF. This suggests that the main fraction of TAP38 resides spatially close to its potential substrate, pLHCII which is exclusively associated with PSI under state 2 conditions (Figure 7a). Moreover, the distribution patterns of TAP38 under state 1 (PSI light) and state 2 (PSII light) were basically unchanged, suggesting a relatively rather stable localization around PSI and not PSII, which localized predominantly to the grana fraction (Figure 7a).

3.2.2 Immunogold labeling suggests a stroma lamellae localization of TAP38

In the immunogold-labeling experiment, envelope-free chloroplasts were extracted from *tap38-3* and *oeTAP38* under LL (state 2) and FR (state 1) light respectively. Following incubation with TAP38-specific primary antibodies, and secondary antibodies which were conjugated to gold particles, the so labeled envelope-free chloroplasts were analyzed by scanning electron microscopy (SEM) (AG Wanner, LMU). The position of TAP38 was marked by the gold particles within the SEM images. Shown in the Figure 7b are grana represented by the flat area and stroma lamellae as well as margin regions illustrated by rough parts. There was hardly any accumulation of TAP38 visible on the chloroplast surface of the *tap38-3* mutant suggesting very low unspecific binding of the TAP38 specific antibody (Figure 7b, upper panel). For the WT, gold particles mainly associated with the uneven regions representing the stroma lamellae and margin domains, which was in line with the results of the differential fractionation experiments (Figure 7b lower panels).

3.3 TAP38 is not regulated by the redox state of the Plastoquinone pool

3.3.1 Constant expression of TAP38 under different light conditions

Light qualities are known to affect the redox state of the plastoquinone (PQ) pool, and the accumulation of STN7 in WT plants was in turn shown to be regulated by redox state of the PQ pool (Wunder et al., 2013). In brief, STN7 protein levels are increased in plants adapted to PSII specific light compared to those adapted to PSI-favoring light (Wunder et al., 2013). Furthermore, it is well accepted that TAP38 counteracts STN7 regarding LHCII phosphorylation and state transition (Pribil et al., 2010; Shapiguzov et al., 2010). However, the LHCII phosphatase TAP38 was previously suggested to be insensitive to redox regulation (Silverstein et al., 1993). To assess the expression of *TAP38* under state 1 (dark or far-red light) or state 2 (low light or PSII light) or high light more comprehensively, WT plants were dark adapted overnight and then transferred to either PSII light for up to 540 min or low light for 120 min, followed by far-red light or high light for a total exposure time of 270 min. Thylakoids were extracted at different time points and TAP38 accumulation was detected by TAP38 specific antibodies. These analyses showed a high and constant expression of TAP38 independent of the applied light conditions (Figure 8a). Based on these findings, we concluded that TAP38 protein levels are not regulated by prolonged changes in light conditions and relative difference in the redox state (Figure 8a). This is in agreement with previous findings showing that there were no significant changes in TAP38 amounts upon transfer of WT plants between different light conditions (Pribil et al., 2010).

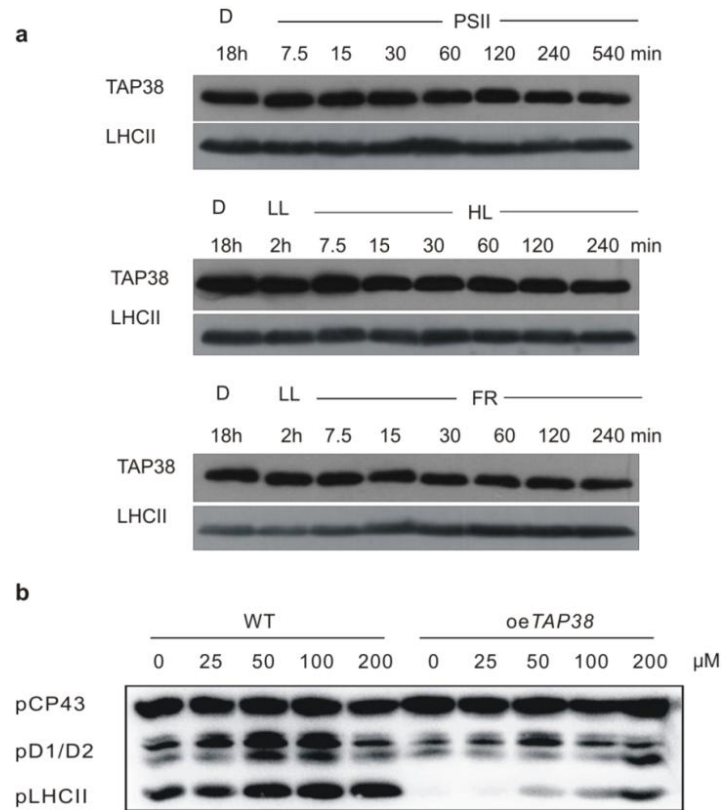


Figure 8 TAP38 is neither regulated at the protein nor activity level by the redox state of the PQ pool.

(a) TAP38 expression after different long term light treatment. WT plants were adapted to dark overnight, and then transferred to PSII light for up to 540 min or low light for 120 min, followed by far-red light or high light exposure for a total of 270 min. Thylakoids were isolated and subjected to Western blotting using TAP38 antibody. (b) Aliquots of thylakoids from dark-adapted plants (no NaF) equivalent to 6 μ g chlorophyll were resolved in 20 μ l phosphorylation buffer containing different NaF concentrations. Following illumination under 60 μ m photons $m^{-2} s^{-1}$ for 15 min, the reactions were stopped by adding the same volume of 4 \times SDS loading buffer and thylakoid phosphorylation was analyzed by Western blot using phosphothreonine specific antibodies.

3.3.2 TAP38 still active in state 2

Based on the above data, the question arose whether TAP38 remains active under light conditions that stimulate LHCII phosphorylation (low light, PSII light). To address this issue, thylakoids from dark-adapted WT and *oeTAP38* were isolated in the absence of NaF, and further exposed to low light for 15 min in the presence of increasing NaF concentrations. Subsequently,

the reactions were stopped by addition of 4xSDS loading buffer and analyzed by immunoblot using phosphothreonine-specific antibodies. In WT, the levels of LHCII denovo phosphorylation accumulated progressively with increasing concentrations of NaF (Figure 8b). This phenomenon was even more enhanced in *oeTAP38*, which showed almost no de novo LHCII phosphorylation in the presence of 0 or 25 mM NaF. However, at NaF concentrations above 50 mM pLHCII began to accumulate and reached its maximum at about 200 mM NaF (Figure 8b). It seemed that the amount of pLHCII correlated directly with NaF quantity applied and inversely with TAP38 abundance (Figure 8b). These observations suggest that TAP38 activity is not regulated by low light exposure, the light condition at which TAP38 inactivation or downregulation could make most sense from a physiological point of view.

3.3.3 TAP38 accumulates and functions normally in mutant lines with over-reduced PQ pool

As previously described, *psad1-1* and *psae1-3*, two mutants affected in PSI accumulation, show a much lower effective yield of PSII (Φ_{II}) and significantly reduced PQ pool (measured as 1-qp or 1-qL) compared to WT. Therefore these lines also show a drastically increased level of pLHCII (Ihnatowicz et al., 2007b; Ihnatowicz et al., 2004; Pesaresi et al., 2009) in contrast to the *oeTAP38* line. To clarify whether constitutive alterations in the redox state of PQ pool caused by defective photosynthetic complexes affect TAP38 accumulation, *oeTAP38* was crossed with *psad1-1* or *psae1-3* and homozygous double mutants were obtained from the F2 generation. In the following, the double mutants (*psad1-1 oeTAP38* and *psae1-3 oeTAP38*), as well as their parental lines were analyzed regarding TAP38 accumulation, growth phenotypes, *in vivo* chlorophyll a fluorescence and PSI-LHCI-LHCII formation.

3.3.3.1 TAP38 could accumulate in mutants with highly-reduced PQ pool

Isolated thylakoids of plants exposed to either LL for 2 h or LL and additional 2 h of FR were analyzed by Western blotting regarding TAP38 expression. TAP38 amounts within different lines did not change significantly between state 1 and state 2 light inducing conditions (Figure 9a). Since the signal of TAP38 was much stronger in *oeTAP38* compared to WT, *psad1-1* and *psae1-3*, the latter did not show a TAP38 signal under the chosen exposure condition (Figure 9a). However, when thylakoids of *oeTAP38* lines were loaded less, clear TAP38 signals could be detected in those lines (Figure 9b). The expression levels of TAP38 in both double mutants

(*psad1-1* oeTAP38 and *psae1-3* oeTAP38) were slightly reduced compared to that of oeTAP38, but still about six times higher than those in the WT and 12-15 times higher than those in *psad1-1* or *psae1-3* in which TAP38 protein amounts are reduced to half or one third of those in WT (Figure 9b). Therefore we conclude that TAP38 could accumulate to normal or even exaggerated levels in plants with reduced PSI amounts and permanently highly-reduced PQ pool.

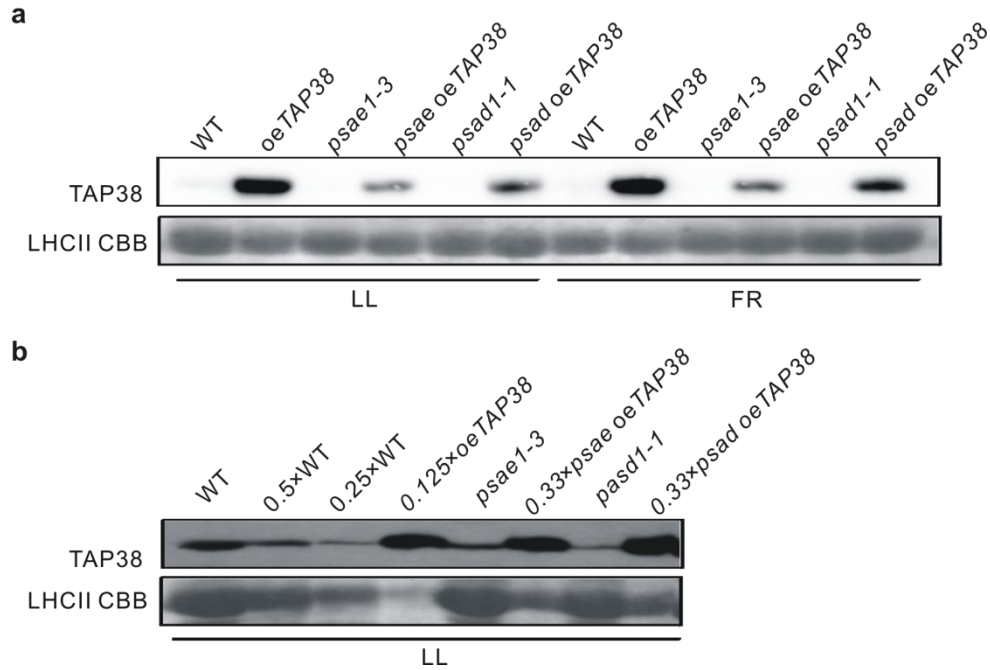


Figure 9 Ectopic expression of TAP38 in mutants with highly-reduced PQ pool (*psae1-3* and *psad1-1*).

(a) TAP38 overexpression in the *psae/d* mutants background under LL and FR. Thylakoids from WT, oeTAP38, *psad1-1*, *psae1-3*, and double mutants were extracted out for LL- or FR-adapted leaves and immunodetected with TAP38 antibodies after Western transfer. (b) Thylakoid proteins isolated after LL treatment were loaded on a SDS gel correspondingly. Reduced thylakoid amounts oeTAP38 or double mutants, corresponding to 12.5% or 33% of the WT levels were loaded and marked as 0.125xoeTAP38 and 0.33x*psae/psad* oeTAP38. Decreasing amounts of WT thylakoids were indicated as 0.5xWT and 0.25xWT. Immunodetection was performed using TAP38-specific antibodies. *psad1-1*, *psae1-3* were abbreviated as *psad* and *psae* respectively in the double mutants; CBB staining of LHCII was shown as a loading control.

3.3.3.2 TAP38 activity is not affected in the double mutants (*psad1-1* oeTAP38 or *psae1-3* oeTAP38)

Plants were grown in a climate chamber under a 16/8 day/night cycle and the phenotypes were assayed. The two double mutants (*psad1-1* oeTAP38 and *psae1-3* oeTAP38) exhibited a dramatically reduced growth rate (Figure 10a), as well as a markedly reduced Φ_{II} , compared to their parental lines (Table 1). In detail, the Φ_{II} reduced from 0.41 in *psad1-1* to 0.31 in *psad1-1* oeTAP38 and from 0.50 in *psae1-3* to 0.36 *psae1-3* oeTAP38. This suggested that the plants were affected more severely than the respective single mutants. Notably, the growth phenotypes of the double mutants resembled those of the *psad1-1* *stn7* or *psae1-3* *stn7* double mutants (Pesaresi et al., 2009). As a control, the double mutants *stn8* *psad1-1* and *stn8* *psae1-3*, were grown and behaved like the single parental mutants (Figure 10a). Those changes in *psad1-1* oeTAP38 and *psae1-3* oeTAP38 could be attributed to an even more severely reduced PQ pool as displayed by a largely increased 1-qL (0.87 in *psad1-1* oeTAP38 compared to 0.78 in *psad1-1* and 0.85 in *psae1-3* oeTAP38 compared to 0.68 in *psae1-3*) although the maximum quantum yield of PSII (F_v/F_m) remained unaltered (Table 1). This suggest that even in plants with a strongly reduced PQ pools like *psad1-1* or *psae1-3*, overexpression of the LHCII phosphatase TAP38 still resulted in a shift of the PQ pool towards an even more reduced state.

Table 1 Chlorophyll Fluorescence Parameters of 4-week-old double mutants of oeTAP38 and PSI defective mutants (*psad1-1*, *psae1-3*).

Measured	WT	oeTAP38	<i>psad1-1</i>	<i>psad1-1</i> oeTAP38	<i>Psae1-3</i>	<i>psae1-3</i> oeTAP38
PAM parameter						
F_v/F_m	0.83±0.02	0.83±0.01	0.79±0.01	0.79±0.00	0.78±0.02	0.80±0.00
Φ_{II}	0.74±0.01	0.67±0.02	0.41±0.02	0.31±0.01	0.50±0.01	0.36±0.01
1-qL	0.33±0.03	0.53±0.03	0.78±0.02	0.87±0.00	0.68±0.04	0.85±0.01

After plants were adapted to darkness for 30 min, minimal fluorescence (F_0) was determined. White light (5000 $\mu\text{mol photons m}^{-2} \text{s}^{-1}$) was given as a pulse (0.8 s) to measure the maximum fluorescence (F_m). The

maximum quantum yield of PSII was calculated according to the equation $(F_m - F_0)/F_m = F_v/F_m$. Actinic light ($40 \mu\text{mol photons m}^{-2} \text{s}^{-1}$) was applied for 10 min before the steady-state fluorescence (F_s) was measured. F_m' was determined after exposure to further saturation pulses (0.8 s , $5000 \mu\text{mol photons m}^{-2} \text{s}^{-1}$). The photosynthetic parameters, Φ_{II} and $1-qL$, were calculated according to the following equations (Maxwell and Johnson, 2000): $\Phi_{II} = (F_m' - F_s)/F_m'$ and $1-qL = 1 - (F_m' - F_s)F_0 / ([F_m' - F_0] F_s)$. Values were averages of 6 plants and the standard deviation was calculated accordingly.

In addition, biochemical analyses indicated that LHCII phosphorylation was almost absent in the double mutants similar to the case of *oeTAP38* (Figure 10b). On the contrary, in the single parental mutant lines *psad1-1* and *psae1-3*, LHCII was phosphorylated strongly under low light and remained phosphorylated to a certain degree upon far-red light exposure (Figure 10b). In agreement with these findings, BN-PAGE analyses showed that the band representing the PSI-LHCI-LHCII complex, which reflects the PSI associated with the mobile pool of pLHCII (Pesaresi et al., 2009) is present in significant amounts in *psad1-1* and *psae1-3* but absent in the double mutants under all light conditions investigated similar to *oeTAP38* (Figure 10c). Correspondingly, an enhancement of the PSI-LHCI band was observed in the double mutants (*psad1-1 oeTAP38* and *psae1-3 oeTAP38*) compared to the respective single mutants (*psad1-1* and *psae1-3*) under all applied conditions (Figure 10c) suggesting the dissociation of LHCII from PSI. The PSI-LHCI band was also increased in the single mutants upon transfer from LL to FR (Figure 10c). In WT, the PSI-LHCI-LHCII complex was formed under low light but disintegrated under far-red light condition as expected (Figure 10c). Based on these findings, we draw the conclusion that TAP38 activity is not affected in mutants with over-reduced PQ pool.

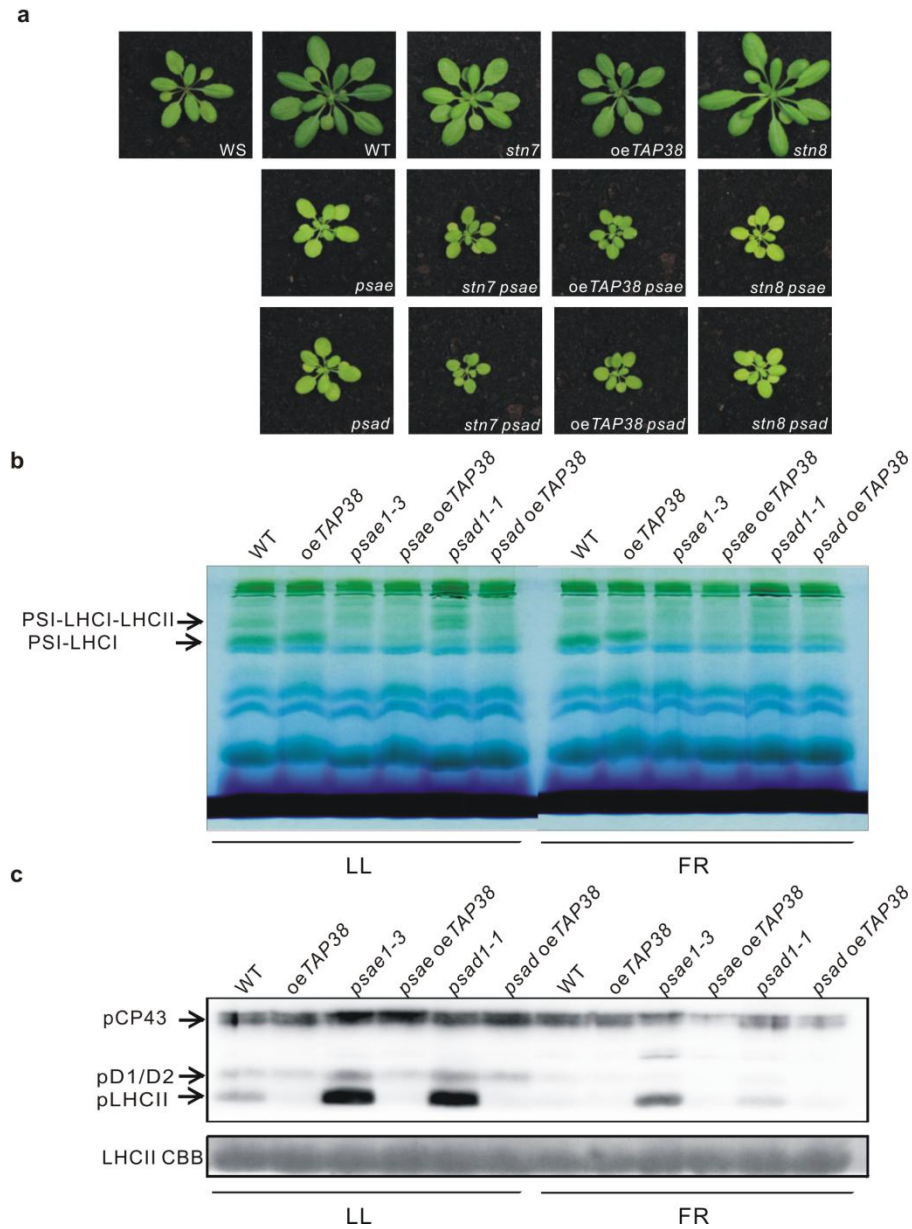


Figure 10 TAP38 could accumulate and functions normally in the double mutants with further over-reduced PQ pool

(a) Exacerbated phenotypes of double mutants of *oeTAP38* or *stn7* with mutants showing an over-reduced PQ pool (*psad1-1* or *psae1-3*). Plants were four-week-old and grown in a climate chamber under 16/8 day/night cycle. (b) Thylakoid protein phosphorylation detected by immunoblot analysis with phosphothreonine-specific antibodies in WT, *oeTAP38*, *psad1-1*, *psae1-3*, and the respective double mutants. Four-week-old plants were adapted to dark for overnight, and then transferred to LL for 2h and subsequently to FR for 2h. Subsequently thylakoids were isolated and fractioned by SDS-PAGE. Phosphorylation of LHCII was detected by immunoblot analysis using phosphothreonine-specific

antibodies. (b) Visualization of PSI-LHCI-LHCII and PSI-LHCI bands in BN-gels. Thylakoid membranes were isolated from same plants described in (b). Identical amounts of thylakoids were loaded for BN-PAGE analysis (see chapter 2.10) and arrows indicate the PSI-LHCI-LHCII and PSI-LHCI complexes.

3.4 TAP38 co-localizes with its putative substrate LHCII and depends on its expression

3.4.1 TAP38 co-localizes with its putative substrate LHCII

To investigate the interaction between TAP38 and its postulated substrates LHCII, sucrose gradient ultracentrifugation was performed with WT plants. Firstly, thylakoids of WT plants were solubilized with β -DM, and then fractionated by sucrose gradient centrifugation. Subsequently, different fractions were collected, separated via SDS-PAGE and analyzed by immunoblotting with TAP38-specific antiserum. A replicate gel was stained with Coomassie brilliant blue (G250) to assess the protein composition of different fractions (Figure 11a). LHCII was predominantly presented in fractions 4-7 of the Coomassie stained gel (Figure 11a). These fractions also contain most of the TAP38 signals detected by Western blot. Those lanes containing TAP38 ranged from the free protein containing fraction to the fractions of low-molecular-weight complexes. This suggests to some extent, association between TAP38 and its putative substrate LHCII.

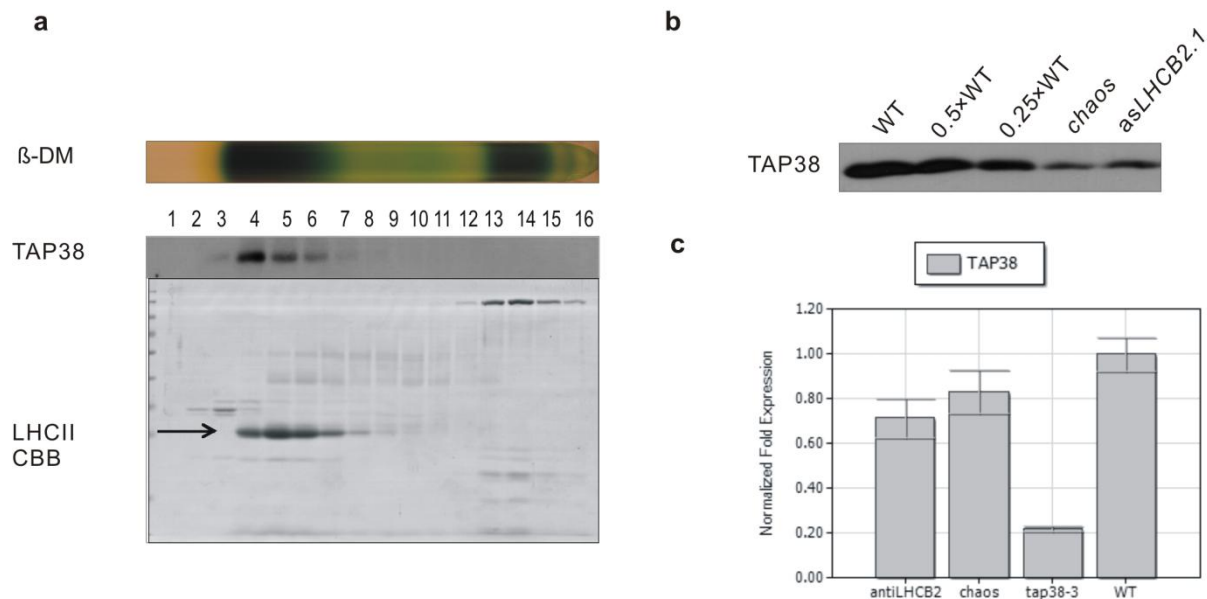


Figure 11 TAP38 co-localizes with its putative direct substrate LHCII and depends on its expression.

(a) TAP38 and LHCII distribution patterns in sucrose gradient ultracentrifugation. The sucrose gradient was prepared from 0.4 M sucrose (frozen and thaw overnight) and WT thylakoids at 1 mg ml⁻¹ chlorophyll

was solubilized in the presence of 1% β -DM. After centrifugation at 16000 *g* for 5 min, the supernatant was fractionated by the sucrose gradient and divided into 16 fractions. All the fractions were separated via 15% AA SDS-PAGE, transferred to PVDF membrane and immunodetected using a TAP38-specific antibody. A replicate gel was stained with Coomassie brilliant blue (CBB). (b) Immunoblot analysis of TAP38 in thylakoids from WT, *tap38-3*, *chaos* and LHCII antisense line (*asLHCII2.1*). Decreasing levels of WT thylakoids were loaded indicated as WT 0.5 (50%) and WT 0.25 (25%). (c) Quantification of TAP38 mRNAs by real-time PCR in WT, *chaos* and *asLHCII2.1*. RNA isolation, cDNA synthesis, PCR and data analysis referred to paragraph 2.18 and 2.19.

3.4.2 TAP38 expression is decreased in mutants defective in LHCII accumulation

To test whether TAP38 requires the association with LHCII to accumulate or whether there is a feedback regulatory mechanism on TAP38 accumulation when its putative substrate is lacking, the accumulation dependency of TAP38 on LHCII was assayed on the protein level using WT and mutant lines, impaired either in the accumulation of LHCII (*asLHCII2.1*) (Andersson et al., 2003) or targeting of LHCII (*chaos*) (Klimyuk et al., 1999). To this end, plants were grown in a climate chamber and thylakoid proteins were isolated, and analyzed by Western blotting using a TAP38-specific antibody (Figure 11b). The results of this assay implied that TAP38 amounts were reduced to less than 20% of WT level in both mutant lines (Figure 11b). To check whether these changes in TAP38 abundance were due to altered TAP38 transcription level, real-time PCR was carried out which showed that TAP38 transcripts of all mutants were reduced by about 20-30% compared to WT (Figure 11c). These results pointed towards a certain correlation between mRNAs level and TAP38 protein. From these observations, one can conclude that the TAP38 expression depends on the LHCII either due to the necessity for a physical binding or a feedback mechanism.

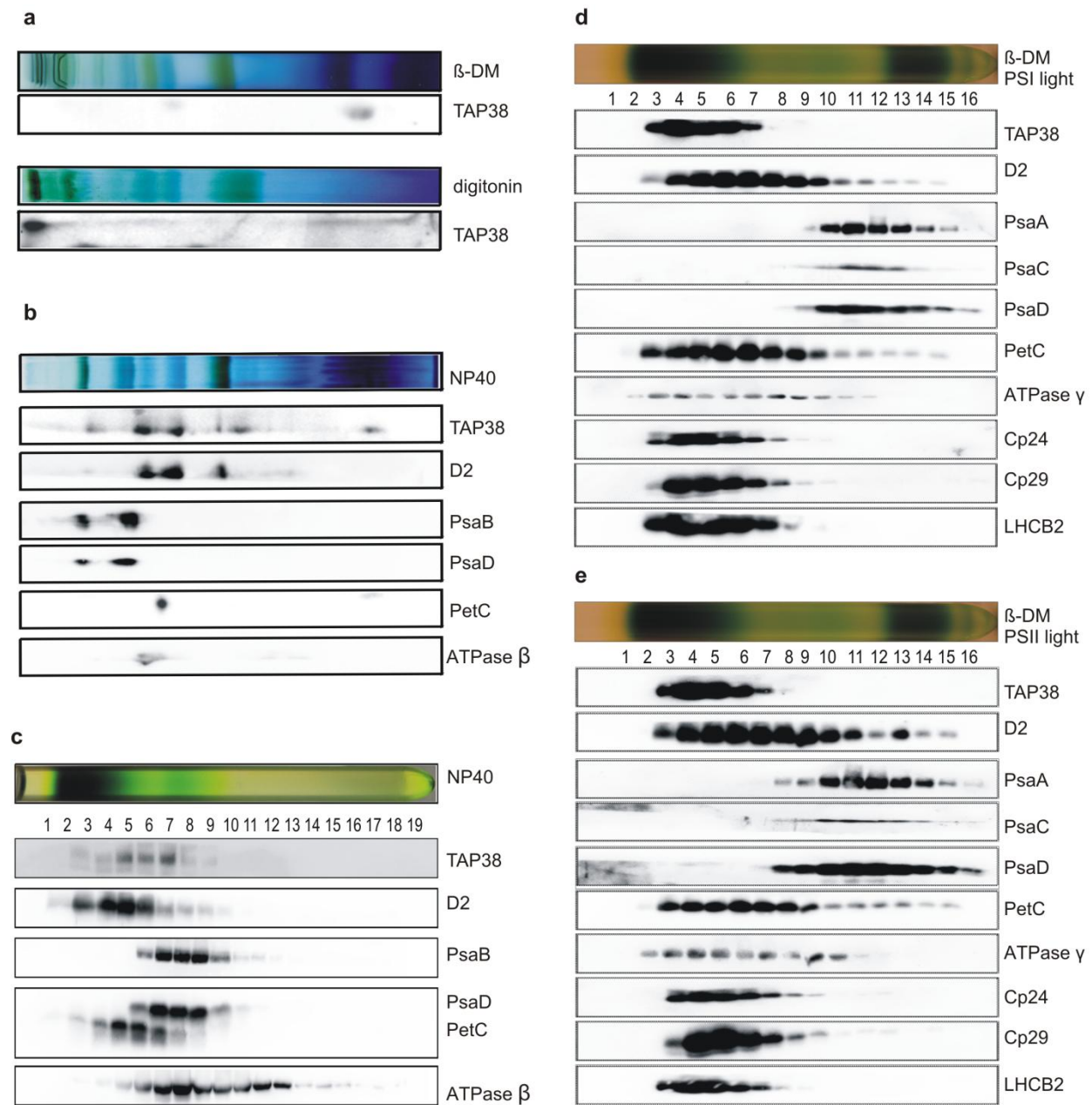


Figure 12 TAP38 is not directly associated with PSI or other major photosynthetic complexes.

Detection of TAP38 in 2D BN/SDS-PAGE using β -DM or digitonin as a detergent. Thylakoids corresponding to 100 μ g Chl from WT plants were solubilized with 1% β -DM or 1.5% digitonin and fractionated by BN-PAGE. The TAP38 signal was detected by Western blot after 2-D PAGE. (b) Detection of TAP38 in 2D BN/SDS-PAGE using NP40 a detergent. Thylakoids (corresponding to 100 μ g Chl) from WT plants were solubilized with 2% NP40 and fractionated as described (chapter 2.10). PsaB, PsaD, PetC, ATPase β , D2 and TAP38 were detected by Western blot using specific antibodies. (c) Detection of TAP38 in sucrose gradient fractions after solubilization of thylakoids using NP40 as a detergent. Sucrose gradient preparation, thylakoid solubilization, ultracentrifugation and gradient preparation, were

performed as described before (see 2.11). The same protein makers were detected by Western blotting as in (b). (d) Detection of TAP38 after sucrose gradient centrifugation using β -DM as a detergent. Plants were treated with PSI light. PsaB, PsaD, PasC, PetC, ATPase γ , D2, LHCII (LHCB1), CP26, CP29 and TAP38 analyses were performed (e) Detection of TAP38 after sucrose gradient centrifugation using β -DM as a detergent. Plants were treated with PSII light. Same proteins as in (d) were detected.

3.5 TAP38 is not directly associated with PSI or other major photosynthetic complexes

3.5.1 TAP38 is not associated with major photosynthetic complexes in BN and sucrose gradient ultracentrifugation

Different detergents were used to solubilize thylakoids of WT, and Western blot results were obtained from second dimension gels of BN-PAGE analyses using TAP38-specific antibodies. When 1% β -DM was employed, TAP38 accumulated in the region of free proteins (Figure 12a upper panel). However, when thylakoids were solubilized with 1.5% digitonin TAP38 associated mainly with supercomplexes of very-high-molecular weight (Figure 12a lower panel). When the detergent NP40 was applied in the same experimental setup, the signals of TAP38 ranged from the free protein to high-molecular-weight complex region (Figure 12b). Additionally, marker proteins for the major photosynthetic complexes were applied, but their distribution patterns did not show a clear co-localization with TAP38 (Figure 12b). Thylakoids were also crosslinked using DTSSP. This time, TAP38 migrated to high molecular regions in the BN-PAGE even β -DM was used for solubilization (Figure 13a). Many photosynthetic complexes were found in this high molecular region that no specific association of TAP38 with any of them could be observed (Figure 13b). The distribution patterns of TAP38 and major photosynthetic complexes in a sucrose gradient using β -DM and NP40 during the solubilization step were also detected by Western blot. Here, TAP38 localized only in the free protein and low molecular weight complexes fractions and its signal did not overlap perfectly with any of the photosynthetic complex signal (Figure 12c, 12d, 12e). Whereas, there was significant overlap between TAP38 and the antenna components LHCII in line with previous observation (Figure 12d, 12e). It is worth noting that the TAP38 distribution patterns were the same after PSI- and PSII-light treatment (Figure 12d, 12e). Therefore, the conclusion could be drawn that no stable association of TAP38 with the major photosynthetic complexes persists in the thylakoid membrane including PSI.

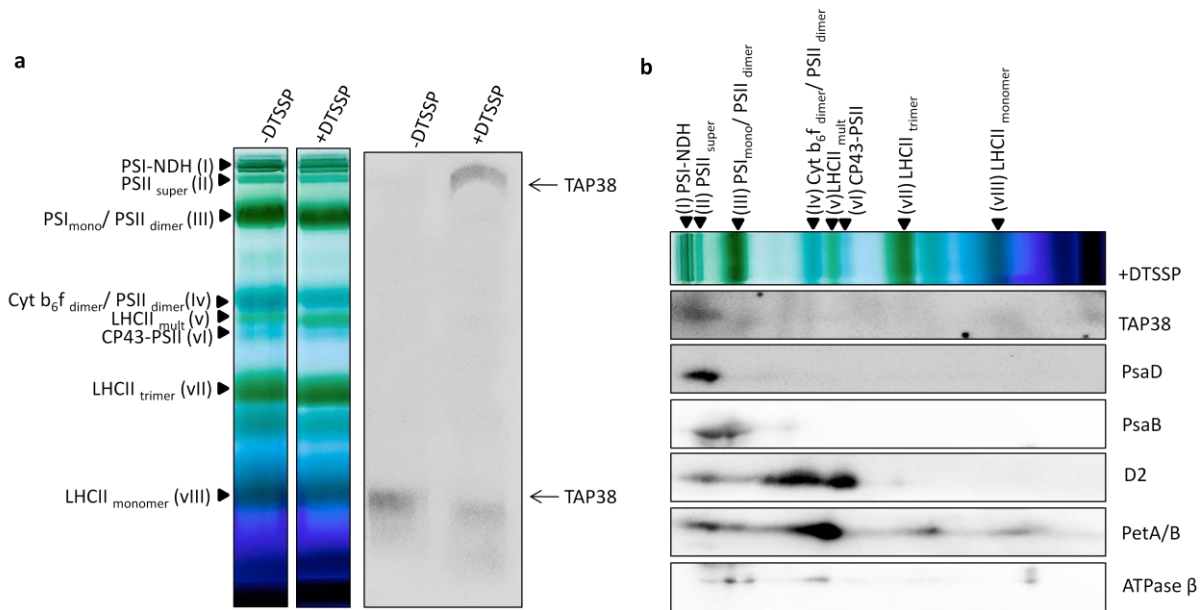


Figure 13 TAP38 is crosslinked to high molecular weight complexes.

(a) Detection of TAP38 in first dimension of BN gel. Thylakoids from WT were crosslinked by DTSSP, solubilized using β -DM, and subsequently subjected to BN separation (see chapter 2.10 and 2.14). TAP38 was detected by Western blotting after first dimension of BN PAGE. (b) Detection of TAP38 in 2D BN/SDS-PAGE. Gel slices from (a) were further separated in SDS-PAGE and PsaB, PsaD, PetA/B, ATPase β , D2 and TAP38 were detected by Western blot using specific antibodies.

3.5.2 The expression of TAP38 is affected in a mutant lacking PSI but not in mutants lacking any other of the major photosynthetic complexes

The dependency of TAP38 expression was assayed by analysis of TAP38 levels in mutant lines lacking PSI (*psad1d2*), PSII (*hcf136*), Cyt *b₆f* (*petc*) or ATPase (*atpd*). These mutants and WT as well as the *tap38-3* mutant were grown for 6 weeks on MS plates, and total proteins were isolated to be analyzed by immunoblotting with TAP38-specific antibodies. TAP38 expression seemed not to be affected in *petc* and *atpd* mutants, but reduced in mutant defective in PSI (*psad1d2*) and PSII (*hcf136*) (Figure 14a). Indeed, in *hcf136* mutant, PSI (PsaD) amount is also significantly downregulated as a secondary effect of lacking PSII. Although results from chapter 3.5.1 showed that TAP38 is not associated with PSI, at least a certain correlation with the amount of PSI is present. Similarly a reduction of TAP38 amount also appeared in *psad1-1* and *psae1-3*

mutants (Figure 9, 10). However, in the double mutants *psad1-1 oeTAP38* and *psae1-3 oeTAP38*, TAP38 could substantially accumulate and dephosphorylate pLHCII (Figure 9, 10), although PSI amounts were dramatically reduced in these lines. Moreover, *psad1-1* or *psae1-3* showed a reduced levels of pLHCII when put under extreme artificial FR light supporting that that TAP38 amounts present in those lines were sufficient to allow for dephosphorylation of LHCII and that the decrease of TAP38 amounts in *psad1-1* or *psae1-3* single mutants was not related to a reduction of TAP38 binding to PSI (Figure 10c). Therefore, it seemed that TAP38 protein reduction in *psad1d2* and *hcf136* was not caused by a lack of PSI as binding site. Thus, to address the question whether *TAP38* was regulated at transcript level, RT-PCR was performed in those lines which showed decreased TAP38 level together with *psad1-1* and *psae1-3* mutants. The results revealed a significantly reduction of *TAP38* mRNA (20% - 60%) in all mutants compared to WT (Figure 14b). Taking together, a reduction of TAP38 accumulation might be not caused directly by lack of PSI as a binding necessity but through a regulation of TAP38 at transcript levels.

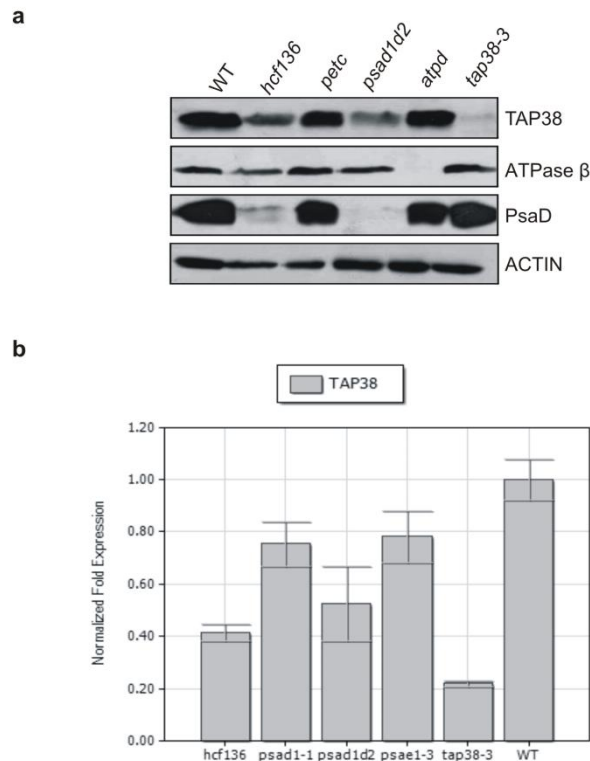


Figure 14 The expression of TAP38 is affected in mutants lacking PSI but not in mutants lacking any of the other photosynthetic complexes

(a) TAP38 expression in WT and *tap38-3* compared to mutants of major photosynthetic complexes (*psad1d2*, *hcf136*, *petc*, *atpd*). Total proteins were isolated from 6-week old plants grown on the MS plates. Immunoblot analyses were carried out using TAP38, D2, ATPase β and PsdD specific antibodies. (b) Real time-PCR analysis on TAP38 accumulation in the mutants listed in (a) in addition with *psa1-3* and *psad1-1*.

3.6 Pull down assay using functional N-terminal HA-Fusion line and C-terminal GFP-Fusion Line of TAP38

3.6.1 Expression of TAP38-HA and TAP38-GFP proteins in the *tap38-3* mutant background

TAP38 protein accumulation in oeTAP38 HA-tagged lines was strongly increased compared to WT (Figure 15a) leading to a reduction in LHCII phosphorylation (Figure 15b) under all analyzed light conditions. State transitions values monitored by PAM-fluorometry in HA-tagged line resembled those of TAP38 overexpressor plants (oeTAP38) indicating that the HA-tagged TAP38 protein was functional (Figure 15e). Surprisingly, lines expressing GFP-tagged TAP38 accumulated TAP38 proteins both in the size of mature TAP38 and of potential GFP-tagged (Figure 15 c), with a total expression level similar to TAP38 accumulation in WT. In line with that, state transitions and LHCII phosphorylation patterns were similar to WT with a tendency towards a slight oeTAP38 phenotype (Figure 14d, 14e). Although it was unclear whether the GFP-tagged variant was able to dephosphorylate pLHCII, its localization was unequivocally confirmed in the thylakoid membrane.

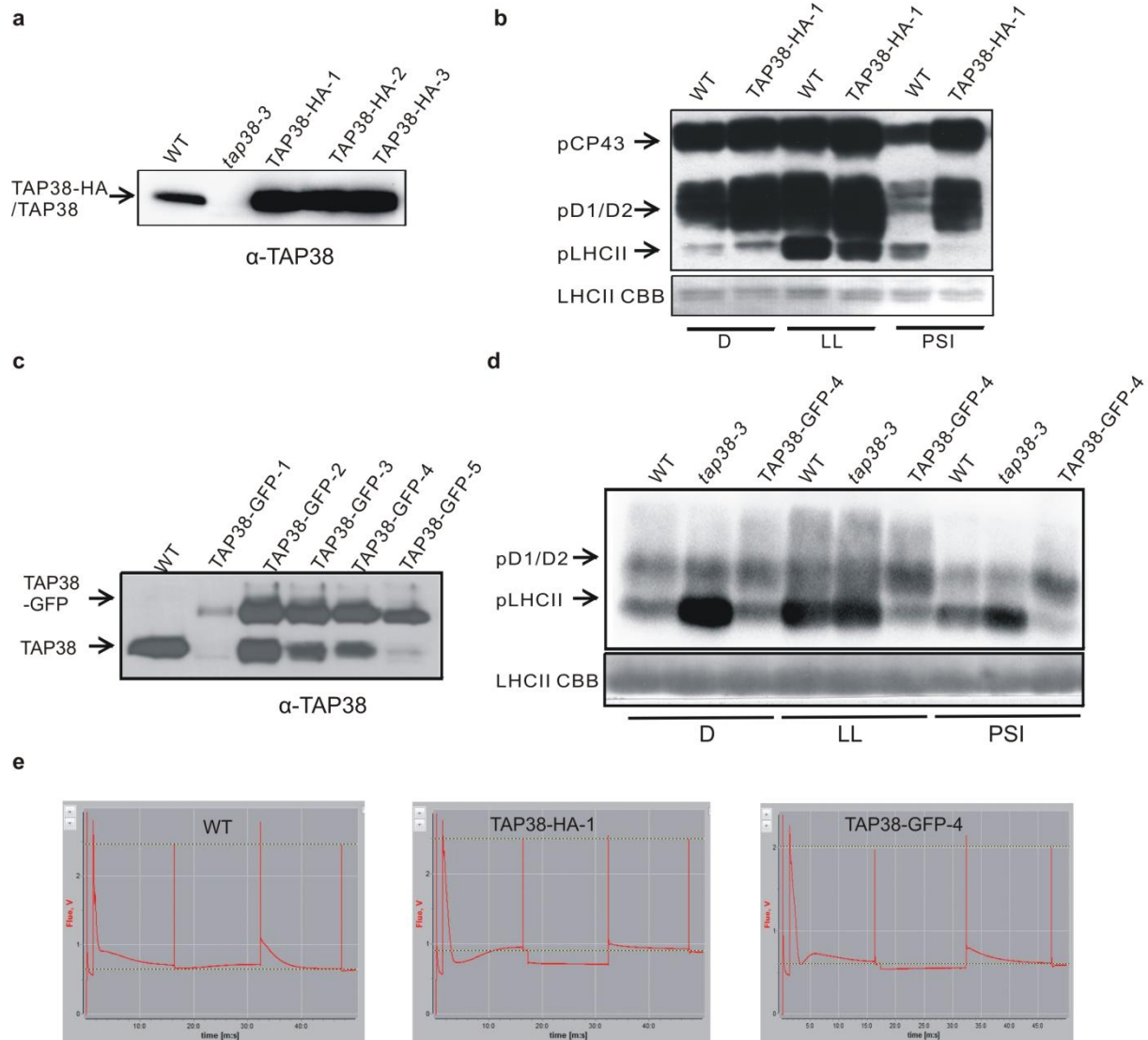


Figure 15 Generation of a functional N-terminal HA and C-terminal GFP Fusion lines of TAP38.

(a) Immunodetection of TAP38 in thylakoids of WT, *tap38-3* and individual TAP38-HA lines generated in the *tap38-3* mutant background. (b) Thylakoids phosphorylation in WT and TAP38-HA plants detected by phospho-threonine specific antibodies. (c) Immunodetection of TAP38 in thylakoids of WT, *tap38-3* and several TAP38-GFP lines generated in the *tap38-3* mutant background. (d) Thylakoids phosphorylation in WT and TAP38-GFP plants detected by phospho-threonine specific antibodies. (e) PAM measurement of state transitions in WT, TAP38-HA-1 and TAP38-GFP-4 line according to the method described in 2.7.2.

3.6.2 Pull down of putative interactors of TAP38 using HA- or GFP-tagged lines

In order to identify interaction partners of TAP38, co-immunoprecipitation (Co-IP) experiments were performed with TAP-HA, TAP38-GFP and WT lines. After solubilization using NP40 and incubation with a HA- or GFP- affinity matrix, the elution fractions were analyzed by Western blot and Mass Spectrometry (MS). Western detection with TAP38 specific antibodies displayed a specific signal within elution fractions of the HA- or GFP- respective tagged line which were absent in WT (Figure 16). These results indicate that tagged TAP38 proteins were specifically pulled down by the interaction between the respective tag and the affinity matrix. Subsequently the elution samples were analyzed by MS. Each Co-IP experiment was performed in at least three biological replicates and the consistency between different experiments was very high. Potential interactor proteins represented the components of PSI including its antenna proteins (i.e. LHCA1, LHCA2, LHCA4) and core proteins (PsaA/B). Also the proteins of the mobile fraction of LHCII (i.e. LHCB2 and LHCB1.5) were identified in the elution fractions (Table 2). As previously described, TAP38 can directly dephosphorylate pLHCII *in vitro* (Pribil et al., 2010) which associates with PSI in state 2. Co-precipitation of TAP38 with LHCII proteins as shown by this MS analysis supported this idea. Co-precipitation of TAP38 with PSI was an indication that TAP38 was localized closely with PSI complex which was consistent with fractionation and immunogold-labeling results (Figure7).

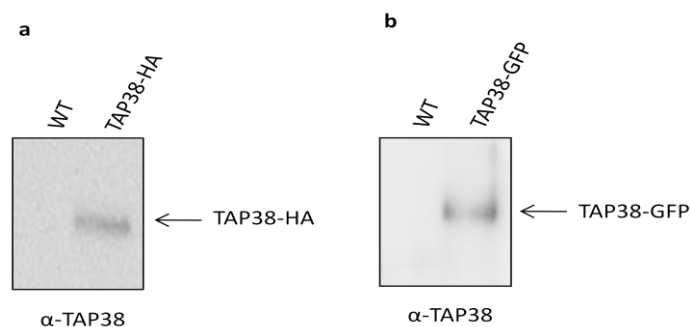


Figure 16 Immunodetection of TAP38 in the elutions of co-immunoprecipitation with HA- and GFP-affinity matrices.

Thylakoids were isolated from WT and lines expressing HA- and GFP tagged TAP38. The Co-IP was performed according to chapter 2.15. The elutions were subjected to SDS-PAGE followed by western blot analyses using TAP38 specific antibody (α -TAP38).

Table 2 Results of the Mass Spectrometry analysis on the Co-IP elutions.

Accession	Protein	TAP38-HA #Peptides	WT #Peptides
light-harvesting chlorophyll-protein complex I subunit A4	LHCA4	9	1
photosystem I light harvesting complex gene 1	LHCA1	5	0
photosystem I light harvesting complex gene 2	LHCA2	3	0
photosystem II light harvesting complex gene 2.1	LHCB2	6	0
photosystem II light harvesting complex gene B1B2	LHCB1.5	5	0
photosystem I subunit D-2	PsaD2	6	1
photosystem I subunit E-2	PsaE2	3	0
Photosystem I, PsaA/PsaB protein	PsaA/PsaB	8	0

Co-IP was performed with thylakoids from WT grown under low light, TAP38-HA and TAP38-GFP line using HA affinity matrix (WT and TAP38-HA line) or GFP trap beads (WT and TAP38-GFP line) (see chapter 2.15). The elutions from the Co-IP were subjected to mass spectrometry (MS) analyses and the MS analyses results from single representation run was shown and only proteins identified with at least 3 unique peptides in all 3 experiments were listed.

3.7 At low light TAP38 is present in lower amounts compared to STN7

To quantify the amount of TAP38 and STN7 in WT thylakoids under low light (state 2), N-terminal His-tag fusions of TAP38 and STN7 proteins were expressed in *E. coli* and purified. Dilution series of heterologously expressed proteins and thylakoids were separated on SDS-PAGE and subjected to immunoblotting using specific antibodies against TAP38 and STN7, respectively (Figure 17). The signal intensities were analyzed with Fusion FX7 image acquisition system (VilberLourmat) and then the protein amount in thylakoids (per μg chlorophyll) were calculated. As listed in table 3, the concentration of STN7 was 0.092 pm per μg of chlorophyll ($\text{pm } \mu\text{g}^{-1} \text{ Chl}$), which is 3 times more than the concentration of TAP38 ($0.028 \text{ pm } \mu\text{g}^{-1} \text{ Chl}$).

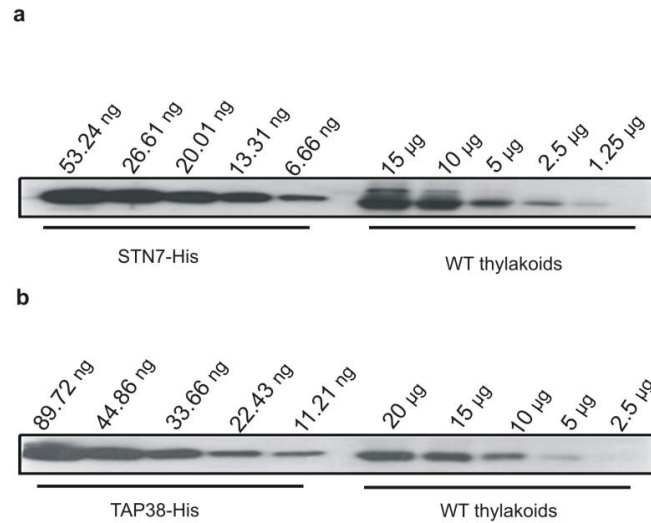


Figure 17 In low light acclimated plants TAP38 is accumulated in lower amounts compared to STN7.

(a) Western detection of STN7 in WT thylakoids. Recombinant STN7 (STN7-His) was expressed in *E. coli* strain BL21 with N-terminal 6 x His-tag and purified via Ni-NTA column. The protein concentration of the purified protein was determined by Amido black staining. Thylakoids were isolated from WT plants grown under LL conditions. Decreasing levels of STN7-His and thylakoids were loaded according to the protein quantity or chlorophyll concentration and analyzed by Western blot using STN7 specific antibody. The image was obtained by Fusion FX7 image acquisition system. (b) Western detection of TAP38 in WT thylakoids. All procedures were performed according to the same procedure as described in (a).

Table 3 Quantification of TAP38 and STN7 in low light adapted thylakoid membranes.

Proteins	Amount (ng/µg Chl)	Molecular amount (pm/µg Chl)
STN7	5.05±0.48	0.092±0.01
TAP38	1.05±0.29	0.028±0.01

The Westernblots signals from Figure 17 were quantified by Fusion FX7 image acquisition system (VilberLourmat) to obtain the STN7 and TAP38 amounts in thylakoids (ng µg⁻¹ Chl), then the corresponding molecular amount of each protein was calculated (pm µg⁻¹ Chl). Values ± standard deviations are shown.

3.8 Is TAP38 the true counter player of STN7?

Long term response (LTR) is a process that leads to the readjustment of the stoichiometry of the photosystems depending on the environmental light conditions. The ratio of chlorophyll a over chlorophyll b (Chl a/b) and steady fluorescence over maximum fluorescence (F_s/F_m) are indicator for changes in photosystem stoichiometry (Bailey et al., 2001; Dietzel and

Pfannschmidt, 2008; Pfannschmidt et al., 2001; Walters, 2005). Chl a/b ratio indicating PSI/PSII ratio is usually higher in PSII-light acclimated plants compared to that in PSI-light acclimated plants. Whereas F_s/F_m value which can also reflect PSII/PSI ratio behaves in the opposite way being higher in PSI-light acclimated plants and lower in PSII-light acclimated plants (Dietzel and Pfannschmidt, 2008).

During a shift between PSI and PSII light, the *stn7* mutant is not able to readjust the stoichiometry between PSI and PSII which can be determined by lack in changes of the F_s/F_m value or the chlorophyll a/b ratio (Pesaresi et al., 2009). Considering that TAP38 counteracts STN7 in state transitions and the *stn7* mutant is devoid of LTR (Bonardi et al., 2005; Pesaresi et al., 2009), the function of TAP38 in LTR was studied using *tap38* mutant and the *oeTAP38* line. WT, *stn7* and *oeSTN7* were selected as controls and LTR was monitored by measuring the F_s/F_m value and the chlorophyll a/b ratio (Chl a/b ratio). At the same time, the chlorophyll fluorescence parameters Φ_{II} and 1-qP were measured to assess PSII efficiency. Φ_{II} represents the effective quantum yield of PSII while the excitation pressure, 1-qP, provides a measure of the fraction of closed PSII centers. PSI and PSII lights were set as described (chapter 2.2). For long term acclimation, plants were initially grown for 10 d under white light, followed an acclimation period. In detail, plants were grown under PSI or PSII light for 6 d (PSI or PSII light) or they were first acclimated to PSI light for 2 d followed by 4 d under the PSII light source or *vice versa* (PSI-II or PSII-I light). All the parameters were measured as described in chapter 2.8.

3.8.1 Response of *tap38-3* and *oeTAP38* to the long term acclimation as monitored by chlorophyll a/b ratios and F_s/F_m values

For WT, the chlorophyll a/b ratios were higher under PSII and PSI-PSII light than under PSI and PSII-I light whereas the F_s/F_m ratio behaved in the opposite manner (Figure 18a, 18b). In the *stn7* mutant, both values for F_s/F_m or Chl a/b ratio remained unaltered under these changing light conditions and were typical for plants acclimated to PSI (Figure 18a, 18b). The overall behaviors of *tap38* mutants and *oeTAP38* resembled that of WT (Figure 18). However, the Chl a/b ratios were in general a bit higher in *tap38* and lower in *oeTAP38* in comparison to WT under all conditions applied (Figure 18a). To address this difference, the Chl a/b ratio was further analyzed with WT, *tap38-3*, and *oeTAP38* and the results confirm this observation (Figure S2).

Noticeably, there was a tendency for F_s/F_m values in *oeTAP38* which were generally higher compared to WT. This tendency was similar to that of *stn7* which is blocked in state 1.

Under all light conditions applied, the Φ_{II} and 1-qP values of *stn7* remained stable and either equally lower or higher than those of WT, indicating that the *stn7* mutant was suffered during the light acclimation process due to its block in state 1 (Figure 18c, 18d). As expected, the WT showed relatively higher 1-qP and lower Φ_{II} values under PSI and PSII-I conditions compared to PII and PI-II light conditions. In accordance to the Chl a/b ratio and F_s/F_m values, the 1-qP and Φ_{II} values in *oeTAP38* and *tap38* mutants resembled WT again suggesting no impairment in LTR. Notably, even if *oeTAP38* showed a certain degree of acclimation, its 1-qP value remained on higher level than that of WT and rather similar to *stn7* (Figure 18c). This tendency could also be observed for the Φ_{II} value (Figure 18d). Taking together, *oeTAP38*, *tap38-1* and *tap38-3* behaved similar to WT regarding the assessed parameters indicating that they are able to perform LTR (Figure 18a, 18b). Neither the absence nor the overexpression of TAP38 resulted in major perturbation in LTR. However *oeTAP38* lines, to certain extent, resemble *stn7* mutants suggesting a moderate role of TAP38 on LTR.

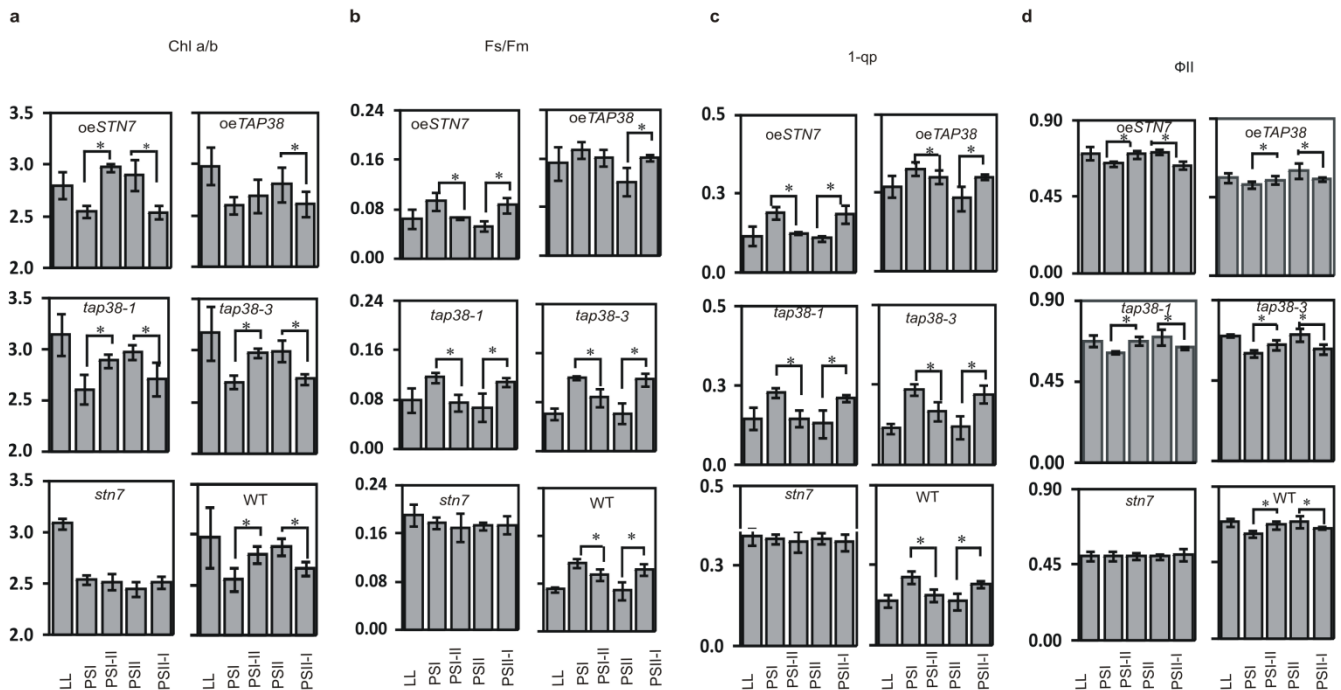


Figure 18 Measurement of LTR-acclimation of TAP38 mutant and overexpressor plants

(a) Chlorophyll a/b ratios of WT, *tap38-1*, *tap38-3*, *stn7*, *oeTAP38* and *oeSTN7* measured after exposure to different light conditions. PSI and PSII lights were set as described (chapter X), and then plants were initially grown for 10 d under white light, followed by an acclimation period. In detail, plants were either grown under PSI or PSII light for 6 d (PSI or PSII plants) or were first acclimated to PSI light for 2 d followed by 4 d exposure to PSII light source or *vice versa* (PSI-II or PSII-I plants). Plant material was harvested under the respective growth light, grinded in liquid nitrogen and pigments were extracted with 80% buffered acetone. Chlorophyll concentrations and Chlorophyll a/b ratios were determined and calculated according to Porra et al. (1989). (b) The F_s/F_m value of WT, *tap38-1*, *tap38-3*, *stn7*, *oeTAP38* and *oeSTN7* measured after exposure to the same light conditions as in (a). The minimal fluorescence (F_0) was determined after 15 min dark adaptation, then leaves were exposed to a 1600-ms flash of saturating white light ($3000 \mu\text{mol photons m}^{-2} \text{s}^{-1}$) to determine maximal fluorescence (F_m), whereas the steady state fluorescence (F_s) was measured after illumination with $90 \mu\text{mol photons m}^{-2} \text{s}^{-1}$ of actinic red light (620 nm) for 10 min. At the end, minimal fluorescence of light adapted plants (F_0') as determined after switching off the actinic red light. (c) The excitation pressure of PSII (1-qP) was measured as in (b), and $1-qP=1-(F_m'-F_s)/(F_m'-F_0)$. (d) Effective quantum yield of PSII (Φ_{II}) was measured as in (b), and $\Phi_{II}=(F_m'-F_s)/F_m'$. Average values (\pm SD) of individual plants were shown and the stars indicate that two data sets are significantly different from each other according to Student's *t*-test.

3.8.2 Microarray analyses on *tap38* and *oeTAP38* show no significant changes on transcriptome level

In the *stn7* mutant, as well as in other mutants defective in LTR (e.g. *psae1-3*, *psad1-1*), a large number of genes are differently regulated relative to WT as described before (Pesaresi et al., 2009). If TAP38 is required for LTR, the transcriptomic profiles of *tap38* mutant and *oeTAP38* would be as well altered compared to WT. To address this question, transcript profiles of *tap38-1*, *oeTAP38* and WT were generated by microarray analyses and additionally compared to already existing data sets of the *stn7* mutant (Pesaresi et al., 2009). As depicted in Figure 19, in total only five genes in *tap38-1* and two genes in *oeTAP38* were identified to be differentially regulated compared to WT. The only one overlap gene between *tap38-1* and *oeTAP38* was *TAP38* itself which was reduced to 5% in *tap38-1* and increase six folds in *oeTAP38*. Another gene (At5g58310, Methyl Esterase 18) altered in *oeTAP38* was also changed in *stn7* in which transcripts of 1191 genes were changed in comparison to WT. Moreover, no overlap was found between *tap38-1* and *stn7*. In case a specific signaling pathway is perturbed in *stn7* regarding

LTR leading to significant changes in the transcript profile, a lack or overexpression of TAP38 does not affect this long term acclimation signaling pathway.

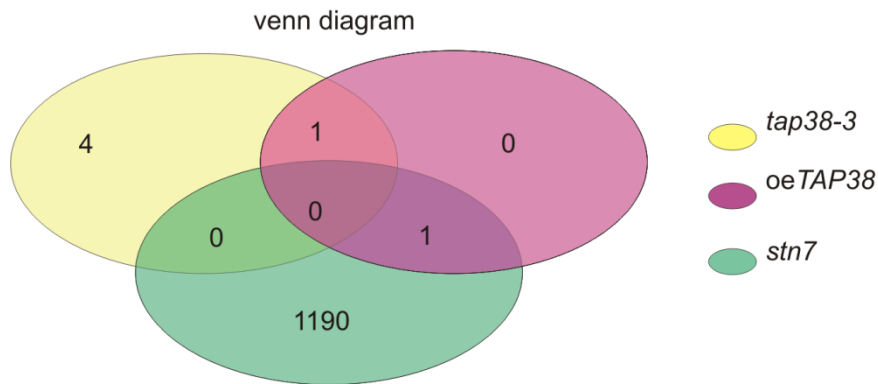


Figure 19 Venn diagram depicting the overlap of genes whose expression was found in Microarray analysis to be differentially regulated.

RNA was isolated from 4-week-old plants (WT, *tap38-1* and *oeTAP38*) using the RNeasy Microarray Tissue Mini Kit (QIAGEN), and in total 1 mg RNA of each genotype was sent to NASC for microarray analysis. The number of genes that were differentially regulated in each line was indicated. The transcript data for the *stn7* mutant was described by Pesaresi et al. (2009).

3.9 Generation of thylakoid hyper- and hypo-phosphorylation double mutants

Despite the fact that *oeSTN7* displays a five-fold increase in STN7 protein levels compared to WT, state transitions are still regulated by PQ pool in this line which can be demonstrated by the phosphorylation of LHCII upon oxidation of PQ pool when *oeSTN7* plants are exposing to FR light (Lemeille et al., 2009; Wagner et al., 2008; Willig et al., 2011; Wunder et al., 2013). The counteracting phosphatase, TAP38, is suggested to be redox-independent (Lemeille et al., 2009), which was confirmed in this work (Figure 8). It was tempting to speculate that the combination of the genetic backgrounds *oeSTN7* and *tap38* mutant could result in hyper-phosphorylation of thylakoid proteins and the combination of *stn7* and *oeTAP38* would lead to hypo-phosphorylation instead. To push thylakoid phosphorylation or dephosphorylation to its extremes, double mutants were generated by crossing *tap38-1* with *oeSTN7*, or *oeTAP38* with *stn7*, respectively. The LHCII phosphorylation in those double mutants was monitored by immunodetection with phosphothreonine specific antibodies under D, LL, and FR conditions. As expected, the WT

showed an increase in pLHCII during transition from state 1(D) to state 2 (LL) followed by a decrease upon PSI light exposure (state 1). The *stn7 oeTAP38* did not show any LHCII phosphorylation under all light conditions applied similar to *stn7* (Figure 20). The observed decrease of pLHCII in *tap38-1* under PSI light might be due to residual amounts of TAP38 which were sufficient to dephosphorylate pLHCII after PSI light treatment. However, the amount of pLHCII was still much higher compared to WT. The decrease of pLHCII in *oeSTN7* could be primarily attributed to STN7 inactivation (Bellafiore et al., 2005; Wunder et al., 2013). Surprisingly, *tap38-1 oeSTN7* showed much higher level of pLHCII than the respective single mutants under PSI light, even if pLHCII levels were similar to *oeSTN7* and *tap38-1* under low light and PSII light (Figure 20). In theory, this double mutant might display increased phosphorylation levels for some phosphoprotein-substrates which are normally phosphorylated to a less extent in WT. Thus, these crossings represent genetic material that could be used to screen for substrates in the future.

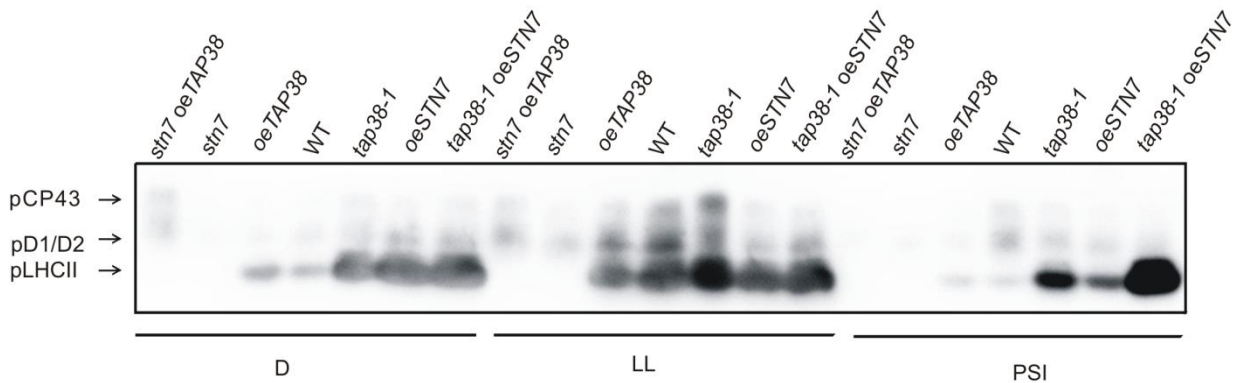


Figure 20 LHCII phosphorylation in hyper- and hypo-phosphorylation mutants.

Various mutants (*stn7 oeTAP38*, *stn7*, *oeTAP38*, *tap38-1*, *oeSTN7* and *tap38-1 oeSTN7*) and WT plants were kept in dark (D), subsequently expose to low light (LL) for 2h, and then to PSI light (PSI) for 2h. Thylakoids were isolated and fractionated by SDS-PAGE and phosphorylation of LHCII was detected by immunoblot analysis using phosphothreonine specific antibodies.

3.10 Second dimension protein separation by isoelectric focusing and SDS-PAGE gel electrophoresis

The chloroplast kinases STN7 and STN8 are suggested to share various substrates, as phosphorylated forms of LHCII and PSII core proteins are completely absent only in the *stn7stn8* double mutant but not in the respective single mutants (Bonardi et al., 2005; Fristedt and Vener, 2011). Likewise the two thylakoids phosphatases, TAP38 and PBCP were shown to exhibit certain substrate overlap (Pribil et al., 2010; Samol et al., 2012). Therefore, TAP38 may have more substrates in the thylakoid membrane besides LHCII, D1, D2 and CaS proteins. Moreover, there is comprehensive evidence for an extensive phosphorylation of both stromal proteins and thylakoid membrane proteins in the chloroplast (Bayer et al., 2012; Laing and Christeller, 1984; Reiland et al., 2009; Sugiyama et al., 2008). As the phosphatase domain of TAP38 protein is exposed to the stroma side (see Figure 6), it is possible that TAP38 also plays a role in stromal protein dephosphorylation. To test these hypotheses, thylakoid and stromal proteins of *tap38-1 oeSTN7*, *stn7*, *oeTAP38* and mutants with hyper-/hypo- phosphorylation (see chapter 3.10) were subjected to second dimension (2D) protein separation by isoelectric focusing (IEF) and SDS-PAGE as described (chapter 2.12).

After precipitation by 80% acetone, 50 µg of thylakoid proteins from *oeSTN7 tap38-1* and *stn7 oeTAP38* were separated in Immobiline™ Drystrips (gradient pH 3–10 NL, GE Healthcare) according to their isoelectric points. Subsequently second dimension separation by SDS-PAGE was carried out and Western blotting analysis was performed using phosphothreonine specific antibodies. As shown in Figure 21a (upper panel), the Coomassie brilliant blue staining (CBB) of the Western blot membrane before antibody application did not show any difference between *tap38-1 oeSTN7* and *stn7 oeTAP38*. Immunodetection using phosphothreonine specific antibodies revealed that all detectable phosphoproteins were distributed in a narrow region on the 2-D IEF-SDS PAGE between pH 4-7 (Figure 21) and several thylakoid proteins (D1, D2, CP43 and CP47) which are known to be phosphorylated in WT could not be detected clearly. However, we observed obvious differences between *oeSTN7 tap38-1* and *tap38-1 oeSTN7*. At least 4 protein signals were exclusively phosphorylated in *oeSTN7 tap38-1* compared to *stn7 oeTAP38* with a protein size of 26, 34, 55-60 and 170 kDa respectively (Figure 21 upper panel). LHCII is a substrate of TAP38 and STN7 (Bellafiore et al., 2005; Pribil et al., 2010); therefore the 26-kDa signal could be attributed to LHCII. The 34-kDa signal could be ascribed to D1/D2 which were

also shown to be partially phosphorylated by STN7 and dephosphorylated by TAP38 (Bonardi et al., 2005; Pribil et al., 2010). The 55-60 kDa spot could be the β -subunit of chloroplast ATPase or/and STN7. Both of them were identified to be phosphorylated via MS and/or biochemical approaches (del Riego et al., 2006; Lohrig et al., 2009; Reiland et al., 2009). However, there was no indication regarding the identity of the 170-kDa signal. Nonetheless, the result suggested that further thylakoid proteins especially the 55-kDa protein might be novel substrates of TAP38 or/and STN7.

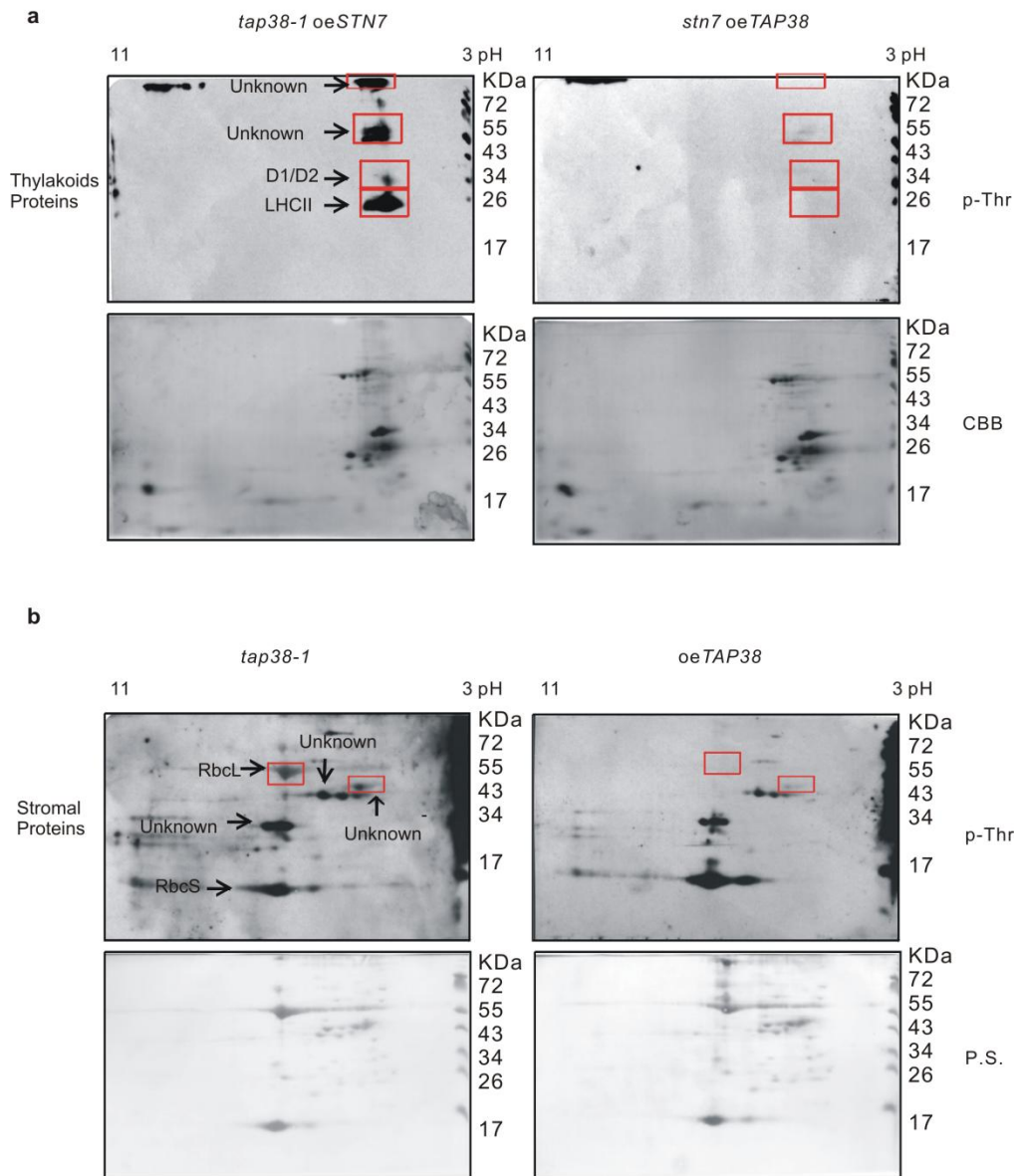


Figure 21 Second dimension-IEF gel analyses of thylakoid and stromal proteins.

(a) Thylakoid proteins (corresponding to 50 μ g Chl) from *tap38-1 oeSTN7* and *stn7 oeTAP38* were subjected to IEF gels as described (see chapter 2.12), and second dimension analyses were carried out by

12% SDS-PAGE. Subsequently, Western blotting was performed on the second dimension using phosphothreonine specific antibodies (p-Thr). The membrane was stained with Coomassie brilliant blue (CBB) prior to immunodetection. Differences between *tap38-1* oe*STN7* and *stn7* oe*TAP38* are highlighted by rectangles and indicated by arrows. (b) Stromal proteins (500 µg) from *tap38-1* and oe*TAP38* were subjected to 2D IEF analyses as described. The membrane was stained with or Ponceau S (P.S.) prior to immunodetection. The rectangles highlight the differences between *tap38-1* and oe*TAP38*. All the detected proteins were including proteins which were equally phosphorylated in these two lines (RbcL, RbcS and unknown proteins) are indicated by arrows. Pre-stained protein markers are shown in kDa and the pH reflects the direction of the first dimension of IEF gel.

Stroma proteins from *tap38-1* and oe*TAP38* were also subjected to 2D IEF-SDS PAGE analyses. The Ponceau S staining for the membranes did not show any difference between these two lines (Figure 21b upper panel). The Western blotting results revealed that several proteins were equally phosphorylated in *tap38-1* and oe*TAP38*, e.g. RbcS (Rubisco small subunit), an unknown 35-kDa protein and another 55-kDa protein. Surprisingly RbcL (Rubisco large subunit) and one protein signal around 60 kDa which were strongly phosphorylated in *tap38-1* totally disappeared in oe*TAP38* (Figure 21b) indicating it was exclusively dephosphorylated by TAP38. Therefore, it seems TAP38 is also responsible for the dephosphorylation of some stroma proteins.

Many efforts were made to reveal the identities of those new potential substrates in the thylakoids and stroma, but it was not possible in the scope of this work to sequence them via MS (data not shown). However, those results were reproducible. Taken together, these findings allowed us to conclude that there seem to be further substrates of TAP38 in the thylakoid membrane and stroma beyond LHCII.

4 Discussion

4.1 TAP38 is not regulated by the PQ pool redox in contrast to the counteracting kinase STN7

The protein amounts of LHCII kinase (STN7 and STT7) proteins become significantly decreased under prolonged state 1 light condition (FR) and HL (Bellafiore et al., 2005; Depege et al., 2003; Lemeille et al., 2009; Willig et al., 2011). To investigate this more comprehensively, STN7 amounts were analyzed under different redox state of the PQ pool including transient and constant changes. Since different light qualities induce changes in the PQ redox state (Wagner et al., 2008), transient changes of the PQ redox state were obtained by exposing plants to different light qualities (Wunder et al., 2013). Results showed that the STN7 protein levels in WT plants adapted to PSII light were significantly higher than those in plants adapted to PSI light (Wunder et al., 2013). This is in line with the PQ pool being more reduced under PSII light compared to PSI light (Wagner et al., 2008; Wunder et al., 2013). Wunder et al. (2013) also addressed the effects of a constitutive alteration in the PQ redox state on STN7 accumulation. In mutants with a permanently over-reduced PQ pool (e.g. *psae1-3*, *psad1-1* and *psal-1*), STN7 levels were increased compared to WT, whereas in mutants with an over-oxidized PQ pool (e.g. *tap38-1*), the STN7 levels were reduced (Wunder et al., 2013). Therefore, STN7 amounts depended on the redox state of PQ pool (Wunder et al., 2013). Furthermore, it was shown that STN7 abundance is also controlled at the transcript level with the protein amounts directly correlating with the respective mRNA levels under prolonged high light and in mutant plants with an over-oxidized PQ pool (Wunder et al., 2013).

Besides STT7/STN7 mRNA and protein amounts also STN7 activity is redox-dependently regulated via the redox state of the PQ pool and the stromal ferredoxin-thioredoxin system. There are two conserved Cysteine residues (68 and 73) at the N-terminal region of STT7 /STN7, which were shown to be essential for STT7 activity and state transitions (Depege et al., 2003). Recently, a new model for STN7 regulation suggested that the activation of the kinase under low light conditions was controlled by the two Cysteines on the luminal side, whereas under high light, the reduction of two conserved stromal exposed Cysteines by thioredoxin could be attributed to the inactivation of the kinase (Puthiyaveetil, 2011).

Bennett (1980) suggested that a potential LHCII phosphatase would be indifferent to light (Bennett, 1980) and based on *in vitro* experiments this phosphatase was not susceptible to redox regulation (Silverstein et al., 1993). To address this hypothesis, we assessed the expression of *TAP38* under state 1 (dark or far-red light), state 2 (low light or PSII light) and high light conditions more comprehensively. To this end, *TAP38* accumulation was detected in WT plants that were adapted to the dark, PSII light, far red light and high light over a longer period. The result was a high and constant expression of *TAP38* independent of the applied light conditions (Figure 8a). Based on these findings, *TAP38* protein levels seem not to be influenced by prolonged changes in light conditions, suggesting that regulation on the protein level via the PQ pool redox state as the case of *STN7* (Figure 8a) does not take place. This is in agreement with previous findings which showed that there were no significant changes in *TAP38* amounts upon short-term transfer of WT plants to different light conditions (Pribil et al., 2010; Shapiguzov et al., 2010).

To gain information on a potential regulation of *TAP38* on the level of its enzymatic activity, *TAP38* activity was assayed *in vitro* by applying different concentrations of NaF, a phosphatase inhibitor, on isolated thylakoids. In WT, the de novo amounts of phosphorylated LHCII accumulated progressively with increasing concentrations of NaF (Figure 8b). In the *TAP38* overexpressor line (*oeTAP38*), significantly higher amounts of NaF had to be added to observe similar effects (Figure 8b). It seemed that the amount of pLHCII correlated positively with NaF amount and inversely with *TAP38* abundance (Figure 8b). These observations suggest that *TAP38* activity was not down-regulated by low light exposure, a light condition under which *TAP38* inactivation would make most sense from a physiological point of view and that there was a clear correlation between *TAP38* amounts and LHCII dephosphorylation capacity. Combining the data on the expression profiles under different light treatments and the activity assay under low light, one can conclude that *TAP38* is not regulated in a redox-dependent manner, at least not dependent on the redox states of PQ pool.

To further investigate whether *TAP38* was regulated by long-term changes of the PQ pool redox state, *oeTAP38* was crossed with the mutant lines *psad1-1* and *psae1-3*, which display a constitutive over reduced PQ pool compared to WT (Ihnatowicz et al., 2008; Ihnatowicz et al., 2004; Pesaresi et al., 2009). *TAP38* was still able to accumulate at high levels (6-fold compared to WT) in these genetic backgrounds showing that *TAP38* accumulation is *per se* independent from that of PSI and occurs also in the presence of a

constantly over-reduced PQ pool (Figure 9b). Furthermore, the *psad1-1 oeTAP38* and *psae1-3 oeTAP38* double mutants showed exacerbated phenotypes (Figure 10a) which could be attributed to an even more severely reduced PQ pool as displayed by a significantly increased 1-qL (Table 1). These behaviors were similar to *stn7 psad1-1* and *psae1-3 stn7* (Pesaresi et al., 2009). Biochemical analyses of these lines indicated that LHCII phosphorylation and the band representing the PSI-LHCI-LHCII complex in BN-PAGE analyses (Pesaresi et al., 2009) were almost absent in the double mutants similar to the situation in *oeTAP38* (Figure 10b). Summarizing this, it seems quite clear that TAP38 is insensitive to the redox state of PQ pool regarding TAP38 accumulation and activity. This suggests that LHCII phosphorylation and therefore state transitions are predominantly controlled via the redox-sensitivity of the STN7 kinase.

4.2 TAP38 is present in lower amounts than STN7

STN7-dependent LHCII phosphorylation and the transition from state 1 to state 2 is at least seven-fold faster than the dephosphorylation reaction of pLHCII by TAP38 and its migration back to PSII (Puthiyaveetil et al., 2012; Silverstein et al., 1993). Puthiyaveetil et al. (2012) proposed two possible explanations for that: (i) the phosphorylation is thermodynamically more favorable than the dephosphorylation reaction due to the free energy of phosphoryl transfer in the kinase reaction; (ii) TAP38/PPH1 is usually associated with PSI, and therefore it dephosphorylates its substrate only when the latter is part of the PSI antenna not part of the PSII antenna (Puthiyaveetil et al., 2012). Here, BN and sucrose gradient experiments were performed in order to confirm an interaction of TAP38 and PSI or any other photosynthetic complexes, but no stable association between TAP38 and PSI could be demonstrated (Figure 12a, 12b, 12c). However, results of Co-immunoprecipitation experiment, showed that PSI antenna proteins (LHCA1, LHCA2, LHCA4 etc.) and further some PSI core proteins (PsaA/B) can be pulled down together with HA- or GFP-tagged TAP38, indicating that TAP38 resides in close proximity to PSI (Table 2). Furthermore, the amounts of TAP38 and STN7 in WT thylakoids under low light conditions (state 2) were quantified by western blot (Figure 16). With a 0.092 pm per μg of chlorophyll the STN7 concentration was more than 3 times higher than the concentration of TAP38 (0.028 pm μg^{-1} Chl). The concentration of PsaD (PSI subunit) and Rieske (Cyt *b₆f* subunit) was 2.16 mmol⁻¹ Chl (2.4 pm per μg^{-1} Chl) and 1.35 mol⁻¹ Chl (1.5 pm per μg^{-1} Chl) respectively in *A.*

thaliana (Ambruster et al., 2013). Based on these findings, the molar ratio between STN7/TAP38 and PSI should be around 1:26/1:86. Consequently, the STN7/TAP38 to LHCII ratio would be 1:260/1:860, suggesting STN7 and TAP38 are acting in catalytic amounts. Notably, STT7 was also demonstrated to be present in substoichiometric amounts with a molar ratio of 1:20 relative to the Cyt *b₆f* complex and 1:200 relative to LHCII in *C. reinhardtii* (Lemeille et al., 2009). Therefore, we suggest in addition to the two explanations given above that a third reason for a lower efficiency of TAP38 relative to STN7 are the significant lower amounts of TAP38 compared to STN7 under state 2 conditions. This finding is also in good agreement with the accumulation of high levels of phosphorylated LHCII under light conditions when STN7 and the TAP38 are both activated.

4.3 TAP38 accumulation is regulated at the transcript level and correlates with the presence of LHCII and PSI.

The protein amounts of TAP38 were significantly reduced in *psad1-1*, *psae1-3*, *hcf136*, *psad1d2*, *chaos* and *asLHCB2.1* mutant lines but nearly unchanged in the *petc* and *atpd* mutants (Figure 9b, Figure 11b, Figure 14a). Notably, in the *psad1d2* double mutant, TAP38 was reduced to a larger extent than in the other mutants. Real-time PCR revealed that the TAP38 mRNA levels in those mutants were reduced by 20% - 60% compared to WT (Figure 6c, Figure 14b) suggesting a certain correlation between *TAP38* transcript and protein amounts. However, the mRNA patterns did not perfectly match the protein patterns and the mRNA levels were generally less reduced than the protein amounts compared to WT, suggesting an involvement of post-translational regulation to a certain extent, such as protein degradation as in the case of STN7 (Bellafiore et al., 2005; Depege et al., 2003; Lemeille et al., 2009; Willig et al., 2011; Wunder et al., 2013).

It is tempting to speculate that the redox state of PQ pool plays a role in the regulation of TAP38 amount although TAP38 was shown to be insensitive to redox changes of the PQ pool (chapter 4.1). Indeed, the PQ pool was highly reduced in *petc* and PSI mutants (*psad1-1*, *psae1-3* and *psad1d2*) (Ihnatowicz et al., 2004; Ihnatowicz et al., 2007), but rather oxidized in *hcf136* considering its lack of PSII complex (Meurer et al., 1998). In case the PQ pool exerts an effect on *TAP38* transcripts, one would expect an opposite regulatory effect on *TAP38* in *hcf136* and PSI mutants (*psad1-1*, *psae1-3* and *psad1d2*). However, the TAP38 abundance decreased in *hcf136* as well as in PSI mutants, but remained almost unaltered in *petc*.

Therefore, the alterations in TAP38 protein/mRNA amounts seem not to follow a clear redox-dependent regulatory scheme.

A second possibility was that a reduction in PSI or LHCII amount causes the decrease of TAP38. Regarding the PSI mutants (*psad1-1*, *psae1-3*, *psad1d2*), PSI abundance was reduced to about 70% of the WT level in *psad1-1*, *psae1-3* (Ihnatowicz et al., 2007; Ihnatowicz et al., 2004) and not even detectable in *psad1d2* (Ihnatowicz et al., 2004). Also in *hcf136* the amount of PsaD (PSI subunit) and TAP38 were markedly decreased (Figure 14a) (Meurer et al., 1998). On the contrary, in *petc* and *atpd* PSI levels and TAP38 amounts did not significantly alter from WT (Figure 14a). In case of mutant lines defective in LHCII, LHCII (LHCB1 and LHCB2) were strongly downregulated to an undetectable level in anti*LHCB2* (Andersson et al., 2003) and the LHCIIb (LHCB2) proteins decreased by ~50% in *chaos* shown by densitometric analysis (Klimyuk et al., 1999). Concluding, it seems that the accumulation of LHCII and PSI affects the abundance of TAP38.

With LHCII being the potential target of TAP38 (Pribil et al., 2010; Shapiguzov et al., 2010) and PSI being a putative anchor for TAP38 localization, as pLCHII is supposed to be associated with PSI, a direct interaction with the components seems a reasonable prerequisite. This hypothesis was supported to a certain extent by the comigration of TAP38 and LHCII in the sucrose gradient (Figure 11a, 12d, 12e) and transient association of TAP38 with LHCII and PSI as shown by co-immunoprecipitation in which the former two were pulled down by tagged-TAP38. However, no stable association of TAP38 with PSI could be observed during our experimental approaches (Figure 12). Furthermore, based on quantitative data, the molecular ratio of TAP38 to LHCII/PSI was 860:1/86:1 (Table 3) (see chapter 4.2). Therefore, the residual amounts of LHCII in *chaos* and the remaining amount of PSI in *psad1-1* and *psae1-3* should be sufficient for TAP38 to bind. In line with this, overexpression of TAP38 in the *psad1-1* and *psae1-3* background was successful (Figure 9, 10b, 10c) and in *psad1d2* mutant in which PSI was totally absent, there was still certain accumulation of TAP38. Overall, it seems that PSI and LHCII *per se* were not essential for TAP38 to accumulate within the thylakoid membrane.

Summarizing, one can conclude that TAP38 accumulation predominantly depends on the availability of its putative substrate (LHCII) and PSI and a potential regulation occurs at the transcript level and, if at all, to a minor extent on the post-transcription level.

4.4 TAP38 localized close to PSI

TAP38 is a thylakoid membrane protein with its N-terminus facing the stroma side (Figure 6). Fractionation and immunogold-labeling experiments both indicate that TAP38 was enriched in stroma lamellae where also its putative substrates (pLHCII) and PSI were localized (Figure 7). But, a lack of TAP38 does not affect the accumulation of any of the major photosynthetic complex (Pribil et al., 2010). Furthermore, no stable association could be observed between PSI and TAP38 in BN gels and sucrose gradient ultracentrifugation although various detergents have been tried (Figure 12). Nonetheless, the behaviors of TAP38 in the BN gel were interesting and worth analyzing. It migrated to very high molecular weight region in the BN-PAGE gel when digitonin was used for thylakoids solubilization but was distributed in the free protein region if β -DM was used as a detergent. However, when thylakoids were crosslinked by DTSSP, TAP38 migrated to high molecular regions in the BN-PAGE even β -DM was used for solubilization (Figure 13a). Many photosynthetic complexes were found in this high molecular region that no specific association of TAP38 with any of them could be observed (Figure 13b). Noticeably, migration patterns of the major photocomplexes were not changed after DTSSP crosslinking suggesting the crosslinker DTSSP was not used in excess amounts (Figure 13a).

In the sucrose gradient ultracentrifugation fractions, TAP38 was present in the free protein region or low molecular weight complex region regardless whether digitonin or β -DM was used as a detergent (figure 12d and 12e) (data for digitonin were not shown). Only the use of NP40 as a detergent led to the accumulation of some intermediate size TAP38 complexes after BN-PAGE analysis and sucrose centrifugation. However, no perfect overlap between TAP38 and PSI or any other photosynthetic complexes could be observed (Figure 12b, 12c). Therefore, it seems that TAP38 localized spatially close to some major photosynthetic complexes, but the physical interaction between them is not strong enough to form a stable complex that can resist detergent treatment. Therefore, in further experiments, it would be worthwhile to perform BN-PAGE and sucrose centrifugation with crosslinked thylakoids.

Despite no stable association was present between TAP38 and PSI, a number of PSI antenna proteins and core proteins were pulled down together with tagged-TAP38 proteins in Co-IP experiments. Based on these results, we conclude that TAP38 localizes in close proximity to PSI and more precisely the LHCA belt. Noticeably, in the same pull down assay, LHCII, the putative substrate of TAP38 was also co-precipitated with TAP38. In line with this,

Pribil et al. (2010) already showed that TAP38 is able to dephosphorylate LHCII. Also, the PSII phosphatase PBCP was demonstrated to directly dephosphorylate PSII core proteins *in vitro* in support of a direct acting mode regarding the catalytic way of the phosphatases in the thylakoid membrane (Samol et al., 2012). These evidences indicate a very high possibility for a direct interaction between TAP38 and LHCII.

To summarize the findings in this and previous chapters, TAP38 is always active regardless of the redox state of the PQ pool and permanently resides in close proximity to PSI where TAP38 dephosphorylates LHCII directly. We propose a working model for TAP38 in LHCII dephosphorylation during state transitions in Figure 22.

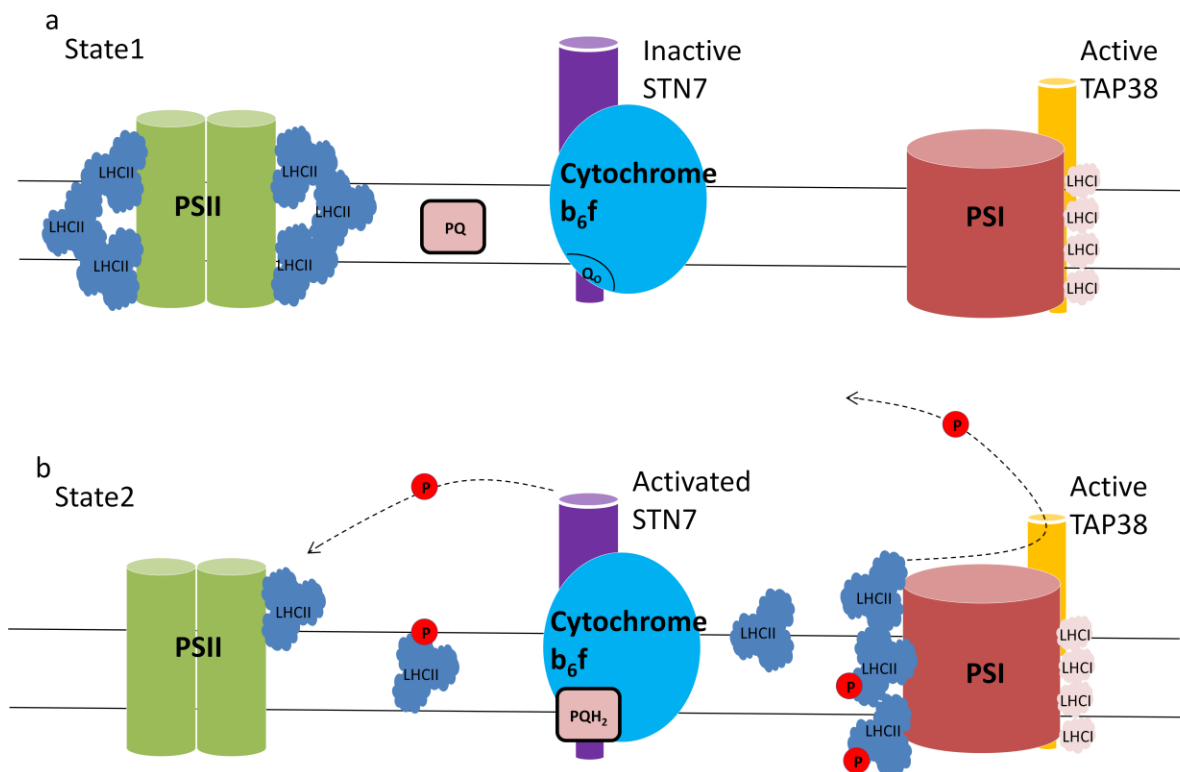


Figure 22 Simplified State transitions model indicating the working dynamic of TAP38.

(a) Under state 1 light conditions, the PQ pool is rather oxidized, STN7 is present in an inactive state and LHCII remains associated with PSII. In this situation, TAP38 resides close to PSI in an active state, however, no substrate (pLHCII) is available. (b) Under state 2 light conditions, the PQ pool becomes reduced and PQH_2 binds to the Q_o site of the Cytochrome b_6f complex. Thereby the STN7 kinase is activated leading to phosphorylation of LHCII. pLHCII subsequently disassociates from PSII and attaches to PSI. Active TAP38 now dephosphorylates pLHCII around PSI. However, the LHCII kinase is more efficient than TAP38, resulting in predominant association of pLHCII with PSI. Modified from Minagawa et al. (2011)

4.5 The function of TAP38 and STN7 in the long term response (LTR)

The long term response (LTR), which involves changes in photosystem stoichiometry, is induced by change in light quality that persists for hours or days. Long time differential excitation of the photosystems is sensed by the redox state of the PQ pool which in turn leads to a signal from the chloroplast to the nucleus, where the respective photosynthetic genes are encoded (Dietzel and Pfannschmidt, 2008; Nott et al., 2006). STN7 was suggested to be the trigger of LTR since *stn7* mutants display no change in the respective parameters (Bonardi et al., 2005; Pesaresi et al., 2009) and to participate in retrograde signaling affecting the expression of nuclear-encoded genes (Leister, 2012; Pesaresi et al., 2009; Wagner et al., 2008).

Considering that TAP38 counteracts STN7 in state transitions and *stn7* mutants lack LTR (Bonardi et al., 2005; Pesaresi et al., 2009), it is feasible to assume TAP38 might also function in LTR. Pesaresi et al. (2009) suggested that the signal transduction pathways associated with state transitions and LTR diverge directly at or immediately downstream of STN7 (Pesaresi et al., 2009). However, the LTR activities in the *tap38* mutant and *oeTAP38* resembled that of WT regarding the parameters F_s/F_m , Chl a/b ratio, Φ_{II} and 1-qP (Figure 11). Noticeably, the respective values of *oeTAP38* were close to those of *stn7* which is blocked in state 1 but they were still following the trend, typical for plants are able to perform LTR. In general, the Chl a/b ratios were a bit higher in *tap38* and lower in *oeTAP38* in comparison to WT under all conditions applied (Figure 11a). And the F_s/F_m values in *oeTAP38* behaved in the opposite way being much higher than those of WT (Figure 11b). In accordance to these, the 1-qP and Φ_{II} values of *oeTAP38* were higher than that of the WT and rather similar to the *stn7* values (Figure 11c). The same tendency could also be observed for the Φ_{II} values (Figure 11d). Taken together, *oeTAP38*, *tap38-1* and *tap38-3* mutant behaved similar to WT regarding the assessed parameters indicating that they are able to perform LTR (Figure 11a, 11b).

It is commonly accepted that LTR involves the regulation of *de novo* synthesis of chlorophyll a and its binding proteins (Murakami et al., 1997). Moreover, photosystem core proteins are mainly regulated on transcriptional level by changes of PQ redox state pool (Pfannschmidt et al., 1999). Depletion of STN7 resulted in the differential expression of a total 1991 genes when plants were grown under controlled growth conditions (Bonardi et al., 2005). Contrarily, in the expression profile of *tap38* and *oeTAP38* mutant lines no more than 5 genes were differentially regulated compared to WT (Figure 12). Out of those 5 genes of which one was TAP38 itself, only 1 gene was conversely regulated compared to *stn7* (Pesaresi et al.,

2009). In case a specific LTR signaling pathway is perturbed in *stn7* which leads to significant changes in the nuclear transcript profile, a lack or overexpression of TAP38 does not affect this long term acclimation signaling pathway.

The expression of many nuclear encoded photosynthetic genes were not affected in *stn7* (Bonardi et al., 2005) and changes in the expression of other genes might be caused by incapability to oxidize the PQ pool which results from imbalance in electron transport due to permanent detachment of LHCII from PSI (Tikkanen et al., 2012). Moreover, the *stn7* mutant showed an increased PSI-PSII ratio under white light which leads to WT like growth size. This implies that *stn7* persists the ability to transfer retrograde signals (Grieco et al., 2012; Tikkanen et al., 2006). In line with this, *stn7* mutant also showed a higher Chl a/b ratio under low light compared to other light conditions for inducing LTR (Figure 17a). Tikkanen et al. (2012) suggested that by controlling LHCII-phosphorylation, STN7 might play an important role in retrograde signaling through ROS but STN7 itself was not the central factor of redox-induced LTR (Tikkanen et al., 2012). The chloroplast sensor kinase (CSK), a further potential sensor of the PQ pool redox state, was described to govern the LTR with the chloroplast factor 1 (SIG1) and plastid transcription kinase (PTK) being its functional partners (Puthiyaveetil, 2011).

It was also observed that under steady state light conditions, the lower Chl a/b ratio in the *stn7* mutant did not result from changes in photosystem stoichiometry (almost no alteration in the accumulation of PSI and PSII subunits and their antenna proteins) suggesting an effect of STN7 on Chl a synthesis or Chl b degradation (Tikkanen et al., 2012; Tikkanen et al., 2006). In line with this, several genes involved in the isoprenoid biosynthesis or degradation were correlated with *STN7* (Tikkanen et al., 2012). *STN7/TAP38* were also suggested to display an activity in the degradation of controlled LHCII (Tikkanen et al., 2012). Since only a few genes were differentially regulated at the transcriptional level in *tap38* or *oeTAP38 mutant* plants (Figure 18), the overall higher or lower Chl a/b ratio in *tap38-3* and *oeTAP38* respectively (Figure 17a, S3) could either be caused by an enhanced or diminished capability to degrade Chl b.

The *Stn7* mutants grown under white light showed distinct photosynthetic protein compositions compared to WT, but the transcript profile remained unchanged. Apparently, STN7 also participates in the post-transcriptional regulation of various gene involved (Tikkanen et al., 2006). Therefore, TAP38 might be involved in the post-transcriptional

regulation of certain photosynthetic proteins leading to a trend of Chl a/b ratio and F_s/F_m values in *tap38-3* and *oeTAP38* towards *stn7*.

Taken all together, lacking or overexpression of TAP38 exerts no significant effects on LTR, but TAP38 may play a role in degradation of Chl b and/or post-transcriptional regulation for a number of photosynthetic genes.

4.6 Potential new substrates of TAP38

According to bioinformatic predictions there should be about 80 protein kinases (PKs) present in the chloroplast (Bayer et al., 2012) whereas only 27 protein phosphatases (PPs) were clearly predicted to be localized in the chloroplast and only 9 of them could actually be experimentally confirmed to be chloroplast located (Schliebner et al., 2008). Apparently, the numbers of PPs in the chloroplast is much lower than those of PKs.

STN8 was demonstrated to predominantly phosphorylate PSII proteins (D1, D2, CP43 and PsbH respectively) (Bonardi et al., 2005; Tikkanen et al., 2008a). However, it further catalyzes the phosphorylation of the calcium-sensing receptor (CaS), PGRL1, the large subunit of RuBisCo (RbcL), CP29 and of two unknown proteins (Lemeille and Rochaix, 2010; Lohrig et al., 2009; Reiland et al., 2011; Vainonen et al., 2008). On the other hand, STN7 predominantly phosphorylates LHCII, with CP29 and TSP9 being further identified as substrates (Bellafiore et al., 2005; Fristedt et al., 2009; Fristedt and Vener, 2011). Only in the *stn7stn8* double mutant, phosphorylated forms of LHCII and PSII core proteins are completely absent but not in the respective single mutant, suggesting STN7 and STN8 overlap to a certain degree in their substrate specificity (Bonardi et al., 2005; Fristedt and Vener, 2011). Likewise, the two thylakoids phosphatases, TAP38 (LHCII phosphatase) and PBCP (PSII phosphatase) show a certain substrate overlap (i.e. D1, D2 and LHCII) (Pribil et al., 2010; Samol et al., 2012). Interestingly, CaS, one of the substrates of STN8, was suggested to be dephosphorylated by TAP38 (Pribil et al., 2010). These findings indicate the network of reversible phosphorylation is indeed very complex within the chloroplast. We therefore postulate that TAP38 must have further substrates in the chloroplast membrane besides the proteins LHCII, D1, D2 and CaS. Indeed, there are various evidences for an extensive phosphorylation of stroma proteins and chloroplast proteins in general (Bayer et al., 2012; Laing and Christeller, 1984; Reiland et al., 2009; Sugiyama et al., 2008). Since the phosphatase domain of TAP38 is exposed to the stroma side (see Figure 6), it is feasible that

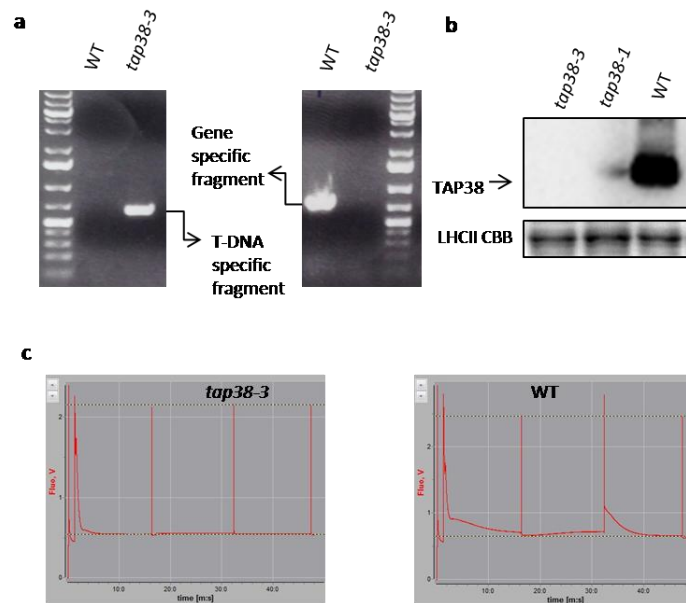
TAP38 also plays a role in stroma protein dephosphorylation. This hypothesis was confirmed by 2D isoelectric focusing (IEF) and SDS-PAGE.

As depicted in Figure 21, in the 2D IEF-SDS PAGE carried out with thylakoids proteins from *stn7 oeTAP38* and *oeSTN7 tap38-1* at least 4 protein signals exclusively phosphorylated in *tap38-1 oeSTN7* compared to *stn7 oeTAP38* with a protein size of 26, 34, 55-60 and 170 kDa respectively. LHCII is one substrate of TAP38 and STN7; therefore the 26-kDa band could be attributed to LHCII. The 34-kDa protein could be ascribed to D1/D2 which was also shown to be partially phosphorylated by STN7 and dephosphorylated by TAP38 (Bonardi et al., 2005; Pribil et al., 2010). In agreement with that, the amount of phosphorylated D1/D2 was decreased in the *stn7 oeTAP38* in comparison to *oeSTN7 tap38-1*. As for the 55-60 kDa double bands, they could represent the β -subunit of the chloroplast ATPase (ATPase β) or/and STN7, both of which were identified to be phosphorylated by mass spectrometry and/or biochemical approaches (del Riego et al., 2006; Lohrig et al., 2009; Reiland et al., 2009). STN7 was phosphorylated and the STN7 amount was significantly increased in the *oeSTN7 tap38-1* line which might explain STN7 detection in this approach (Figure S3). So far no kinase was found to be responsible for STN7 phosphorylation; therefore STN7 might show antophosphorylation (Willig et al., 2011). Moreover, the phosphorylation of STN7 which occurs at four conserved residues (Ser⁵²⁶, Thr⁵³⁷, Thr⁵³⁹ and Thr⁵⁴¹) was demonstrated to play a role in its turnover (Willig et al., 2011). In line with that, thylakoids used in this approach were obtained from plants grown under low light which favors the accumulation of STN7. The α/β -subunit of ATPase were also identified to be phosphorylated at multiple residues (mainly serine and threonine) in Spinach, Barley and *Arabidopsis* (del Riego et al., 2006; Lohrig et al., 2009; Reiland et al., 2009). Moreover, casein kinase II (CKII) was reported to be involved in the phosphorylation of the β -subunit of ATPase in Spinach chloroplast (Kanekatsu et al., 1998). Regarding the 170 kDa signal, no known phosphoprotein is available.

Furthermore, stroma proteins of *tap38-1* and *oeTAP38* were subjected to 2D IEF-SDS PAGE, and westernblot analyses showed the large subunit of Rubisco (RbcL) and one protein spot around 50 kDa were solely phosphorylated in *tap38-1* (Figure 21b). RbcL and RbcS have been previously reported to be phosphorylated (Budde and Chollet, 1988; Guitton and Mache, 1987) and MS analyses revealed that phosphorylation occurs at multiple serine and threonine sites (Lohrig et al., 2009; Reiland et al., 2009). In spinach, the phosphorylation of RbcL enhanced dramatically with addition of NaF an inhibitor of phosphatase, suggesting an

involvement of phosphatase (Guitton and Mache, 1987). However, Reiland et al. (2011) suggested that RbcL might be phosphorylated by STN8. Regarding the protein spot at around 50 kDa, there was no clear indication with respect to its identity. Based on all of these findings, it is most likely that TAP38 has further substrates besides LHCII, both within the thylakoid membrane and the stroma. Thus a function of TAP38 beyond state transitions seems very likely.

Appendix 1

**Figure S1 Identification of homozygous *tap38-3* lines.**

(a) PCR amplifications on the T-DNA insertion and *TAP38* gene. Left panel was amplified using primers specific for detection of T-DNA insertion and right panel showed a specific signal of *TAP38* gene using primers designed from *TAP38* gene. Gene specific Primers were used. (b) Western blot analysis using *TAP38* specific antibodies to confirm the knockout of *TAP38* in the *tap38-3* mutant line. Thylakoids corresponding to 10 µg of Chl were loaded for WT, *tap38-1* and *tap38-3*. (c) PAM measurement for state transitions process in WT and *tap38-3* as described in chapter 2.7.2.

Appendix 2

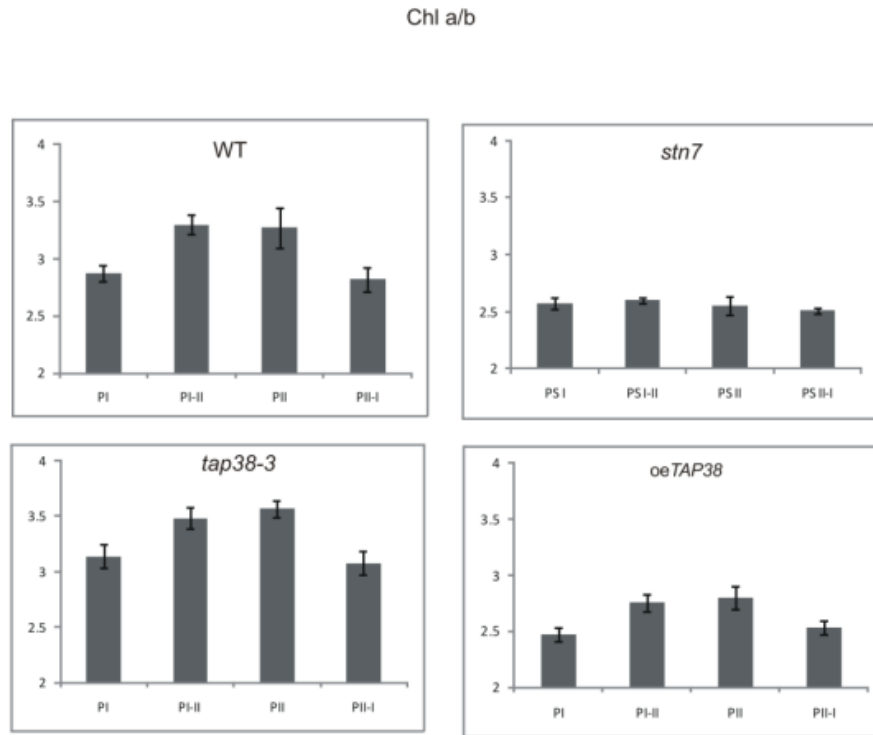


Figure S2 Chl a/b ratios of *TAP38* mutant and overexpressor plants during LTR acclimation.

Chlorophyll a/b ratios of WT, *tap38-1*, *tap38-3*, *stn7* and *oeTAP38* measured after exposure to different light conditions. In detail, plants were grown under PSI or PSII light for 6 d (PSI or PSII plants) or they were first acclimated to PSI light for 2 d followed by 4 d under PSII light source or *vice versa* (PSI-I or PSII-I plants). Plant material was harvested under the respective growth light and grinded in liquid nitrogen and then pigments were extracted with 80% buffered acetone. Chlorophyll concentrations and Chlorophyll a/b ratios were determined and calculated according to (Porra et al., 1989).

Appendix 3

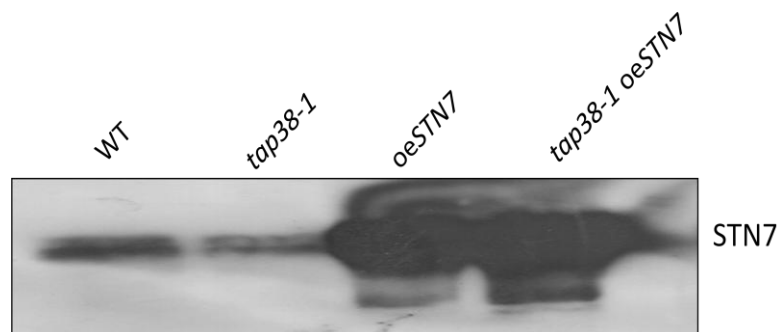


Figure S3 Overexpression of STN7 in the double mutant *tap38-1 oeSTN7*.

Thylakoids were isolated from WT, *tap38-1*, *oeSTN7* and *tap38-1 oeSTN7* and separated on 12% SDS-PAGE followed by immunodetection using STN7 specific antibodies.

5 References

A

- Allen, J.F. (1983). Regulation of photosynthetic phosphorylation. *Crc Cr Rev Plant Sci* 1, 1-22.
- Allen, J.F. (1984a). Photosynthesis and phosphorylation of light-harvesting chlorophyll a/b protein in intact chloroplasts - effects of uncouplers. *FEBS lett* 166, 237-244.
- Allen, J.F. (1984b). Protein-phosphorylation and optimal production of Atp in photosynthesis. *Biochem Soc T* 12, 774-775.
- Allen, J.F. (1992). Protein-phosphorylation and LHCII structure - Reply. *Trends Biochem Sci* 17, 346-347.
- Allen, J.F. (1996). Redox control of gene expression involving iron-sulfur proteins. Change of oxidation-state or assembly disassembly of Fe-S clusters? Reply. *FEBS lett* 382, 220-221.
- Allen, J.F., Bennett, J., Steinback, K.E., and Arntzen, C.J. (1981). Chloroplast Protein-Phosphorylation Couples plastoquinone redox State to distribution of excitation-energy between photosystems. *Nature* 291, 25-29.
- Allen, J.F., and Forsberg, J. (2001). Molecular recognition in thylakoid structure and function. *Trends in plant sci* 6, 317-326.
- Andersson, B., Akerlund, H.E., Jergil, B., and Larsson, C. (1982). Differential phosphorylation of the light-harvesting chlorophyll protein complex in appressed and non-appressed regions of the thylakoid membrane. *FEBS lett* 149, 181-185.
- Andersson, J., Wentworth, M., Walters, R.G., Howard, C.A., Ruban, A.V., Horton, P., and Jansson, S. (2003). Absence of the Lhcb1 and Lhcb2 proteins of the light-harvesting complex of photosystem II - effects on photosynthesis, grana stacking and fitness. *Plant J* 35, 350-361.
- Armbruster, U., Zuhlke, J., Rengstl, B., Kreller, R., Makarenko, E., Ruhle, T., Schunemann, D., Jahns, P., Weisshaar, B., Nickelsen, J., *et al.* (2010). The *Arabidopsis* thylakoid protein PAM68 is required for efficient D1 biogenesis and photosystem II assembly. *Plant cell* 22, 3439-3460.
- Armbruster, U., Labs, M., Pribil, M., Viola, S., Xu W., Scharfenberg M., Hertle A. P., Rojahn, U., Jensen P. E., Rappaport, F., Joliot P., Dörmann, P., Wanner G., and Leister, D. (2013) CURT1 Proteins Modify Thylakoid Architecture by Inducing Membrane Curvature. *Plant cell* Submitted.
- Arnon, D.I., Allen, M.B., and Whatley, F.R. (1954). Photosynthesis by isolated chloroplasts. *Nature* 174, 394-396.

Aro, E.M., Suorsa, M., Rokka, A., Allahverdiyeva, Y., Paakkarinen, V., Saleem, A., Battchikova, N., and Rintamaki, E. (2005). Dynamics of photosystem II: a proteomic approach to thylakoid protein complexes. *J Exp Bot* 56, 347-356.

Aro, E.M., Virgin, I., and Andersson, B. (1993). Photoinhibition of photosystem-2 - inactivation, protein damage and turnover. *Biochim et biophys acta* 1143, 113-134.

Aronsson, H., and Jarvis, P. (2002). A simple method for isolating import-competent *Arabidopsis* chloroplasts. *FEBS lett* 529, 215-220.

Arvidsson, P.O., and Sundby, C. (1999). A model for the topology of the chloroplast thylakoid membrane. *Aust J Plant Physiol* 26, 687-694.

B

Bailey, S., Horton, P., and Walters, R.G. (2004). Acclimation of *Arabidopsis thaliana* to the light environment: the relationship between photosynthetic function and chloroplast composition. *Planta* 218, 793-802.

Bailey, S., Walters, R.G., Jansson, S., and Horton, P. (2001). Acclimation of *Arabidopsis thaliana* to the light environment: the existence of separate low light and high light responses. *Planta* 213, 794-801.

Barber, J. (1982). Influence of surface-charges on thylakoid structure and function. *Annu Rev Plant Phys* 33, 261-295.

Bassi, R., and Caffarri, S. (2000). Lhc proteins and the regulation of photosynthetic light harvesting function by xanthophylls. *Photosynth res* 64, 243-256.

Bassi, R., Marquardt, J., and Lavergne, J. (1995). Biochemical and functional-properties of photosystem-II in agranal membranes from maize mesophyll and bundle-sheath chloroplasts. *Eur J Biochem* 233, 709-719.

Bassi, R., Rigoni, F., Barbato, R., and Giacometti, G.M. (1988). Light-harvesting chlorophyll a/b proteins (LHCII) populations in phosphorylated membranes. *Biochim et biophys acta* 936, 29-38.

Bayer, R.G., Stael, S., Rocha, A.G., Mair, A., Vothknecht, U.C., and Teige, M. (2012). Chloroplast-localized protein kinases: a step forward towards a complete inventory. *J Exp Bot* 63, 1713-1723.

Bellafiore, S., Barneche, F., Peltier, G., and Rochaix, J.D. (2005). State transitions and light adaptation require chloroplast thylakoid protein kinase STN7. *Nature* 433, 892-895.

Ben-Shem, A., Frolov, F., and Nelson, N. (2003). Crystal structure of plant photosystem I. *Nature* 426, 630-635.

- Bennett, J. (1980). Chloroplast Phosphoproteins - Evidence for a thylakoid-bound phosphoprotein phosphatase. *Eur J Biochem* 104, 85-89.
- Bennett, J. (1983). Regulation of photosynthesis by reversible phosphorylation of the light-harvesting chlorophyll a/b Protein. *Biochemical J* 212, 1-13.
- Black, M.T., Lee, P., and Horton, P. (1986). Changes in topography and function of thylakoid membranes following membrane-protein phosphorylation. *Planta* 168, 330-336.
- Boekema, E.J., Hankamer, B., Bald, D., Kruij, J., Nield, J., Boonstra, A.F., Barber, J., and Rogner, M. (1995). Supramolecular structure of the photosystem-II complex from green plants and cyanobacteria. *P Natl Acad Sci USA* 92, 175-179.
- Bonardi, V., Pesaresi, P., Becker, T., Schleiff, E., Wagner, R., Pfannschmidt, T., Jahns, P., and Leister, D. (2005). Photosystem II core phosphorylation and photosynthetic acclimation require two different protein kinases. *Nature* 437, 1179-1182.
- Bonavent.C, and Myers, J. (1969). Fluorescence and oxygen evolution from *Chlorella pyrenoidosa*. *Biochim Biophys Acta* 189, 366-383.
- Buchanan, B.B., Gruissem, W., and Jones, R. (2002). *Biochemistry and Molecular Biology of Plants*. John Wiley & Sons.
- Budde, R.J.A., and Chollet, R. (1988). Regulation of enzyme-activity in plants by reversible phosphorylation. *Physiol Plantarum* 72, 435-439.
- Bulte, L., Gans, P., Rebeille, F., and Wollman, F.A. (1990). Atp control on state transitions *in vivo* in *Chlamydomonas reinhardtii*. *Biochim Biophys Acta* 1020, 72-80.

C

- Caffarri, S., Kouril, R., Kereiche, S., Boekema, E.J., and Croce, R. (2009). Functional architecture of higher plant photosystem II supercomplexes. *Embo J* 28, 3052-3063.
- Chuartzman, S.G., Nevo, R., Shimoni, E., Charuvi, D., Kiss, V., Ohad, I., Brumfeld, V., and Reich, Z. (2008). Thylakoid membrane remodeling during state transitions in *Arabidopsis*. *Plant Cell* 20, 1029-1039.
- Clough, S.J., and Bent, A.F. (1998). Floral dip: a simplified method for agrobacterium-mediated transformation of *Arabidopsis thaliana*. *Plant J* 16, 735-743.
- Cohen, P. (1989). The structure and regulation of protein phosphatases. *Annu Re Biochem* 58, 453-508.
- Cohen, P. (2000). The regulation of protein function by multisite phosphorylation--a 25 year update. *Trends Biochem Sci* 25, 596-601.

D

DalCorso, G., Pesaresi, P., Masiero, S., Aseeva, E., Schünemann, D., Finazzi, G., Joliot, P., Barbato, R., and Leister, D. (2008). A complex containing PGRL1 and PGR5 is involved in the switch between linear and cyclic electron flow in Arabidopsis. *Cell* 132, 273-285.

Dekker, J.P., and Boekema, E.J. (2005). Supramolecular organization of thylakoid membrane proteins in green plants. *BBA-Bioenergetics* 1706, 12-39.

del Riego, G., Casano, L.M., Martin, M., and Sabater, B. (2006). Multiple phosphorylation sites in the beta subunit of thylakoid ATP synthase. *Photosynth Res* 89, 11-18.

Delosme, R., Olive, J., and Wollman, F.A. (1996). Changes in light energy distribution upon state transitions: An in vivo photoacoustic study of the wild type and photosynthesis mutants from *Chlamydomonas reinhardtii*. *BBA-Bioenergetics* 1273, 150-158.

DemmigAdams, B., Adams, W.W., Barker, D.H., Logan, B.A., Bowling, D.R., and Verhoeven, A.S. (1996). Using chlorophyll fluorescence to assess the fraction of absorbed light allocated to thermal dissipation of excess excitation. *Physiol Plantarum* 98, 253-264.

Depege, N., Bellafiore, S., and Rochaix, J.D. (2003). Role of chloroplast protein kinase Stt7 in LHCII phosphorylation and state transition in *Chlamydomonas*. *Science* 299, 1572-1575.

Dietzel, L., Brautigam, K., and Pfannschmidt, T. (2008). Photosynthetic acclimation: state transitions and adjustment of photosystem stoichiometry--functional relationships between short-term and long-term light quality acclimation in plants. *FEBS J* 275, 1080-1088.

Dietzel, L., Brautigam, K., Steiner, S., Schuffler, K., Lepetit, B., Grimm, B., Schottler, M.A., and Pfannschmidt, T. (2011). Photosystem II supercomplex remodeling serves as an entry mechanism for state transitions in *Arabidopsis*. *Plant Cell* 23, 2964-2977.

Dietzel, L., and Pfannschmidt, T. (2008). Photosynthetic acclimation to light gradients in plant stands comes out of shade. *Plant Signal Behav* 3, 1116-1118.

E

Eberhard, S., Finazzi, G., and Wollman, F.A. (2008). The Dynamics of Photosynthesis. *Annu Rev Genet* 42, 463-515.

F

Fey, V., Wagner, R., Brautigam, K., and Pfannschmidt, T. (2005a). Photosynthetic redox control of nuclear gene expression. *J Expl Bot* 56, 1491-1498.

- Fey, V., Wagner, R., Brautigam, K., Wirtz, M., Hell, R., Dietzmann, A., Leister, D., Oelmüller, R., and Pfannschmidt, T. (2005b). Retrograde plastid redox signals in the expression of nuclear genes for chloroplast proteins of *Arabidopsis thaliana*. *J Bio Chem* 280, 5318-5328.
- Finazzi, G., Furia, A., Barbagallo, R.P., and Forti, G. (1999). State transitions, cyclic and linear electron transport and photophosphorylation in *Chlamydomonas reinhardtii*. *BBA-Bioenergetics* 1413, 117-129.
- Finazzi, G., Rappaport, F., Furia, A., Fleischmann, M., Rochaix, J.D., Zito, F., and Forti, G. (2002). Involvement of state transitions in the switch between linear and cyclic electron flow in *Chlamydomonas reinhardtii*. *Embo Rep* 3, 280-285.
- Finazzi, G., Zito, F., Barbagallo, R.P., and Wollman, F.A. (2001). Contrasted effects of inhibitors of cytochrome b6f complex on state transitions in *Chlamydomonas reinhardtii*: the role of Q_o site occupancy in LHCII kinase activation. *J Bio Chem* 276, 9770-9774.
- Fristedt, R., Carlberg, I., Zygadlo, A., Piippo, M., Nurmi, M., Aro, E.M., Scheller, H.V., and Vener, A.V. (2009). Intrinsically unstructured phosphoprotein TSP9 regulates light harvesting in *Arabidopsis thaliana*. *Biochemistry* 48, 499-509.
- Fristedt, R., and Vener, A.V. (2011). High light induced disassembly of photosystem II supercomplexes in *Arabidopsis* requires STN7-dependent phosphorylation of CP29. *PLoS one* 6, e24565.

G

- Grieco, M., Tikkanen, M., Paakkarinen, V., Kangasjarvi, S., and Aro, E.M. (2012). Steady-state phosphorylation of light-harvesting complex II proteins preserves photosystem I under fluctuating white light. *Plant Physiol* 160, 1896-1910.
- Guillon, C., and Mache, R. (1987). Phosphorylation invitro of the large subunit of the ribulose-1,5-bisphosphate carboxylase and of the glyceraldehyde-3-phosphate dehydrogenase. *Eur J Biochem* 166, 249-254.

H

- Haldrup, A., Jensen, P.E., Lunde, C., and Scheller, H.V. (2001). Balance of power: a view of the mechanism of photosynthetic state transitions. *Trends in plant sci* 6, 301-305.
- Haldrup, A., Naver, H., and Scheller, H.V. (1999). The interaction between plastocyanin and photosystem I is inefficient in transgenic *Arabidopsis* plants lacking the PSI-N subunit of photosystem I. *Plant J* 17, 689-698.

Hammer, M.F., Sarath, G., and Markwell, J. (1995). Dephosphorylation of the thylakoid membrane light-harvesting complex-II by a stromal protein phosphatase. *Photosynth Res* 45, 195-201.

Hansson, M., and Vener, A.V. (2003). Identification of three previously unknown in vivo protein phosphorylation sites in thylakoid membranes of *Arabidopsis thaliana*. *Mol Cell Proteomics* 2, 550-559.

Heinemeyer, J., Eubel, H., Wehmhoner, D., Jansch, L., and Braun, H.P. (2004). Proteomic approach to characterize the supramolecular organization of photosystems in higher plants. *Phytochemistry* 65, 1683-1692.

Hertle, A.P., Blunder, T., Wunder, T., Pesaresi, P., Pribil, M., Armbruster, U., and Leister, D. (2013). PGRL1 is the elusive ferredoxin-plastoquinone reductase in photosynthetic cyclic electron flow. *Mol cell* 49, 511-523.

Horton, P., and Hague, A. (1988). Studies on the induction of chlorophyll fluorescence in isolated barley protoplasts .IV. Resolution of non-photochemical quenching. *Biochim Biophys Acta* 932, 107-115.

Horton, P., and Ruban, A. (2005). Molecular design of the photosystem II light-harvesting antenna: photosynthesis and photoprotection. *J Expl Bot* 56, 365-373.

I

Ihnatowicz, A., Pesaresi, P., and Leister, D. (2007). The E subunit of photosystem I is not essential for linear electron flow and photoautotrophic growth in *Arabidopsis thaliana*. *Planta* 226, 889-895.

Ihnatowicz, A., Pesaresi, P., Lohrig, K., Wolters, D., Müller, B., and Leister, D. (2008). Impaired photosystem I oxidation induces STN7-dependent phosphorylation of the light-harvesting complex I protein Lhca4 in *Arabidopsis thaliana*. *Planta* 227, 717-722.

Ihnatowicz, A., Pesaresi, P., Varotto, C., Richly, E., Schneider, A., Jahns, P., Salamini, F., and Leister, D. (2004). Mutants for photosystem I subunit D of *Arabidopsis thaliana*: effects on photosynthesis, photosystem I stability and expression of nuclear genes for chloroplast functions. *Plant J* 37, 839-852.

Iwai, M., Takahashi, Y., and Minagawa, J. (2008). Molecular remodeling of photosystem II during state transitions in *Chlamydomonas reinhardtii*. *Plant Cell* 20, 2177-2189.

J

- Jansson, S. (1999). A guide to the Lhc genes and their relatives in *Arabidopsis*. Trends in plant sci 4, 236-240.
- Jensen, P.E., Haldrup, A., Zhang, S., and Scheller, H.V. (2004). The PSI-O subunit of plant photosystem I is involved in balancing the excitation pressure between the two photosystems. J Bio Chem 279, 24212-24217.
- Johnson, G.N. (2011). Physiology of PSI cyclic electron transport in higher plants. BBA-Bioenergetics 1807, 384-389.
- Joliot, P., and Joliot, A. (2006). Cyclic electron flow in C3 plants. BBA-Bioenergetics 1757, 362-368.

K

- Kanekatsu, M., Saito, H., Motohashi, K., and Hisabori, T. (1998). The beta subunit of chloroplast ATP synthase (CF₀CF₁-ATPase) is phosphorylated by casein kinase II. Biochem Mol Biol Int 46, 99-105.
- Karnauchov, I., Herrmann, R.G., and Klosgen, R.B. (1997). Transmembrane topology of the Rieske Fe/S protein of the cytochrome *b6/f* complex from spinach chloroplasts. FEBS lett 408, 206-210.
- Klimyuk, V.I., Persello-Cartieaux, F., Havaux, M., Contard-David, P., Schuenemann, D., Meierhoff, K., Gouet, P., Jones, J.D.G., Hoffman, N.E., and Nussaume, L. (1999). A chromodomain protein encoded by the *Arabidopsis* CAO gene is a plant-specific component of the chloroplast signal recognition particle pathway that is involved in LHCP targeting. Plant Cell 11, 87-99.
- Koivuniemi, A., Aro, E.M., and Andersson, B. (1995). Degradation of the D1- and D2-proteins of photosystem II in higher plants is regulated by reversible phosphorylation. Biochemistry 34, 16022-16029.
- Kouril, R., Zygadlo, A., Arteni, A.A., de Wit, C.D., Dekker, J.P., Jensen, P.E., Scheller, H.V., and Boekema, E.J. (2005). Structural characterization of a complex of photosystem I and light-harvesting complex II of *Arabidopsis thaliana*. Biochemistry 44, 10935-10940.
- Kovacs, L., Damkjaer, J., Kereiche, S., Ilioaia, C., Ruban, A.V., Boekema, E.J., Jansson, S., and Horton, P. (2006). Lack of the light-harvesting complex CP24 affects the structure and function of the grana membranes of higher plant chloroplasts. Plant Cell 18, 3106-3120.
- Kovacs, L., Wiessner, W., Kis, M., Nagy, F., Mende, D., and Demeter, S. (2000). Short- and long-term redox regulation of photosynthetic light energy distribution and photosystem

stoichiometry by acetate metabolism in the green alga, *Chlamydomonas reinhardtii*. *Photosynth Res* 65, 231-247.

Kruse, O. (2001). Light-induced short-term adaptation mechanisms under redox control in the PS II-LHCII supercomplex: LHCII state transitions and PSII repair cycle. *Die Naturwissenschaften* 88, 284-292.

L

Laing, W.A., and Christeller, J.T. (1984). Chloroplast phosphoproteins - distribution of phosphoproteins within spinach-chloroplasts. *Plant Sci Lett* 36, 99-104.

Larsson, U.K., Jergil, B., and Andersson, B. (1983). Changes in the lateral distribution of the light-harvesting chlorophyll-a/b protein complex induced by its phosphorylation. *Eur J Biochem* 136, 25-29.

Leister, D. (2012). Retrograde signaling in plants: from simple to complex scenarios. *Frontiers in plant science* 3, 135.

Lemeille, S., and Rochaix, J.D. (2010). State transitions at the crossroad of thylakoid signalling pathways. *Photosynth Res* 106, 33-46.

Lemeille, S., Turkina, M.V., Vener, A.V., and Rochaix, J.D. (2010). Stt7-dependent phosphorylation during state transitions in the green alga *Chlamydomonas reinhardtii*. *Mol Cell Proteomics* 9, 1281-1295.

Lemeille, S., Willig, A., Depege-Fargeix, N., Delessert, C., Bassi, R., and Rochaix, J.D. (2009). Analysis of the chloroplast protein kinase Stt7 during state transitions. *PLoS biology* 7, e45.

Lichtenthaler, H.K. (1987). Chlorophylls and carotenoids - pigments of photosynthetic biomembranes. *Method Enzymol* 148, 350-382.

Lohrig, K., Müller, B., Davydova, J., Leister, D., and Wolters, D.A. (2009). Phosphorylation site mapping of soluble proteins: bioinformatical filtering reveals potential plastidic phosphoproteins in *Arabidopsis thaliana*. *Planta* 229, 1123-1134.

Lunde, C., Jensen, P.E., Haldrup, A., Knoetzel, J., and Scheller, H.V. (2000). The PSI-H subunit of photosystem I is essential for state transitions in plant photosynthesis. *Nature* 408, 613-615.

M

Maiwald, D., Dietzmann, A., Jahns, P., Pesaresi, P., Joliot, P., Joliot, A., Levin, J.Z., Salamini, F., and Leister, D. (2003). Knock-out of the genes coding for the Rieske protein and the ATP-synthase delta-subunit of *Arabidopsis*. Effects on photosynthesis, thylakoid protein composition, and nuclear chloroplast gene expression. *Plant Physiol* 133, 191-202.

- Margulis, L. (1992). *Symbiosis in Cell Evolution*. San Francisco: Freeman.
- Martin, W., Rujan, T., Richly, E., Hansen, A., Cornelsen, S., Lins, T., Leister, D., Stoebe, B., Hasegawa, M., and Penny, D. (2002). Evolutionary analysis of Arabidopsis, cyanobacterial, and chloroplast genomes reveals plastid phylogeny and thousands of cyanobacterial genes in the nucleus. *P Natl Acad Sci USA* *99*, 12246-12251.
- Maxwell, K., and Johnson, G.N. (2000). Chlorophyll fluorescence - a practical guide. *J Expl Bot* *51*, 659-668.
- Meurer, J., Plucken, H., Kowallik, K.V., and Westhoff, P. (1998). A nuclear-encoded protein of prokaryotic origin is essential for the stability of photosystem II in *Arabidopsis thaliana*. *Embo J* *17*, 5286-5297.
- Michel, H., Griffin, P.R., Shabanowitz, J., Hunt, D.F., and Bennett, J. (1991). Tandem mass-spectrometry identifies sites of 3 posttranslational modifications of spinach light-harvesting chlorophyll protein-II - proteolytic cleavage, acetylation, and phosphorylation. *J of Biol Chem* *266*, 17584-17591.
- Minagawa, J. (2011). State transitions - the molecular remodeling of photosynthetic supercomplexes that controls energy flow in the chloroplast. *Biochim Biophys Acta* *1807*, 897-905.
- Müller, P., Li, X.P., and Niyogi, K.K. (2001). Non-photochemical quenching. A response to excess light energy. *Plant Physiol* *125*, 1558-1566.
- Mullineaux, P.M., and Rausch, T. (2005). Glutathione, photosynthesis and the redox regulation of stress-responsive gene expression. *Photosynth Res* *86*, 459-474.
- Munekage, Y., Hojo, M., Meurer, J., Endo, T., Tasaka, M., and Shikanai, T. (2002). PGR5 is involved in cyclic electron flow around photosystem I and is essential for photoprotection in *Arabidopsis*. *Cell* *110*, 361-371.
- Murakami, A., Kim, S.J., and Fujita, Y. (1997). Changes in photosystem stoichiometry in response to environmental conditions for cell growth observed with the cyanophyte *Synechocystis* PCC 6714. *Plant Cell Physiol* *38*, 392-397.
- Murata, N. (1969). Control of excitation transfer in Photosynthesis .II. Magnesium ion-dependent distribution of excitation energy between two pigment systems in spinach chloroplasts. *Biochim Biophys Acta* *189*, 171-181.

Nellaepalli, S., Kodru, S., and Subramanyam, R. (2012). Effect of cold temperature on regulation of state transitions in *Arabidopsis thaliana*. *J Photoch Photobio B* 112, 23-30.

Nellaepalli, S., Mekala, N.R., Zsiros, O., Mohanty, P., and Subramanyam, R. (2011). Moderate heat stress induces state transitions in *Arabidopsis thaliana*. *Biochim Biophys Acta* 1807, 1177-1184.

Nield, J., Orlova, E.V., Morris, E.P., Gowen, B., van Heel, M., and Barber, J. (2000). 3D map of the plant photosystem II supercomplex obtained by cryoelectron microscopy and single particle analysis. *Nat Struct Biol* 7, 44-47.

Nott, A., Jung, H.S., Koussevitzky, S., and Chory, J. (2006). Plastid-to-nucleus retrograde signaling. *Annu Rev Plant Biol* 57, 739-759.

O

Ogrzewalla, K., Piotrowski, M., Reinbothe, S., and Link, G. (2002). The plastid transcription kinase from mustard (*Sinapis alba* L.). A nuclear-encoded CK2-type chloroplast enzyme with redox-sensitive function. *Eur J Biochem* 269, 3329-3337.

Olsen, J.V., Blagoev, B., Gnad, F., Macek, B., Kumar, C., Mortensen, P., and Mann, M. (2006). Global, in vivo, and site-specific phosphorylation dynamics in signaling networks. *Cell* 127, 635-648.

P

Peng, L.W., Yamamoto, H., and Shikanai, T. (2011). Structure and biogenesis of the chloroplast NAD(P)H dehydrogenase complex. *BBA-Bioenergetics* 1807, 945-953.

Pesaresi, P., Hertle, A., Pribil, M., Kleine, T., Wagner, R., Strissel, H., Ihnatowicz, A., Bonardi, V., Scharfenberg, M., Schneider, A., Pfannschmidt, T., Leister D. (2009). *Arabidopsis* STN7 kinase provides a link between short- and long-term photosynthetic acclimation. *Plant Cell* 21, 2402-2423.

Petroutsos, D., Busch, A., Janssen, I., Trompelt, K., Bergner, S.V., Weinl, S., Holtkamp, M., Karst, U., Kudla, J., and Hippler, M. (2011). The chloroplast calcium sensor CaS is required for photoacclimation in *Chlamydomonas reinhardtii*. *Plant Cell* 23, 2950-2963.

Pfannschmidt, T. (2003). Chloroplast redox signals: how photosynthesis controls its own genes. *Trends in plant sci* 8, 33-41.

Pfannschmidt, T., Brautigam, K., Wagner, R., Dietzel, L., Schroter, Y., Steiner, S., and Nykytenko, A. (2009). Potential regulation of gene expression in photosynthetic cells by redox and energy state: approaches towards better understanding. *Annals of botany* 103, 599-607.

- Pfannschmidt, T., Nilsson, A., and Allen, J.F. (1999). Photosynthetic control of chloroplast gene expression. *Nature* 397, 625-628.
- Pfannschmidt, T., Schutze, K., Brost, M., and Oelmüller, R. (2001). A novel mechanism of nuclear photosynthesis gene regulation by redox signals from the chloroplast during photosystem stoichiometry adjustment. *J Bio Chem* 276, 36125-36130.
- Pfannschmidt, T., Schutze, K., Fey, V., Sherameti, I., and Oelmüller, R. (2003). Chloroplast redox control of nuclear gene expression - A new class of plastid signals in interorganellar communication. *Antioxid Redox Sign* 5, 95-101.
- Porra, R.J. (2002). The chequered history of the development and use of simultaneous equations for the accurate determination of chlorophylls a and b. *Photosynth Res* 73, 149-156.
- Porra, R.J., Thompson, W.A., and Kriedemann, P.E. (1989). Determination of accurate extinction coefficients and simultaneous-equations for assaying chlorophyll-a and chlorophyll-b extracted with 4 different solvents - verification of the concentration of chlorophyll standards by atomic-absorption spectroscopy. *Biochim Biophys Acta* 975, 384-394.
- Pribil, M., Pesaresi, P., Hertle, A., Barbato, R., and Leister, D. (2010). Role of plastid protein phosphatase TAP38 in LHClI dephosphorylation and thylakoid electron flow. *PLoS biology* 8, e1000288.
- Puthiyaveetil, S. (2011). A mechanism for regulation of chloroplast LHC II kinase by plastoquinol and thioredoxin. *FEBS lett* 585, 1717-1721.
- Puthiyaveetil, S., Ibrahim, I.M., and Allen, J.F. (2012). Oxidation-reduction signalling components in regulatory pathways of state transitions and photosystem stoichiometry adjustment in chloroplasts. *Plant Cell Environ* 35, 347-359.
- Puthiyaveetil, S., Ibrahim, I.M., Jelacic, B., Tomasic, A., Fulgosi, H., and Allen, J.F. (2010). Transcriptional control of photosynthesis genes: The evolutionarily conserved regulatory mechanism in plastid genome function. *Genome Biol Evol* 2, 888-896.
- Puthiyaveetil, S., Kavanagh, T.A., Cain, P., Sullivan, J.A., Newell, C.A., Gray, J.C., Robinson, C., van der Giezen, M., Rogers, M.B., and Allen, J.F. (2008). The ancestral symbiont sensor kinase CSK links photosynthesis with gene expression in chloroplasts. *P Natl Acad Sci USA* 105, 10061-10066.

Q

Qi, Y., Armbruster, U., Schmitz-Linneweber, C., Delannoy, E., de Longevialle, A.F., Rühle, T., Small, I., Jahns, P., and Leister, D. (2012). *Arabidopsis* CSP41 proteins form multimeric complexes that bind and stabilize distinct plastid transcripts. *J Exp Bot* 63, 1251-1270.

R

Reiland, S., Finazzi, G., Endler, A., Willig, A., Baerenfaller, K., Grossmann, J., Gerrits, B., Rutishauser, D., Gruissem, W., Rochaix, J.D., Baginsky, S. (2011). Comparative phosphoproteome profiling reveals a function of the STN8 kinase in fine-tuning of cyclic electron flow (CEF). *P Natl Acad Sci USA* 108, 12955-12960.

Reiland, S., Messerli, G., Baerenfaller, K., Gerrits, B., Endler, A., Grossmann, J., Gruissem, W., and Baginsky, S. (2009). Large-scale *Arabidopsis* phosphoproteome profiling reveals novel chloroplast kinase substrates and phosphorylation networks. *Plant Physiol* 150, 889-903.

Richly, E., and Leister, D. (2004). An improved prediction of chloroplast proteins reveals diversities and commonalities in the chloroplast proteomes of *Arabidopsis* and rice. *Gene* 329, 11-16.

Ruban, A.V., and Johnson, M.P. (2009). Dynamics of higher plant photosystem cross-section associated with state transitions. *Photosynth Res* 99, 173-183.

Ryrie, I.J. (1983). Freeze-fracture analysis of membrane appression and protein segregation in model membranes containing the chlorophyll-protein complexes from chloroplasts. *Eur J Biochem* 137, 205-213.

S

Salinas, P., Fuentes, D., Vidal, E., Jordana, X., Echeverria, M., and Holuigue, L. (2006). An extensive survey of CK2 alpha and beta subunits in *Arabidopsis*: Multiple isoforms exhibit differential subcellular localization. *Plant Cell Physiol* 47, 1295-1308.

Samol, I., Shapiguzov, A., Ingelsson, B., Fucile, G., Crevecoeur, M., Vener, A.V., Rochaix, J.D., and Goldschmidt-Clermont, M. (2012). Identification of a photosystem II phosphatase involved in light acclimation in *Arabidopsis*. *Plant Cell* 24, 2596-2609.

Schaffne, W., and Weissman, C. (1973). Rapid, sensitive, and specific method for determination of protein in dilute-solution. *Anal Biochem* 56, 502-514.

Schagger, H., von Jagow, G. (1991) Blue native electrophoresis for isolation of membrane protein complexes in enzymatically active form. *Anal Biochem* 199, 223–231.

- Scheller, H.V., Jensen, P.E., Haldrup, A., Lunde, C., and Knoetzel, J. (2001). Role of subunits in eukaryotic Photosystem I. *BBA-Bioenergetics* 1507, 41-60.
- Schliebner, I., Pribil, M., Zuhlke, J., Dietzmann, A., and Leister, D. (2008). A survey of chloroplast protein kinases and phosphatases in *Arabidopsis thaliana*. *Curr Genomics* 9, 184-190.
- Schweer, J., Turkeri, H., Link, B., and Link, G. (2010). AtSIG6, a plastid sigma factor from *Arabidopsis*, reveals functional impact of cpCK2 phosphorylation. *Plant J* 62, 192-202.
- Shapiguzov, A., Ingelsson, B., Samol, I., Andres, C., Kessler, F., Rochaix, J.D., Vener, A.V., and Goldschmidt-Clermont, M. (2010). The PPH1 phosphatase is specifically involved in LHCII dephosphorylation and state transitions in *Arabidopsis*. *P Natl Acad Sci USA* 107, 4782-4787.
- Silverstein, T., Cheng, L.L., and Allen, J.F. (1993). Chloroplast thylakoid protein phosphatase reactions are redox-independent and kinetically heterogeneous. *FEBS lett* 334, 101-105.
- Snyders, S., and Kohorn, B.D. (1999). TAKs, thylakoid membrane protein kinases associated with energy transduction. *J of Biol Chem* 274, 9137-9140.
- Snyders, S., and Kohorn, B.D. (2001). Disruption of thylakoid-associated kinase 1 leads to alteration of light harvesting in *Arabidopsis*. *J of Biol Chem* 276, 32169-32176.
- Stael, S., Rocha, A.G., Wimberger, T., Anrather, D., Vothknecht, U.C., and Teige, M. (2012). Cross-talk between calcium signalling and protein phosphorylation at the thylakoid. *J Exp Bot* 63, 1725-1733.
- Sugiyama, N., Nakagami, H., Mochida, K., Daudi, A., Tomita, M., Shirasu, K., and Ishihama, Y. (2008). Large-scale phosphorylation mapping reveals the extent of tyrosine phosphorylation in *Arabidopsis*. *Mol Syst Biol* 4, 193.
- Sun, G., Bailey, D., Jones, M.W., and Markwell, J. (1989). Chloroplast thylakoid protein phosphatase is a membrane surface-associated activity. *Plant Physiol* 89, 238-243.

T

- Taiz, L., and Zeiger, E. (2010). *Plant Physiology*. Sinauer Associates.
- Telfer, A., Allen, J.F., Barber, J., and Bennett, J. (1983). Thylakoid protein phosphorylation during State 1 - State 2 transitions in osmotically shocked pea chloroplasts. *Biochim Biophys Acta* 722, 176-181.
- Tikkanen, M., Gollan, P.J., Suorsa, M., Kangasjarvi, S., and Aro, E.M. (2012). STN7 operates in retrograde signaling through controlling redox balance in the electron transfer chain. *Fron Plant Sci* 3, 277.

Tikkanen, M., Grieco, M., Kangasjarvi, S., and Aro, E.M. (2010). Thylakoid protein phosphorylation in higher plant chloroplasts optimizes electron transfer under fluctuating light. *Plant Physiol* 152, 723-735.

Tikkanen, M., Nurmi, M., Kangasjarvi, S., and Aro, E.M. (2008a). Core protein phosphorylation facilitates the repair of photodamaged photosystem II at high light. *Biochim Biophys Acta* 1777, 1432-1437.

Tikkanen, M., Nurmi, M., Suorsa, M., Danielsson, R., Mamedov, F., Styring, S., and Aro, E.M. (2008b). Phosphorylation-dependent regulation of excitation energy distribution between the two photosystems in higher plants. *Biochim Biophys Acta* 1777, 425-432.

Tikkanen, M., Piippo, M., Suorsa, M., Sirpio, S., Mulo, P., Vainonen, J., Vener, A.V., Allahverdiyeva, Y., and Aro, E.M. (2006). State transitions revisited-a buffering system for dynamic low light acclimation of *Arabidopsis*. *Plant Mol Biol* 62, 779-793.

Tokutsu, R., Iwai, M., and Minagawa, J. (2009). CP29, a monomeric light-harvesting complex II protein, is essential for state transitions in *Chlamydomonas reinhardtii*. *J Bio Chem* 284, 7777-7782.

V

Vainonen, J.P., Hansson, M., and Vener, A.V. (2005). STN8 protein kinase in *Arabidopsis thaliana* is specific in phosphorylation of photosystem II core proteins. *J Bio Chem* 280, 33679-33686.

Vainonen, J.P., Sakuragi, Y., Stael, S., Tikkanen, M., Allahverdiyeva, Y., Paakkarinen, V., Aro, E., Suorsa, M., Scheller, H.V., Vener, A.V., *et al.* (2008). Light regulation of CaS, a novel phosphoprotein in the thylakoid membrane of *Arabidopsis thaliana*. *FEBS J* 275, 1767-1777.

Vasilikiotis, C., and Melis, A. (1994). Photosystem II reaction center damage and repair cycle: chloroplast acclimation strategy to irradiance stress. *P Natl Acad Sci USA* 91, 7222-7226.

Vener, A.V., Vankan, P.J.M., Gal, A., Andersson, B., and Ohad, I. (1995). Activation/deactivation cycle of redox-controlled thylakoid protein-phosphorylation. Role of plastoquinol bound to the reduced cytochrome *bf* complex. *J of Biol Chem* 270, 25225-25232.

Vener, A.V., VanKan, P.J.M., Rich, P.R., Ohad, I., and Andersson, B. (1997). Plastoquinol at the quinol oxidation site of reduced cytochrome *bf* mediates signal transduction between light and protein phosphorylation: Thylakoid protein kinase deactivation by a single-turnover flash. *P Natl Acad Sci USA* 94, 1585-1590.

Wagner, R., Dietzel, L., Brautigam, K., Fischer, W., and Pfannschmidt, T. (2008). The long-term response to fluctuating light quality is an important and distinct light acclimation mechanism that supports survival of *Arabidopsis thaliana* under low light conditions. *Planta* 228, 573-587.

W

Walters, R.G. (2005). Towards an understanding of photosynthetic acclimation. *J Expl Bot* 56, 435-447.

Willig, A., Shapiguzov, A., Goldschmidt-Clermont, M., and Rochaix, J.D. (2011). The phosphorylation status of the chloroplast protein kinase STN7 of *Arabidopsis* affects its turnover. *Plant Physiol* 157, 2102-2107.

Wollman, F.A., and Lemaire, C. (1988). Studies on kinase-controlled state transitions in photosystem-II and *b6f* mutants from *Chlamydomonas reinhardtii* which lack quinone-binding proteins. *Biochim Biophys Acta* 933, 85-94.

Wunder, T., Liu, Q., Aseeva, E., Bonardi, V., Leister, D., and Pribil, M. (2013). Control of STN7 transcript abundance and transient STN7 dimerisation are involved in the regulation of STN7 activity. *Planta* 237, 541-558.

Z

Zhang, S., and Scheller, H.V. (2004). Light-harvesting complex II binds to several small subunits of photosystem I. *J Bio Chem* 279, 3180-3187.

Zito, F., Finazzi, G., Delosme, R., Nitschke, W., Picot, D., and Wollman, F.A. (1999). The Qo site of cytochrome *b6f* complexes controls the activation of the LHCII kinase. *Embo J* 18, 2961-2969.

Acknowledgements

I would like to express my deepest appreciation to Prof. Dr. Dario Leister for accepting me as a PhD student, providing me with a nice studying environment, supervising and supporting my work.

A special gratitude I give to my supervisor Dr. Mathias Pribil who helped me with my project including discussions, guidance, especially in writing this thesis. Also, I am really thankful for his kindness in solving problems in my daily life.

Furthermore I would also like to acknowledge with much appreciation the crucial role of my colleagues Wenteng Xu and Dr. Tobias Wunder for pleasant cooperation, help and discussions.

I would also like to thank Chinese Scholarship Council their financial support granted through predoctoral fellowship.

I would like to thank Dr. Mathias Pribil, Dr. Nikolay Manavski, Wenteng Xu, Dr. Tobias Wunder, Mathias Labs, Luca Tadini, Salar Torabi, Jafar Razegi and Elisabeth Gerick for correction of my thesis and/or useful suggestions in some experiments.

I would like to thank Dr. Alexander Hertle and Dr. Yafei Qi for supporting me with their wide range of knowledge.

I would like to thank AG Wanner (LMU) for taking all the Scanning Electron Microscope pictures.

I am most thankful to the whole AG Leister including Angela Dietzmann, Deniz Sawo, the gardeners et al. I feel so happy to meet all of you. And at last I would like to thank my family and Hongke Li for supporting.

Curriculum vitae

PERSONAL DATA

Name: Qiuping Liu

Date of birth: 30.08.1983

Place of birth: Chongqing

Citizenship: China

RESEARCH EXPERIENCES

10/2009 – 08/2013 Ludwig-Maximilians-University Munich (Germany)

Department Biology I, Botany

PhD “Shedding light on TAP38: A study on its regulation, site of action and antagonistic function towards STN7”

- Supervisor Prof. Dr. Dario Leister

09/2006 – 07/2009 Northwest Agriculture and Forestry University (China)

College of Plant Protection, Plant disease

Diploma thesis “Interaction of *Phytophthora sojae* and *Arabidopsis thaliana* and Genetic Analysis of a Susceptible Mutant”

- Supervisor Prof. Dr. Weixing Shan

EDUCATION

09/2006 – 07/2009 Studies of Plant disease in College of Plant Protection at the Northwest Agriculture and Forestry University (China)

09/2002 – 07/2006 Studies of Plant science in College of Agriculture at the Northwest Agriculture and Forestry University (China)

09/1996 – 07/2002 Number 3 middle school of Chabuchaer, Xinjiang (China)

PUBLICATIONS

Liu Qiuping#, Xu Wenteng#, Wunder Tobias, Steinberger Iris, Sela Noa, Pfannschmidt Thomas, Leister Dario and Pribil Mathias. A study on TAP38: its regulation, site of action and antagonistic function towards STN7. (in preparation)

Wunder T, Liu Q, Aseeva E, Bonardi V, Leister D, Pribil M (2013) Control of STN7 transcript abundance and transient STN7 dimerisation are involved in the regulation of STN7 activity. *Planta* 237(2): 541-558

Qiuping Liu, Hua Cao, Maojin Yao, Ying Ma, Binsheng Deng, Junli Quan, Weixing Shan. Nonhost (2010) Interaction of *Phytophthora sojae* and *Arabidopsis thaliana* and Genetic Analysis of a Susceptible Mutant. *Bulletin of Botany* 45(5):548-555.

Declaration/Eidesstattliche Erklärung

Ich versichere hiermit an Eides statt, dass die vorgelegte Dissertation von mir selbständig und ohne unerlaubte Hilfe angefertigt ist. Der Autor hat zuvor nicht versucht, anderweitig eine Dissertation einzureichen oder sich einer Doktorprüfung zu unterziehen. Die Dissertation wurde keiner weiteren Prüfungskommission weder in Teilen noch als Ganzes vorgelegt.

München, 8. Juni 2013

.....
Qiuping Liu